A cell-based gene therapy approach for dysferlinopathy using *Sleeping Beauty* transposon

Inaugural-Dissertation
to obtain the academic degree
Doctor rerum naturalium (Dr. rer. nat.)

submitted to
the Department of Biology, Chemistry and Pharmacy
of Freie Universität Berlin

by

HELENA ESCOBAR FERNÁNDEZ

from León, Spain

August 2015

This work was prepared from October 2011 to July 2015 under the supervision of Dr. Zsuzsanna Izsvák (Max-Delbrück Center for Molecular Medicine, Berlin, Germany) and Prof. Simone Spuler (Experimental and Clinical Research Center, Berlin, Germany). All the experiments were conducted in the laboratories of Dr. Izsvák and Prof. Spuler.

1st reviewer: **Prof. Dr. med. Simone Spuler**
Institute for Chemistry and Biochemistry
Department of Biology, Chemistry and Pharmacy
Freie Universität, Berlin

and

Department of Muscle Sciences and University Outpatient Clinic for Muscle Disorders
Experimental and Clinical Research Center, Berlin

2nd reviewer: **Prof. Dr. Sigmar Stricker**
Institute for Chemistry and Biochemistry
Department of Biology, Chemistry and Pharmacy
Freie Universität, Berlin

and

Development and Disease Group
Max Planck Institute of Molecular Genetics, Berlin

Date of Defense: November 18th, 2015

Preface

The experiments with human muscle fiber fragments were done in collaboration with Dr. Andreas Marg, from the laboratory of Prof. Simone Spuler. Dr. Marg performed the isolation of human fiber fragments and the full characterization of the fiber fragment culture model. I performed the mouse irradiation and transplantation of human fiber fragments into mice. Dr. Marg also performed the mouse irradiation and the analysis of all grafted muscles.

Acknowledgements

First of all, I want to thank Dr. Zsuzsanna Izsvák for supervising this work and giving me opportunity to carry out my PhD in her laboratory. I want to thank Dr. Luis García for agreeing to be my MyoGrad co-supervisor from Paris.

I want to thank Prof. Simone Spuler for her supervision, support and encouragement, especially during the last two years of my PhD.

I want to thank MyoGrad for the economic support not only to my doctoral studies but to a great number of local and international scientific events. I especially want to thank Susanne Wissler for her help with organizational issues. I also want to thank AFM-Téléthon for supporting me with a fourth year scholarship to complete my PhD.

I want to thank Dr. Andreas Marg for being an excellent mentor, for his constructive criticism, for being always open to helpful discussions and for sharing his solid expertise with me. It made me a better scientist.

I want to thank my colleagues in the lab of Zsuzsanna Izsvák for making work days fun. Especially, I want to thank Dr. Attila Szvetnik and Dr. Enikö Eva Nagy for many scientific and non-scientific late evening discussions, for being interested and always sincerely willing to help me and others. I want to thank Dr. Csaba Miskey, for being the best bench neighbor when I arrived at the lab. I want to thank Dr. Anantharam Devaraj for being a very friendly presence in my early days in the lab and for sharing his knowledge in transposons and molecular biology techniques.

I want to thank Dr. Anna Osiak and Dr. Sanam Bashir and her family for their open minds and their friendship, advice and the fun times spent together.

I want to thank Ana Jiménez Orgaz for being a great colleague and friend as well as the best companion to explore Berlin.

I want to thank Angélica García Pérez and Julia Rugor for being the fellow PhD students and friends that prevailed with me until the end. For all the favors, the help, the discussions, the support, the fun, the trips, the trust. I especially want to thank Angélica for her incredible generosity and the huge amount of help she has given me.

I want to thank Dr. Esther Grueso, Marta Holstein (to me, Pinito) and Alexander Holstein, for making me feel at home during my first months in Berlin. I want to thank Esther for singing in the cell culture in the evening and making it so easy to work until late, for being a great friend and my most thorough judge of scientific posters and applications.

I really miss all of those who have left Berlin but I am thankful that they have given me such great memories of this time.

From the lab of Simone Spuler, I want to thank Adrienne Rothe for her excellent technical support and for helping me with the mouse irradiation. I want to thank Kornelia Gräning for introducing me to the muscle histology techniques and for performing the histological stains for

this work. I want to thank Stephanie Meyer-Liesener and Dr. Verena Schöwel for their help in the immunoblot analysis of some samples. I also want to thank Verena for her help with the applications for animal experiments.

I want to thank Dr. Markus Kufeld and Diana Pasemann from the Cyberknife center of the Charité for their help with the mouse irradiation.

I want to thank my friend Alena for being my family in Berlin, for her immense friendship and strong support and for sharing all good and bad moments here.

Last, I want to thank my wonderful family, especially my parents Rosi and Félix, and my sister Laura. I want to thank them for encouraging me to look forward and always keep learning, for understanding my itinerant life style, and for taking part in it, for being always there.

Table of contents

Summary

Miyoshi myopathy (MM), limb girdle muscular dystrophy 2B (LGMD2B) and distal anterior compartment myopathy (DACM) are rare autosomal recessive muscle disorders caused by mutations in dysferlin. They are encompassed by the term dysferlinopathy and affect the proximal and/or distal muscles of the limbs. Patients usually become wheelchair bound within 15 years of disease onset due to progressive muscle degeneration, weakness and atrophy. No treatment is available. The dysferlin gene spans over 150 kb of genomic DNA in chromosome 2p13 and comprises 55 exons that form a coding sequence of 6.2 kb. Dysferlin is a 237 kDa protein of the ferlin family. It is expressed in many tissues, but more strongly in muscle, where it is found in mature myofibers and to some extent also in satellite cells and myoblasts. It has important roles in membrane repair and in maintaining the transverse tubule structure in myofibers. Besides alterations of these two functions, defects in dysferlin cause increased inflammatory attack to muscle fibers thereby enhancing the muscle pathology.

Muscle regeneration relies on muscle stem cells, called satellite cells, and their progeny of muscle precursors, the myoblasts. Upon muscle injury caused by severe trauma or muscle disorders, they are capable of extensive proliferation to repair the damaged tissue. Satellite cells are marked by the expression of the transcription factor Pax7, they can be isolated based on specific surface markers and have a robust engraftment potential when transplanted into regenerating muscles. Therefore, autologous or allogeneic satellite cell and myoblast transplantation are envisioned as promising therapeutic alternatives. Given that a single gene is causative for dysferlinopathy, gene therapy also holds great promise. However, the large size of the full-length dysferlin coding sequence represents a challenge for gene transfer approaches because most viral vectors used in gene therapy have a lower cargo capacity. *Sleeping Beauty* transposon is a non-viral bi-component vector system consisting of a transposon DNA sequence and a transposase protein. The transposase excises the transposon from a donor plasmid and integrates it into the target genome. Since the transposon can be engineered to carry any sequence of interest, *Sleeping Beauty* is very valuable as a genetic tool for stable gene transfer and has been widely used in gene therapy. *Sleeping Beauty* system can be used to integrate transgenes up to ~8 kb with high efficiency. It is therefore well-suited for delivery of full-length dysferlin.

In this work, I developed a non-viral cell-based gene therapy approach for dysferlinopathy. Using *Sleeping Beauty* transposon, I transferred the full-length human dysferlin cDNA into dysferlin deficient H2K A/J mouse myoblasts, leading to restoration of dysferlin protein expression *in vitro*. I transplanted the corrected myoblasts into dysferlin deficient Scid/blAJ mice following local irradiation of the recipient muscles. This step was necessary to ablate the endogenous satellite cells and promote engraftment of the transplanted cells. I found up to ~90 dysferlin expressing myofibers 3 and 6 weeks post-transplantation. Inducing regeneration in the recipient muscles simultaneously to cell transplantation by injection of cardiotoxin, a snake venom toxin that causes acute damage to myofibers, further enhanced engraftment of the donor cells. In muscles treated with cardiotoxin in addition to irradiation, I found up to ~1000 donor-derived myofibers 3 and 6 weeks after grafting, which were present almost along the entire length of the muscles. Moreover, I found numerous Pax7+ cells in the vicinity of donor-derived myofibers in the grafted muscles. Given that recipient muscles were irradiated prior to grafting, this suggests that donor myoblasts were able to repopulate the host satellite cell compartment upon transplantation. Engraftment as satellite cells would ensure long-term contribution of donor-

derived cells to muscle regeneration. These results show the feasibility of long-term full-length dysferlin reconstitution in skeletal muscle through *ex vivo* gene transfer with *Sleeping Beauty*.

Zusammenfassung

Miyoshi Myopathie (MM), Gliedergürteldystrophie Typ 2B (engl. limb girdle muscular dystrophy 2B, LGMD2B) und die DACM (distal anterior compartment myopathy) sind seltene, autosomal rezessiv vererbte Krankheiten, die durch Mutationen im Dysferlin-Gen verursacht werden. Diese muskulären Erkrankungen werden unter dem Begriff Dysferlinopathie zusammengefasst und betreffen die proximale und/oder die distale Muskulatur der Extremitäten. Durch eine zunehmende Schwächung und Atrophie der Muskeln sind Patienten normalerweise bereits 15 Jahre nach Krankheitsbeginn an den Rollstuhl gebunden. Behandlungsmöglichkeiten gibt es hier keine. Das Dysferlin-Gen umfasst einen 150 kb-Bereich der genomischen DNA auf Chromosom 2p13 und beinhaltet 55 Exons mit einer kodierenden Sequenz von 6,2 kb. Dysferlin ist ein 237 kDa Protein der Ferlinfamilie. Es ist in vielen Geweben vorhanden, vor allem im Muskelgewebe, wo es in ausgereiften Muskelfasern, aber auch in Satellitenzellen und Myoblasten exprimiert wird. Dysferlin spielt eine wichtige Rolle bei der Membranreparatur und der Aufrechterhaltung der T-Tubuli Struktur in den Muskelfasern. Auβer dem erhöht sich durch ein defektes Dysferlinprotein die Entzündungsanfälligkeit der Muskelfasern.

Die Regenerationsfähigkeit von Muskeln beruht auf den Muskelstammzellen (Satellitenzellen) und ihren Abkömmlingen, den Muskelvorläuferzellen (Myoblasten). Bei Muskelverletzungen, z.B. durch schwere Verwundungen oder durch Muskelerkrankungen, vermehren sich diese Zellen extensiv um das geschädigte Gewebe zu reparieren. Satellitenzellen sind durch die Expression des Transkriptionsfaktors Pax7 gekennzeichnet. Ihre Isolation basiert auf spezifischen Oberflächenmarkern. Zudem haben sie ein hohes Anwachspotential, wenn sie in sich regenerierendes Muskelgewebe tranplantiert werden. Deshalb gilt die autologe oder allogene Transplantation von Satellitenzellen oder Myoblasten als vielversprechende therapeutische Alternative. Da Dysferlinopathien durch ein einzelnes Gen verursacht werden, ist zudem die Gentherapie hier sehr erfolgversprechend. Allerdings werden Gentransferversuche durch die Größe der kodierenden Dysferlinsequenz erschwert, da die meisten viralen Vektoren, welche für Gentherapiezwecke benutzt werden, eine zu geringe Ladungskapazität besitzen. Das *Sleeping Beauty* Transposon ist ein nicht-virales 2-Komponenten Vektorsystem, welches aus der DNA Sequenz des Transposons und einem Transposase Protein besteht. Die Transposase schneidet das Transposon aus dem Donorplasmid heraus und integriert es in das Zielgenom. Da das Transposon so verändert werden kann, dass es jede Zielsequenz beinhalten kann, ist *Sleeping Beauty* ein sehr wichtiges, nicht-virales, genetisches Werkzeug, das einen stabilen Gentransfer ermöglicht und deshalb häufig in der Gentherapie verwendet wird. Durch das *Sleeping Beauty* System kann ein bis zu 8 kb groβes Transgen effizient integriert werden. Damit ist es auch für die Integration des vollständigen Dysferlin-Gens sehr gut geeignet.

Im Rahmen dieser Arbeit habe ich eine Methode entwickelt, welche einen nicht-viralen zellbasierten Ansatz zur Gentherapie von Dysferlinopathien ermöglicht. Durch Nutzung des *Sleeping Beauty* Transposons ist es mir gelungen, die vollständige humane Dysferlin cDNA-Sequenz in Dysferlin-defiziente H2K A/J Myoblasten der Maus zu transferieren und die Dysferlinexpression *in vitro* wieder herzustellen. Die so korrigierten Myoblasten habe ich in Dysferlin-defiziente Scid/blAJ Mäuse transplantiert, in denen der Empfängermuskel zuvor lokal bestrahlt wurde. Dieser Schritt war notwendig, um die Anzahl der endogenen Satellitenzellen zu verringern und das Anwachsen der transplantierten Zellen zu fördern. 3-6 Wochen nach der Transplantation konnte ich eine Dysferlinexpression in bis zu 90 Muskelfasern nachweisen. Eine

gleichzeitig zur Transplantation stattfindende Injektion des Zellgiftes Cardiotoxin führte zu einem wesentlich verbesserten Anwachsen der Donorzellen. Muskeln, welche zusätzlich zur Bestrahlung noch mit Cardiotoxin geschädigt wurden, wiesen 3 bis 6 Wochen nach der Transplantation bis zu 1000 Dysferlin exprimierende Muskelfasern auf. Zudem konnte ich in den transplantierten Muskeln eine Vielzahl von Pax7 positiven Zellen in der Umgebung der von den Spenderzellen abgeleiteten Myofibrillen identifizieren. Da der Empfängermuskel vor der Transplantation bestrahlt wurde, deutet dieses darauf hin, dass das Satellitenzellkompartiment des Empfängermuskels nach der Transplantation wieder neu besiedelt wurde. Das Anwachsen der Myoblasten als Satellitenzellen würde daher einen dauerhaften Beitrag der Spenderzellen zur Regeneration des Muskels belegen. Diese Ergebnisse zeigen, dass eine Rekonstruktion des vollständigen Dysferlin Proteins in Skelettmuskeln durch *Sleeping Beauty* vermittelten Gentransfer möglich ist.

List of figures

List of tables

List of abbreviations

AAV	adeno-associated virus
AON	antisense oligonucleotide
ATP	adenosine triphosphate
BAC	bacterial artificial chromosome
BMD	Becker muscular dystrophy
BMT	bone marrow transplantation
CDS	coding sequence
CK	creatine kinase
CMD	congenital muscular dystrophy
CT	computed tomography
CTX	cardiotoxin
DACM	distal anterior compartment myopathy
DGC	dystrophin glycoprotein complex
DHPR	dihydropyridine receptor
DMD	Duchenne muscular dystrophy
EBD	Evans blue dye
ES	embryonic stem
FACS	fluorescence activated cell sorting
GFP	green fluorescent protein
Gy	gray
HDR	homology directed repair
H&E	hematoxylin and eosin
HMFF	human muscle fiber fragment
HRP	horseradish peroxidase
HSC	hematopoietic stem cell
HT	hypothermic treatment
IF	immunofluorescence

iPS	induced pluripotent stem
IRES	internal ribosome entry site
ITR	inverted terminal repeat
LGMD	limb girdle muscular dystrophy
LTR	long terminal repeat
MM	Miyoshi myopathy
NADH	reduced nicotinamide adenine dinucleotide
NMJ	neuromuscular junction
NMR	nuclear magnetic resonance
OPMD	oculopharyngeal muscular dystrophy
ORF	open reading frame
PCR	polymerase chain reaction
PTM	pre-*trans*-splicing molecule
qRT-PCR	quantitative reverse transcription PCR
R.T.	room temperature
RyR	ryanodine receptor
SB	*Sleeping Beauty*
SCID	severe combined immunodeficiency
SmaRT	spliceosome-mediated RNA *trans*-splicing
Spc5-12	synthetic promoter c5-12
SR	sarcoplasmic reticulum
TA	tibialis anterior
T-tubule	transverse tubule
TSS	transcription start site
WAS	Wiskott Aldrich syndrome
WB	western blot
YAC	yeast artificial chromosome

1 Introduction

1.1 Dysferlinopathy

The term dysferlinopathy encompasses several autosomal recessive muscle diseases caused by mutations in dysferlin. Those include Miyoshi myopathy (MM) (J. Liu et al., 1998; Matsuda et al., 1999), limb girdle muscular dystrophy 2B (LGMD2B) (Bashir et al., 1998; J. Liu et al., 1998) and distal anterior compartment myopathy (DACM) (Illa et al., 2001).

1.1.1 Clinical and histological aspects of dysferlinopathy

The clinical presentation of dysferlinopathy is strikingly variable regarding the types of muscles involved and the degree of severity. The age of onset also varies between the patients, but is most common during or after puberty. Depending on which muscles are affected first, the patients can be classified into LGMD2B, MM or DACM. However, some patients have combined phenotypes and rarer forms with unusual presentation have also been reported.

A common characteristic of dysferlinopathy patients is a highly increased level of serum creatine kinase (CK), a marker of muscle damage. CK levels can also be moderately elevated in asymptomatic carriers. The histological and ultrastructural alterations of skeletal muscle are common for MM, LGMD2B and DACM patients. They were first described by Miyoshi and colleagues (Miyoshi, Kawai, Iwasa, Kusaka, & Nishino, 1986) and include:

- Decreased number of fibers and replacement by fatty-fibrous tissue
- Marked variation in myofiber size
- Fiber splitting
- Presence of necrotic fibers, some associated with phagocytosis
- Increased number of regenerating fibers with centralized myonuclei
- Absence of 'ragged red' fibers, nemaline bodies or rimmed vacuoles, which are characteristic of other myopathies
- No apparent abnormalities in the intramuscular nerves
- Atrophy and degeneration of type 1 and 2 fibers, but no obvious fiber type predominance or type grouping
- Disorganization of the intermyofibrillar network
- Zig-zag irregularity and streaming of the Z-band as well as narrowing of myofibrils due to loss of myofilaments
- Increased number of mitochondria and dilatation of the sarcoplasmic reticulum and transverse tubule (T-tubule) system in areas where myofibrils had disappeared

The disease progression of both distal and proximal phenotypes is slow, and the patients remain ambulant for several years although they generally become wheelchair-bound within 15 years of disease onset.

1.1.1.1 The distal myopathies – MM and DACM

The distal myopathies are a group of muscle disorders characterized by progressive muscle weakness and atrophy presenting in the distal muscles of the limbs. The British neurologist Sir

William Richard Gowers was the first to formally use this term to describe a case of distal weakness in 1902 (Gowers, 1902). Two of those disorders, MM (J. Liu et al., 1998; Matsuda et al., 1999) and DACM (Illa et al., 2001), are caused by mutations in the gene encoding dysferlin.

Miyoshi et al. described in 1986 a new form of distal myopathy with autosomal recessive inheritance (Miyoshi et al., 1986). MM patients usually present with muscle weakness and atrophy leading to motor dysfunction during early adolescence to young adulthood. Muscle weakness can be accompanied by disturbance of gait, tendency to fall and difficulty in standing up, running fast and climbing stairs. The affected muscles in the lower parts of the legs, like gastrocnemius and soleus, become very thin due to prominent wasting. The muscle atrophy eventually spreads to the proximal limb muscles during disease progression.

In DACM, the most severely affected muscles are those of the anterior compartment group (Illarioshkin et al., 2000). The disease, also called "distal myopathy with anterior tibial onset", was first described in 2001 as a new form of autosomal recessive distal myopathy caused by mutations in dysferlin (Illa et al., 2001).

1.1.1.2 The limb girdle muscular dystrophies – LGMD2B

LGMD defines a group of muscle diseases caused by mutations in different genes and characterized by progressive weakness with onset in the proximal muscles of the limbs. The distal muscles can be involved in later stages of disease progression. Heart and respiratory muscles may also be affected, whilst facial and extraocular muscles are spared. The onset of clinical manifestations is variable but typically non-congenital, and a muscle biopsy is usually needed to establish differential diagnosis with Duchenne and other forms of muscular dystrophy.

Regarding nomenclature, autosomal dominant forms of LGMD are designated as LGMD1 and autosomal recessive as LGMD2. The assignment of a letter is given in chronological order corresponding to the identification of the associated locus. So far, thirty one LGMD loci have been identified, eight of them autosomal dominant and 23 autosomal recessive. The autosomal recessive forms of LGMD have a cumulative prevalence of 1:15000. The autosomal dominant forms represent less than 10% of all LGMD (reviewed in (Nigro & Savarese, 2014)). As mentioned before, dysferlin mutations are responsible for LGMD type 2B.

A brief history of the LGMDs: the term LGMD was introduced in the 1950s by Walton and Nattrass (Walton & Nattrass, 1954) to describe an autosomal recessive and very heterogeneous clinical condition. The heterogeneity of the LGMDs would later be confirmed when the first LGMD loci were discovered. Kate Bushby published in 1995 a unifying compilation of criteria for the diagnosis of LGMD (Bushby, 1995). The inclusion criteria were:

1. Onset at any age presenting with weakness in pelvic or shoulder girdle muscles or both simultaneously
2. Autosomal dominant or recessive inheritance
3. Greatly elevated CK levels in recessive cases and less elevated in dominant cases
4. Non-specific myopathic or dystrophic changes in muscle biopsies or electromyography

Excluded were: onset of weakness in distal, facial or extraocular muscles, evidence of dystrophinopathy, namely Duchenne muscular dystrophy (DMD) or its milder phenotypic variant Becker muscular dystrophy (BMD), and muscle biopsy findings that would be indicative of a neuropathic disease, inflammatory changes, metabolic or mitochondrial abnormalities.

Until then, only a few genetic associations had been established for LGMD and no gene was known to be causative for any form of LGMD.

1.1.2 Genetic basis of dysferlinopathy

The human dysferlin gene (*DYSF*) was discovered in 1998 in two independent studies (Bashir et al., 1998; J. Liu et al., 1998) that came after a series of works on linkage analysis in families and patients with recessively inherited LGMD and MM phenotypes.

In 1994 Bashir and colleagues reported the finding of a new LGMD2 locus in chromosome 2p (Bashir et al., 1996). This work represented the discovery of the second locus for autosomal recessive LGMD, leading to the designation of the disease as LGMD2B.

Already in 1996 the results obtained in two independent studies suggested that there may be a common genetic origin for LGMD2B and MM.

Weiler and colleagues found two independent mutant alleles in an inbred, aboriginal Canadian kindred with members affected by muscular dystrophy consistent with either MM or LGMD (Weiler et al., 1996). The two mutations, however, could not explain the clinical variability between the patients, suggesting that the phenotypic differences could be due to additional factors.

Linkage analysis on another large and highly consanguineous Russian family with members affected by clinical, histological and ultrastructural symptoms of either MM or LGMD2 pointed towards a common locus in chromosome 2p (Illarioshkin et al., 1996), the same that had been previously associated with LGMD2B (Bashir et al., 1996).

1.1.2.1 Discovery of the dysferlin gene

The definitive discovery of a causative gene for MM and LGMD2B would not come until 1998, when two studies by the groups of Kate Bushby and Robert H. Brown identified dysferlin as a new protein coding gene that was mutated in both diseases (Bashir et al., 1998; J. Liu et al., 1998).

In the work by Bashir et al. (Bashir et al., 1998), the haplotype information of a previously described family allowed the mapping of the LGMD2B critical genomic region to chromosome 2p13. Two yeast artificial chromosomes (YACs) were used to find expressed sequence tags (ESTs) mapping to this region that were expressed in skeletal muscle. This allowed the identification of a 7 kb transcript expressed predominantly in skeletal muscle but also present in other tissues.

In a simultaneously published work, Liu et al. used a previously constructed a P1-derived artificial chromosome (PAC) contig spanning the MM/LGMD2B candidate region and analysed polymorphic markers found in MM families to find out the precise locus (J. Liu et al., 1998). Derived from this locus, they identified a 6.9 kb transcript with an open reading frame (ORF) of 6,243 bp predicted to encode a 2,080 aa protein and beginning with the Kozak consensus sequence for a start codon. Interestingly, they also reported the occurrence of an alternative start codon, in the same frame but +75 bp downstream.

Since the predicted protein was homologous to the C. elegans protein fer-1 expressed in primary spermatocyte, the new protein was named ‘dysferlin’ for dystrophy-associated, fer-1-like protein. The gene was assigned the symbol *DYSF* (J. Liu et al., 1998).

1.1.2.2 *DYSF* mutations and lack of genotype-phenotype correlation

Disease-causing mutations in *DYSF* span the entire length of the gene with an absence of hot-spots and are strikingly variable in their clinical manifestation (Cacciottolo et al., 2011; Krahn et al., 2009). The same mutations have been associated with different degrees of severity, ages of onset or types of muscles involved (Ceyhan-Birsoy et al., 2015; Krahn et al., 2009). In 2009, a

dysferlin mutation analysis done in the largest patient cohort screened thus far (134 patients with suspected LGMD2B or MM) identified 212 deleterious mutations, most present at a homozygous or compound heterozygous pattern, which had no apparent correlation with the observed MM and LGMD2B phenotypes (Krahn et al., 2009).

Very recently, mutations in dysferlin have been associated with more infrequent clinical presentations such as congenital muscular dystrophy (CMD) (Ceyhan-Birsoy et al., 2015; Paradas et al., 2009). Ceyhan-Birsoy and colleagues reported in 2015 a case study of two siblings with a CMD phenotype and complete absence of dysferlin protein caused by a mutation previously associated to cases of adult-onset hyper-CKemia and LGMD.

A secondary reduction in dysferlin protein can occur in muscular dystrophies caused by alternative gene defects such as caveolin-3 (*CAV3*) mutations, which cause LGMD1C (Matsuda et al., 2001). Nevertheless, a study performed in 65 patients with a LGMD/MM phenotype showed that a marked reduction of Dysferlin protein (<20%) in skeletal muscle is caused primarily by *DYSF* mutations (Cacciottolo et al., 2011).

1.2 Dysferlin

1.2.1 *DYSF* gene and dysferlin transcript variants

DYSF spans over 150 kb of genomic DNA in chromosome 2p13.3-p13.1 and comprises 55 exons (Aoki et al., 2001; Bashir et al., 1998; J. Liu et al., 1998). 509 genomic variants are registered in the Leiden Muscular Dystrophy Pages database (http://www.dmd.nl/).

Fourteen transcript variants have so far been identified as arising from the human dysferlin gene through alternative splicing and usage of two different transcription start sites (TSS) (Pramono et al., 2009). Exon 1 of *DYSF* encodes the first C2 domain of dysferlin, C2A. The use of the alternative TSS, contained within intron 1 and preceded by a consensus Kozak sequence, incorporates a different first exon to the mRNA, which is derived from intron 1. This alternative exon 1 encodes a structurally different C2A domain, C2Av1, whereas the rest of the mRNA remains the same (Pramono, Lai, Tan, Takeda, & Yee, 2006).

In addition, seven processed mRNA variants are generated from each of the two pre-mRNAs transcribed from the two TSS. The two variants with canonical splicing are *DYSF* and *DYSF_v1*, transcribed respectively from the canonical and the alternative promoter. The remaining transcripts are produced by alternative splicing inducing exclusion of exon 17 (Salani et al., 2004), in-frame inclusion of alternative exon 5a via exonization of a sequence derived from intron 5, and in-frame inclusion of alternative exon 40a, derived from intron 40 (Pramono et al., 2009).

These protein coding variants are differentially expressed depending on developmental stage, tissue type and disease condition (Pramono et al., 2006; Pramono et al., 2009; Salani et al., 2004). Expression analysis by Northern blot conducted with probes specific to exon 1 of *DYSF* or *DYSF_v1*identified the presence of transcripts detected only by either one of the probes in samples from various tissues. The longest transcript of ~7.5 kb was always present in skeletal muscle. Likewise, qRT-PCR analysis on mRNA samples from human skeletal muscle and blood revealed a different abundancy of the fourteen transcript variants in those tissues (Pramono et al., 2006).

1.2.2 Dysferlin protein

Dysferlin belongs to the ferlin family, an ancient family of large (~200–240 kDa) proteins with roles in vesicle trafficking and fusion that are present in all eukaryotic kingdoms and protozoans. Mammals have six ferlin genes (*Fer1L1–L6*), *DYSF* being *Fer1L1*. Ferlins are the proteins containing the highest number of tandem C2 domains (5-7 depending on the protein). These domains function in lipid and protein binding and are characteristic of proteins involved in vesicle fusion. One such example is the synaptotagmins, which contain two of those structural motifs. Ferlin proteins also contain a single-pass transmembrane domain in their C-terminus for anchoring to the membrane. They are divided into two subgroups according to the presence or absence of a dysF domain. The most studied family members are myoferlin, otoferlin and dysferlin (reviewed in (Lek, Evesson, Sutton, North, & Cooper, 2012)).

Myoferlin is required for myoblast fusion during muscle development and regeneration. Otoferlin is involved in vesicle fusion in the inner hair cells of the cochlea. There, it localizes to the presynaptic membrane and is thought to participate in Ca^{2+}-dependent vesicle exocytosis for neurotransmitter release. Defects in otoferlin cause profound deafness in humans and mice (Lek et al., 2012).

Dysferlin, as predicted based on its amino acid sequence, is a 237 kDa protein (Anderson et al., 1999). It is expressed early during human fetal development, being detected by immunolabeling on lysates of fetal limb tissues already at embryonic age 5-6 weeks. In rat protein lysates, the full-length protein is strongly detected in skeletal muscle, heart and kidney and to a lesser extent in stomach, lung, uterus, liver, spleen and nervous tissue (cerebellum, brain stem, spinal cord and sciatic nerve). Faint smaller bands (~40-60 kDa) are also detected in lysates from brain stem, spinal cord and sciatic nerve, possibly indicating the presence of smaller isoforms. In human it has been detected by immunolabeling in protein lysates of heart, term placenta, skeletal muscle (Anderson et al., 1999) and blood monocytes (Ho et al., 2002).

In skeletal muscle tissue, dysferlin is already expressed in cultured human myoblasts and in satellite cells from muscle biopsy specimens, although to a much lesser extent than in differentiated myotubes and myofibers (De Luna, Gallardo, & Illa, 2004; Salani et al., 2004). Dysferlin is absent or expressed at very low levels in skeletal muscle of dysferlinopathy patients (Anderson et al., 1999; Matsuda et al., 1999; Vainzof et al., 2001). The expression of dysferlin in blood monocytes correlates with that of skeletal muscle. This allows the use of blood samples for diagnosis of dysferlinopathy when good quality muscle biopsies are not available (Gallardo et al., 2011; Ho et al., 2002).

1.2.2.1 Dysferlin domain structure

The C2 domains of the ferlin family proteins otoferlin, myoferlin and dysferlin bind to lipid bilayers and actively promote remodeling of membrane structures. These alterations enable a variety of processes like membrane fusion or recruitment of other proteins involved in membrane-trafficking (Marty, Holman, Abdullah, & Johnson, 2013).

Dysferlin contains seven C2 domains, C2A to C2G (Therrien, Dodig, Karpati, & Sinnreich, 2006). All of them display Ca^{2+} binding activity albeit with very different affinities. The most sensitive ones are the C2A and C2C domains (Abdullah, Padmanarayana, Marty, & Johnson, 2014; Fuson et al., 2014; Marty et al., 2013). The protein also contains three Fer domains (FerA, FerB and FerI), one C-terminal single pass transmembrane domain, a short extracellular domain and two dysF domains (Figure 1. 1), one inserted into the other by gene duplication (Ponting, Mott, Bork, & Copley, 2001). Cristal structures are only available for the human dysferlin inner dysF domain (Sula, Cole, Yeats, Orengo, & Keep, 2014), and for the C2A

and C2Av1 domains (Fuson et al., 2014). They were solved with high resolution by molecular replacement using the NMR structure of the inner DysF and C2A domains of myoferlin, respectively.

Figure 1. 1: Domain architecture of human dysferlin protein.

Modified from (Sula et al., 2014).

The C2A and C2Av1 domains of dysferlin differ in their Ca^{2+} binding activity. C2A contains a high affinity Ca^{2+} binding site that stabilizes the domain and a set of low-affinity Ca^{2+} binding sites responsible for interactions with the negatively charged lipid membrane. On the contrary, C2Av1 binds to negatively charged lipids in a Ca^{2+} independent manner. Nevertheless, studies in C2C12 myoblasts have shown that the full-length dysferlin isoforms containing either C2A or C2Av1 are equally active in their membrane targeting activity (Fuson et al., 2014). Mutations in certain C2 domains of dysferlin can cause protein aggregation due to misfolding and formation of amyloid deposits in skeletal muscle (Spuler et al., 2008).

1.2.2.2 Dysferlin protein localization in skeletal muscle

In skeletal muscle tissue, dysferlin was first described as a membrane protein of muscle fibers (Anderson et al., 1999). However, additionally to its classic sarcolemmal distribution (Figure 1. 2), many authors have reported an intracellular localization of dysferlin in muscle fibers. Recent studies have detected a significant amount of dysferlin at the T-tubule membranes (Figure 1. 5), where it aligns with the dihydropyridine receptor (DHPR) and the Ryanodine Receptor (RyR) present at the triads (Ampong, Imamura, Matsumiya, Yoshida, & Takeda, 2005; Y. Huang et al., 2007; Kerr et al., 2013; Klinge et al., 2010; Klinge et al., 2007; Roche et al., 2011).

A secondary reduction and/or abnormal cytoplasmic staining pattern of dysferlin has also been observed in dystrophin glycoprotein complex (DGC) related myopathies (α-, β- and γ-sarcoglycanopathies and DMD/BMD) as well as in patients unspecifically diagnosed of “LGMD” or “muscular dystrophy” (Piccolo, Moore, Ford, & Campbell, 2000).

1.2.2.3 Dysferlin function in membrane repair

The most widely studied role for dysferlin in skeletal muscle is Ca^{2+}-dependent membrane repair. Bansal et al. first showed that the sarcolemma of some fibers was damaged in dysferlin knock-out mice. When injected with the membrane impermeant dye Evans blue (EBD), dysferlin-null muscles showed a higher dye uptake compared to control muscles. The sites of disrupted sarcolemma in dysferlinopathic muscles were enriched in dysferlin and had vesicles accumulated underneath (Bansal et al., 2003). They demonstrated that proper membrane resealing is impaired in dysferlin-null myofibers by developing a functional assay whereby isolated muscle fibers were injured with a laser in the presence of the membrane-impermeant dye FM 1-43. This molecule fluoresces when bound to lipidic bilayers and serves as an indicator of increased endo-membrane at wound sites, which is removed after repair (Figure 1. 3).

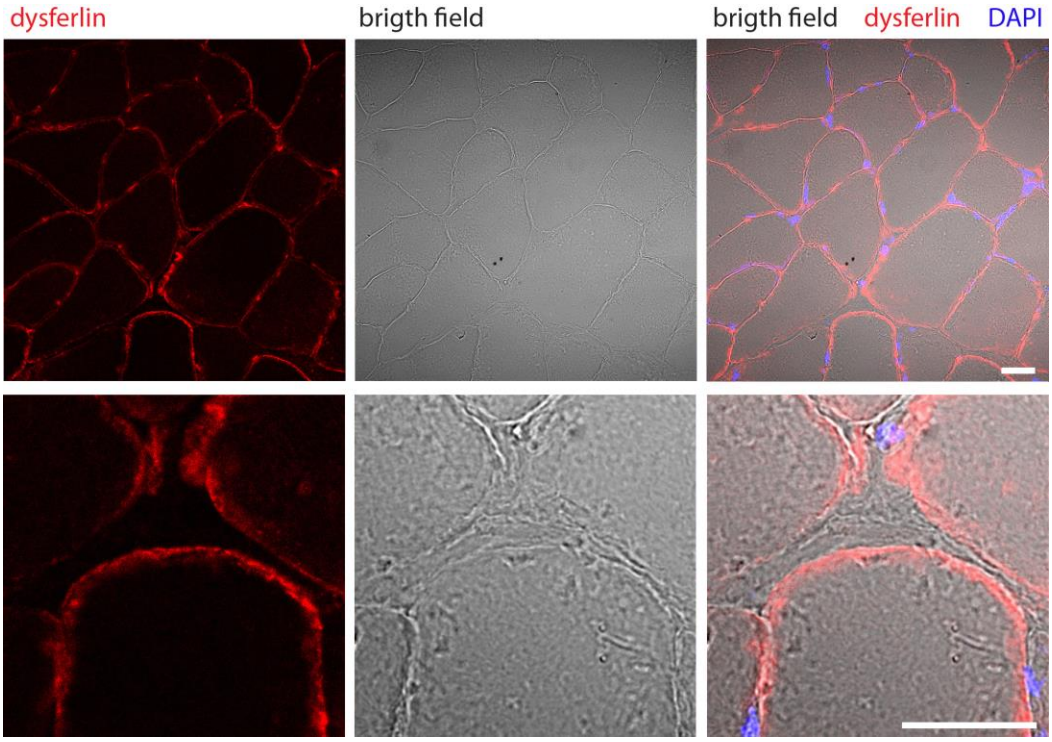

Figure 1. 2: Sarcolemmal localization of dysferlin in mouse muscles.

Confocal microscopy images of one cryosection from a C57BL/6J quadriceps muscle immunostained with an antibody against dysferlin (red). Nuclei were counterstained with DAPI (blue). Scale bars: 20 µm.

Several studies have shown that following membrane injury, dysferlin rapidly relocates to the wound site. Throughout differentiation of mouse C2C12 myoblasts, dysferlin localizes predominantly to the developing T-tubule system. However, in response to membrane wounding using glass beads, it translocates to the plasma membrane and accumulates at the sites of injury in a Ca^{2+}-dependent fashion (Klinge et al., 2007). In muscles of zebrafish embryos, dysferlin localizes to the sarcolemma and the T-tubules in undamaged fibers. In response to laser induced injury *in vivo*, it relocates rapidly to the membrane lesion. This relocation requires dysferlin's transmembrane domain, as it does not occur in truncation mutants lacking this part of the protein. In addition to dysferlin, annexins 6 (Anxa6) and 11a (Anxa11a) also relocate to the site of injury with a fast kinetics. Moreover, both dysferlin and Anxa6 are required for the accumulation of other annexins at the wound and a correct formation of a repair patch (Roostalu & Strahle, 2012).

Complete repair and resolution of a membrane wound in normal myotubes is reportedly a slow process that involves dysferlin and Ca^{2+}-dependent formation of a repair dome at the injury site for over 60 minutes post-injury. This raised ridged structure is enriched in annexin A1 and F-actin, and progressively accumulates dysferlin and the membrane-bender EH-domain-containing protein EHD2 (Marg et al., 2012).

Dysferlin interacts with caveolin-3 and the Tri-partite motif (TRIM) family protein mitsugumin 53 (MG53) in skeletal muscle cells (Cai et al., 2009; Matsuda et al., 2001; Matsuda et al., 2012). Disruption of this complex leads to membrane repair defects (Cai et al., 2009). The role MG53 in sarcolemmal repair was further characterized in a model of ballistics-induced membrane injury in human myotubes (Lek et al., 2013). Dysferlin and MG53 compartments interact and form a condensed lattice encircling the membrane lesions. This process is Ca^{2+}-dependent, as

chelation of Ca^{2+} with EGTA or blocking of voltage-gated calcium channels (VGCCs) impairs the recruitment of both dysferlin and MG53 to the wound site.

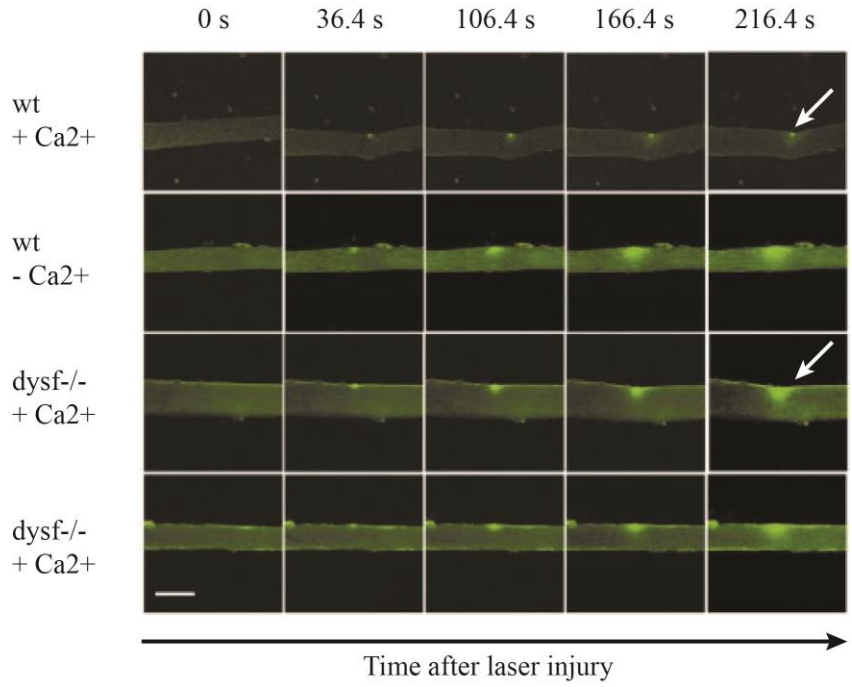

Figure 1. 3: Membrane resealing is impaired in dysferlin deficient skeletal muscle.

Laser wounding assay on single muscle fibers isolated from wild-type (wt) and dysferlin-null (dysf-/-) mice. The membrane damage was induced a t = 20 s in the presence or absence of Ca^{2+}. Compared to wild-type fibers, dysferlin-null fibers are incapable of repairing the membrane lesion and continue to accumulate endomembrane, as indicated by the increasing signal from FM 1-43 fluorescent dye at t = 216.4 s (white arrows). Modified from (Bansal et al., 2003).

Interestingly, myotube damage induces the calpain-mediated cleavage of full-length dysferlin to produce a ~72 kDa C-terminal isoform, mini-dysferlin$_{C72}$, that accumulates at the lesion in a Ca^{2+} dependent manner (Lek et al., 2013). This cleavage is done by calpains in the alternatively spliced exon 40a of dysferlin and it is not specific to myotubes but occurs also in other cells like human umbilical cord endothelial vein cells (HUVEC), mouse astrocytes and microglia, or secondary human oligodendrocytes (MO3.13). Notably, human myotubes subjected to ballistics injury accumulate exon 40a-containg dysferlin around the membrane wounds (Redpath et al., 2014).

Both the actin cytoskeleton (McDade, Archambeau, & Michele, 2014) and microtubules (McDade & Michele, 2014) are involved in the trafficking of dysferlin-containing vesicles during repair. The role of the actin cytoskeleton was uncovered by live-imaging using a fusion protein with a pH-sensitive GFP reporter as a C-terminal tag to dysferlin (dysf-pHGFP) (McDade et al., 2014). In myofibers of transgenic mice expressing dysf-pHGFP, injury triggers a rapid recruitment of dysferlin derived mainly from the sarcolemma in the vicinity of the wound. Inhibition of actin polymerization by Cytochalasin D blocks this trafficking and impairs resealing of the membrane. Microtubule-mediated trafficking of dysferlin-containing vesicles in response to injury is dependent on the kinesin heavy chain motor, KIF5B. These compartments fuse with lysosomes to form large cytoplasmic vesicles adjacent to the lesion and throughout the cytoplasm. This could be observed by live-cell imaging and fast freezing in rat L6 myotubes (McDade &

Michele, 2014). The defects in membrane repair of dysferlin deficient myoblasts have also been attributed to a decrease in acid sphingomyelinase (ASM) secretion by lysosomes in response to membrane injury. This secretion deficit is likely due to a lower number of membrane-proximal lysosomes. Also, dysferlin-null mouse myoblasts show reduced injury-triggered lysosomal exocytosis. It is noteworthy that ASM restores the membrane repair deficit of patient-derived myoblasts and myofibers isolated from dysferlin deficient Bla/J mice after focal laser injury (Defour et al., 2014). This may be interesting as a potential treatment.

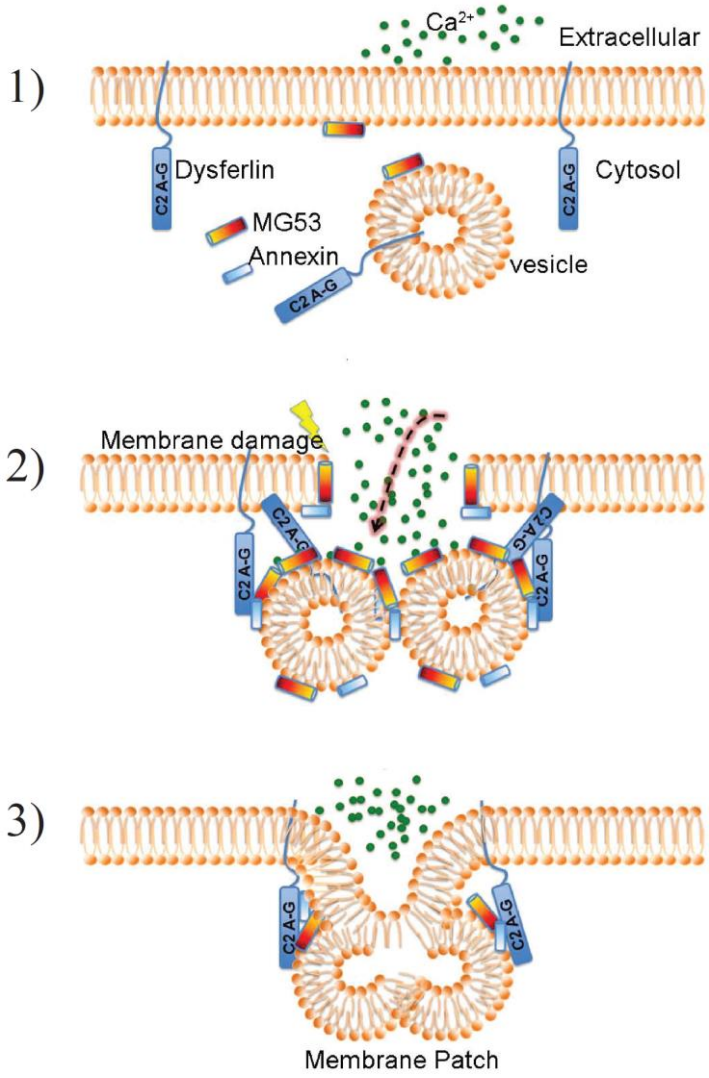

Figure 1. 4: Model for dysferlin-mediated muscle membrane repair.

1) Uninjured membrane. (2) In response to membrane damage and subsequent Ca^{2+} influx, dysferlin and MG53, aided by annexins, mediate the exocytosis of vesicles towards the membrane wound and the vesicle-vesicle fusion to generate larger membranous structures. (3) A membrane "patch" is formed to reseal the membrane wound. Modified from (Han, 2011).

Finally, as mentioned previously, the C2A and C2Av1 domains of dysferlin have differential Ca^{2+} binding affinities and Ca^{2+}-dependent or independent phospholipid binding properties. This has been proposed as a mechanism for concurrent activity of both domains in tightly regulating the membrane repair process (Fuson et al., 2014).

1.2.2.4 T-tubule associated functions

Dysferlin's T-tubule localization has been precisely defined by overexpressing C-terminal or N-terminal tagged pHluorin-dysferlin (a pH-sensitive GFP fused to dysferlin) in isolated adult mouse myofibers. These experiments showed that dysferlin is bound to the T-tubule membrane with its C-terminus exposed to the extracellular space (Kerr et al., 2013). Dysferlin deficient myofibers of A/J and Bla/J mice show and inability to cope with experimentally induced osmotic stress injury (OSI). In these mouse models, OSI causes an uncontrolled influx of extracellular Ca^{2+}, altering Ca^{2+} signaling and ultimately leading to a disruption of the T-tubule network. This effect is ablated by removal of extracellular Ca^{2+}, by treatment with diltiazem (an L-type Ca^{2+} channel blocker that prevents the entry of Ca^{2+} through the DHPR) or by re-expression of full-length dysferlin in dysferlin-null myofibers (Kerr et al., 2013).

During early regeneration of adult rat skeletal muscle induced by myotoxin injury, dysferlin localizes predominantly to the cytoplasm of myotubes and myofibers. There, it is enriched in longitudinal structures identified as T-tubules by the presence of DHPR. In later stages of regeneration, and once the process is completed, dysferlin labelling is more prominent at the sarcolemma of mature fibers. Dysferlin is also increased in the cytoplasm of regenerating human fibers labelled with neonatal myosin heavy chain, desmin and laminin-α5 (Klinge et al., 2010).

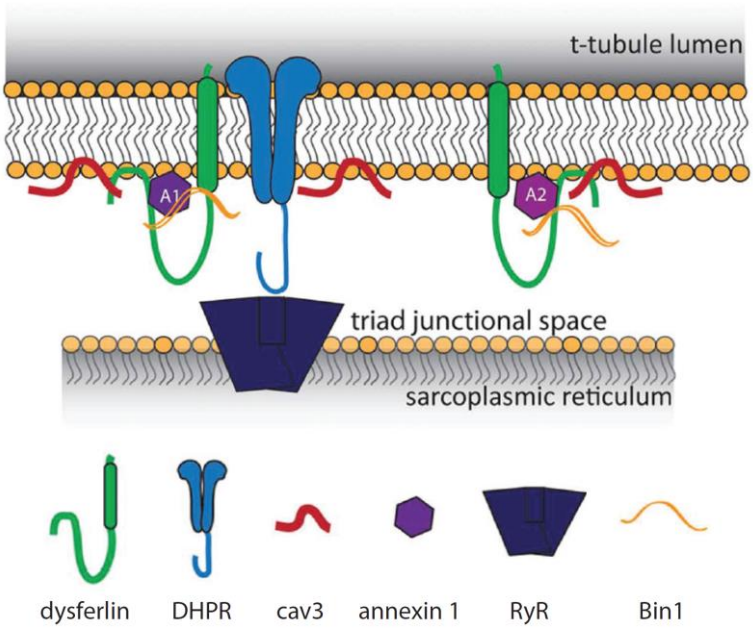

Figure 1. 5: Model for dysferlin's localization at the T-tubule membranes.

Dysferlin is anchored to the membrane with its C-terminal domain exposed towards the lumen of the T-tubule. Dysferlin is located in close proximity to proteins of the triad junction: the DHPR (anchored to the T-tubule membrane) and the RyR (in the sarcoplasmic reticulum), which are part of the excitation-contraction coupling mechanism. Dysferlin is also nearby or associated with its known interaction partners caveolin3, annexins and Bin1. Modified from (Kerr, Ward, & Bloch, 2014).

A similar cytoplasmic redistribution in regenerating fibers has been reported for the dysferlin interactors AHNAK (Y. Huang et al., 2007) and Caveolin-3 (Klinge et al., 2010; Matsuda et al., 2001).

In zebrafish embryos, knockdown of dysferlin using morpholinos doesn't markedly alter myofiber development at early developmental stages. However, it causes major pathogenic changes in myofiber ultrastructure, such as vesicle accumulation and disorganization of the myofibrils and the T-tubule system. Interestingly, knockdown of Anxa6, also involved in membrane repair, affects myofiber ultrastructure but produces a milder phenotype than dysferlin knockdown (Roostalu & Strahle, 2012).

This differential localization, together with the ultrastructural changes in the T-tubule network observed in dysferlin deficient mouse models, suggests a role for dysferlin in T-tubulogenesis and in maintaining the T-tubule structure in mature fibers.

1.2.2.5 Dysferlin, immunity and inflammation

A hallmark for dysferlinopathy is the enhanced activation of the complement system and attack to myofibers (Han et al., 2010; Wenzel et al., 2005). Wenzel et al. first described that the complement inhibitory decay-accelerating factors DAF/CD55 are downregulated in the skeletal muscle of SJL/J mice and LGMD2B patients as compared to control C57BL/6 mice and healthy controls, respectively (Wenzel et al., 2005). This correlates with the finding that the sarcolemma of both murine and human dysferlin-deficient muscle fibers is devoid of DAF/CD55 (Wenzel et al., 2005). The lack of these complement inhibitory factors promotes the deposition of the membrane attach complex C5b9-MAC, the end product of the complement pathway's activation, even on non-necrotic muscle cells (Han et al., 2010; Wenzel et al., 2005). Also, incubation of myotubes derived from control and dysferlinopathy patients with normal human serum resulted in complement-mediated lysis of the dysferlin deficient myotubes, an effect that could be partially inhibited by pre-incubation with anti-CD55 antibodies (Wenzel et al., 2005).

Similarly, Han et al. found that the complement factors C1q, CFB and C4 are elevated in the muscle of dysferlin-null SJL/J as compared to control mice. Rescue of dysferlin expression specifically in skeletal muscle not only reverses the myopathic changes of dysferlin-null mice but also restores the normal expression levels of the complement factors C1qA and CFB. Moreover, knock-out of the central component of the complement pathway, C3, in dysferlin-null mice, although having no effects on the membrane repair capacity of myofibers, is enough to ameliorate the muscle pathology. This, however, is not true for ablation of the terminal complement factor C5, thus suggesting that it is not the terminal activation of the complement pathway but rather of its central component C3 that contributes to disease progression in dysferlinopathy (Han et al., 2010).

The induction of alternative vesicle trafficking pathways in dysferlin deficient muscle has also been proposed to contribute to the inflammatory milieu of dysferlinopathy by increasing the release of pro-inflammatory molecules. Human skeletal muscle lacking dysferlin shows an increase in the synaptotagmin-like protein Slp2a/SYTL2 and its effector, the small GTPase Rab27A, which are involved in vesicle trafficking. An up-regulation of Rab27A and Slp2a in dysferlinopathic muscle could be a compensatory mechanism of vesicle trafficking for membrane repair in the absence of dysferlin (Kesari et al., 2008).

In addition, an increased expression of proteins of the inflammasome complex has also been observed in muscle from LGMD2B patients and SJL/J mice compared to their control counterparts and to DMD and *mdx* muscle, respectively (Rawat et al., 2010). The inflammasome mediates the activation of inflammatory caspases and processing of the pro-inflammatory cytokine pro-interleukin (IL)-1β to mature IL-1β. Myoblasts isolated from dysferlin deficient SJL/J mice show constitutive expression of IL-1β at low levels, indicating the presence of basal inflammasome activity. In response to lipopolysaccharide (LPS) stimulation, SJL/J myoblasts and myotubes display significantly higher levels of IL-1β and increased secretion compared with

control myoblasts. This effect has been attributed primarily to defects in dysferlin, since shRNA knockdown of dysferlin in wild-type muscle cells and in a macrophage cell line also leads to increased IL-1β secretion (Rawat et al., 2010). A proposed model is that the increased inflammasome activity in the absence of dysferlin may be mediated by activation of toll-like receptors (TLR). These would be activated by pro-inflammatory molecules secreted due to leakage through the damaged membrane and to the aforementioned induction of a compensatory vesicle trafficking pathway involving Rab27A and Slp2a (Kesari et al., 2008; Rawat et al., 2010).

Human dysferlinopathic muscle has more infiltrating mononuclear and dendritic cells. This observation goes along with the finding that monocytes isolated from SJL/J mice have a higher phagocytic activity in comparison to control mouse monocytes when incubated with fluorescently labelled *E. coli* bacteria. Knockdown of dysferlin in wild-type mouse macrophages leads to increased phagocytic activity (Nagaraju et al., 2008). In human monocytes and macrophages, dysferlin expression is up-regulated during differentiation and plays a role in regulating cell adhesion and motility (de Morree et al., 2013). In differentiated THP1 cells, a monocyte-like leukemia cell, dysferlin is strongly accumulated at cell-cell contacts. Knockdown of dysferlin affects intercellular interactions by up-regulating the expression of integrins and fibronectin, thereby leading to a strong decrease in cell adhesion. As a result, dysferlin depleted cells are more motile. This increase in cell motility has also been observed *in vitro* in primary macrophages from LGMD2B patients compared to control macrophages (de Morree et al., 2013). Altogether, this suggests that the enhanced monocyte and macrophage infiltration observed in patients is a direct or indirect consequence of the dysferlin defect and may be due to an increase in cell motility.

The role of the immune system in dysferlinopathy does not seem to be restricted to innate immunity. Dysferlin-null Scid/blAJ mice, which lack T and B lymphocytes but have a normally functioning innate immunity, have a delayed and milder myopathic phenotype than their control immunocompetent strain, the Bla/J mice. These milder myopathic features include reduced number of necrotic fibers, decreased phagocytosis and less variation in myofiber size. The skeletal muscle of Scid/blAJ mice also shows a decreased complement deposition and a lower percentage of pro-inflammatory M1 macrophages in comparison to immunocompetent Bla/J mice (Farini et al., 2012). It is known that the resolution of the inflammatory process that accompanies acute injury-induced muscle regeneration is delayed in dysferlin deficient mouse models compared with wild-type mice (Chiu et al., 2009). Interestingly, Scid/blAJ mice also display a faster clearing of inflammation upon injection of notexin compared to Bla/J mice (Farini et al., 2012).

1.2.2.6 Dysferlin function in muscle growth, regeneration and myoblast fusion

Dysferlinopathic muscle shows delayed regeneration (Chiu et al., 2009), defects in myoblast fusion (Cohen, Cohen, & Partridge, 2012; Demonbreun et al., 2011) and failure to respond to growth factor stimulation (Demonbreun et al., 2011). Some of these defects are tightly connected to the immune response alterations observed in dysferlinopathic muscle.

The muscle biopsies of dysferlinopathy patients show a higher percentage (56.3%) of fibers in late stages of regeneration compared with biopsies taken from LGMD2A, DMD/BMD and LGMD2I patients (Chiu et al., 2009). Moreover, experiments performed on dysferlin-null C57BL/10.SJL-Dysf mice have shown a lower amount of infiltrated mononuclear cells at early stages of regeneration (3 days post-myotoxin injection). This was accompanied by a failure to resolve the inflammatory process and a delayed removal of necrotic fibers compared to control muscle. Additionally, regenerating dysferlin-null muscle displays reduced specific force and maximum isometric force. Neither the expression pattern of satellite cell activation and

differentiation markers nor myoblast to myotube/myofiber fusion are altered in regenerating dysferlin-null muscle. However, dysferlin deficient myoblasts show altered secretion of the pro-inflammatory cytokine MCP-1 (Chiu et al., 2009). It therefore appears that the regeneration defect of dysferlinopathic muscle is caused by alterations in the recruitment of inflammatory cells that is necessary for early regeneration.

On the other hand, another study showed that *in vitro* differentiated myotubes derived from dysferlin-null mice had smaller diameters and contained significantly fewer nuclei than those of wild-type mice. This was reflected by lower transcript levels of differentiation markers during early and late stages of myoblast differentiation. These *in vitro* differentiation defects are linked to an increased NFκB signaling in dysferlin-null myoblasts. Inhibition of NFκB signaling with celastrol rescues the fusion deficit in cultured myoblasts (Cohen et al., 2012). In line with those findings, the glucocorticoid receptor agonist dexamethasone has been shown to enhance dysferlin expression and promote differentiation of C2C12 myoblasts (Belanto et al., 2010).

Dysferlin deficient A/J mice have increased levels of the NFκB activator TNF-α. However, treatment of A/J mice with celastrol, although decreasing muscle inflammation, did not improve muscle function and overall had rather detrimental effects (Dillingham et al., 2015). Therefore, targeting inflammation alone does not appear to be a viable therapy to improve muscle function in dysferlinopathy.

1.2.2.7 Dysferlin function in the heart

Dysferlin is also necessary for laser injury-induced membrane repair in mouse cardiomyocytes. In addition, the cardiac muscle of aged dysferlin-null mice shows more necrotic fibers and a higher degree of fibrosis and collagen deposits in comparison to age-matched controls. Aged dysferlin-null mice also present increased levels of serum troponin T, a marker for active cardiac muscle necrosis. They show an altered response to stress exercise, reduced heart rate, increased left ventricular end-systolic volume and appearance of sporadic EBD-positive myocytes (Han et al., 2007). Dysferlin-null mouse hearts also show reduced mechanical stress resistance as well as altered expression of Z-disc and signal transduction proteins when compared to wild-type mouse hearts. Surprisingly, however, they do not present histological abnormalities. Wenzel et al. showed that dysferlinopathy patients can occasionally present with cardiac abnormalities, such as dilated cardiomyopathy with left ventricular hypertrophy and altered left ventricular function (Wenzel et al., 2007).

1.2.2.8 Other functions of dysferlin

The sea urchin homolog of dysferlin has been implicated in membrane injury-triggered intercellular signaling events in early stage (≥4-cell) embryos (Covian-Nares, Koushik, Puhl, & Vogel, 2010). This process seems to be mediated by Ca^{2+} influx through opening of voltage-gated Ca^{2+} channels in the wounded cell in response to membrane depolarization. That in turn likely triggers exocytosis of ATP from the wounded blastomere, inducing Ca^{2+} spikes in neighboring cells. Dysferlin has been proposed to play a role in the release of ATP-containing vesicles, as morpholinos against sea urchin dysferlin inhibit this intercellular signaling. This effect is reversed by perfusion of the embryos with ATP.

1.3 Skeletal muscle regeneration

Skeletal muscle is responsible for voluntary contraction and movement and it is the most abundant tissue in the human body. It accounts for around 40% of the body mass of an adult

person. A muscle is made of fascicles of myofibers aligned longitudinally and connected at their extremities to the tendons forming myotendinous junctions, which attach the muscles to the bones. Each fascicle of fibers is surrounded by connective tissue called perimysium, and the whole muscle is itself surrounded by the epimysium. Each myofiber is at the same time covered by a protein envelope called basal lamina, which is composed of extracellular matrix proteins like laminins, collagens and fibronectin.

Myofibers are syncytial cells that contain multiple postmitotic nuclei within a large, continuous cytoplasm. They are mostly composed of myofibrils, longitudinal assemblies of sarcomeres. Sarcomeres are contractile units containing actin and myosin filaments that overlap and interconnect to allow sarcomere shortening, responsible for contraction in response to signals from the motor neurons. Following the release of neurotransmitters at the neuromuscular junction (NMJ), myofibers undergo membrane depolarization, which triggers Ca^{2+} release from the sarcoplasmic reticulum (SR) and induces sarcomere contraction.

Muscle fibers are formed by the fusion of myoblasts, myogenic precursors. During development, myoblasts derive from Pax3 and Pax7 expressing progenitors that originate in the somites, mesoderm structures at both sides of the neural tube and the notochord. From the somites they migrate to form the muscles of the extremities and the trunk. Some craniofacial muscles, on the other hand, originate from different mesoderm structures and their progenitors are defined by a different gene expression signature (reviewed in (Bentzinger, Wang, & Rudnicki, 2012)).

Adult muscle is a highly plastic tissue that is continuously subjected to mechanical stress due to exercise or just wear and tear. During this everyday process, tissue homeostasis ensures the long-term maintenance of muscle structure and function. But muscle is not only able to respond to these routine challenges. In conditions of severe and/or persistent damage, like after a trauma or in muscular dystrophy, homeostasis is compromised and myofiber architecture may be disrupted. The tissue then needs to regenerate, repair and remodel. In both situations adult muscle requires its stem cells, the satellite cells (Mauro, 1961). They are capable of extensive proliferation to generate myoblasts, which will fuse to existing fibers or to one another in order to generate new fibers (reviewed in (Yin, Price, & Rudnicki, 2013)). Following injury, skeletal muscle regeneration proceeds in three major phases:

1) **Infiltration of inflammatory cells:** a few hours after tissue damage, muscle is infiltrated by neutrophils. They are subsequently followed first by pro-inflammatory macrophages, which clear the cellular debris, and afterwards by anti-inflammatory macrophages. The latter have a role in promoting satellite cell proliferation and myoblast fusion, and are the last to disappear from the tissue once inflammation is cleared (reviewed in (Saclier, Cuvellier, Magnan, Mounier, & Chazaud, 2013)).
2) **Satellite cell proliferation and myoblast fusion:** a few days after damage, satellite cells start to proliferate, differentiate and fuse to repair the damaged myofibers or to make new ones. Regenerating fibers have some special features like a smaller diameter and centrally located myonuclei, as well as differential expression of some protein isoforms (e.g. developmental myosin heavy chain). Following myoblast fusion to an existing fiber, the newly incorporated nuclei go to the center of the fiber, from where later on they migrate towards the periphery (Yin et al., 2013).
3) **Tissue remodeling and maturation of new myofibers:** if regeneration proceeds as normal, at the end of the process the structure of the regenerated muscle is indistinguishable from that before the injury (Yin et al., 2013).

1.3.1 Satellite cells

Satellite cells were first discovered by Alessandro Mauro in 1961 as small, mononuclear cells with a wedged morphology in electron micrographs of skeletal muscle. They were named satellite cells due to their very defined position underneath the basal lamina and closely in contact with the sarcolemma of muscle fibers (Mauro, 1961). Morphologically, they are characterized by their large nuclear-to-cytoplasmic ratio, small nucleus with condensed interphase chromatin and few organelles, indicative of their quiescent state and low transcriptional activity (Schultz, Gibson, & Champion, 1978).

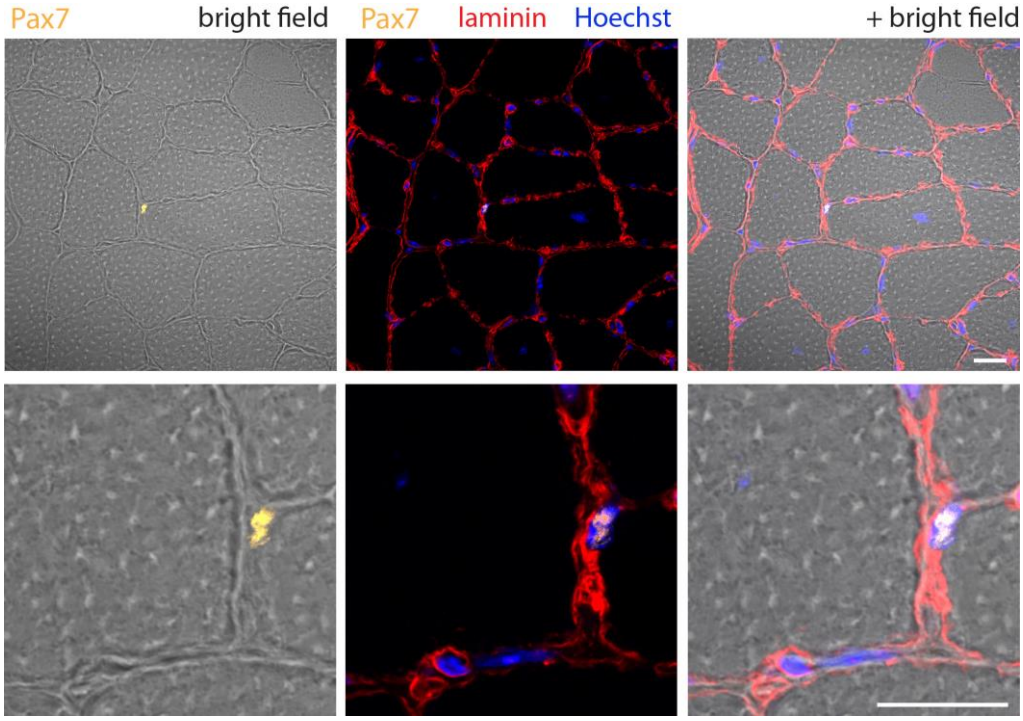

Figure 1. 6: Satellite cell identification in skeletal muscle.

Confocal microscopy images of one cryosection from a Scid/blAJ mouse tibialis anterior muscle immunostained with antibodies against Pax7 (yellow) and laminin (red). Nuclei were counterstained with Hoechst (blue). One satellite cell (yellow) appears adjacent to the myofiber and beneath the basal lamina (red). Scale bars: 20 µm.

The paired box transcription factor Pax7 is the bona fide and unequivocal marker of satellite cells in adult muscle fibers. It is expressed by all satellite cells, both quiescent and activated, of many organisms, including mouse (Seale et al., 2000) and human (Marg et al., 2014; McLoon & Wirtschafter, 2003). Some but not all satellite cells also express Pax3 (Relaix et al., 2006).

Satellite cells constitute only 2-6% of the total nuclei in a muscle fiber. Upon muscle injury, they are activated, exit quiescence and proliferate to regenerate the damaged tissue. This complex, step-by-step process depends on multiple niche factors and intricate crosstalk of signaling pathways (reviewed in (Brack & Rando, 2012; Yin et al., 2013)). During development and regeneration, satellite cells can not only act within their original basal lamina unit but also migrate to other fibers and even muscles (Hughes & Blau, 1990; Watt, Morgan, Clifford, & Partridge, 1987). In the mouse, the pool of quiescent satellite cells that will serve as muscle stem cells during adult life is established around 3 weeks after birth. Until that moment, the pre-

existing pool of progenitors will continue to proliferate extensively and fuse to myofibers during the phase of postnatal muscle growth (Yin et al., 2013).

Once established, the size of the satellite cell pool, in terms of numbers of satellite cells per fiber, remains constant and functional throughout the life of an organism, with their function being impaired only at very old age (Sousa-Victor et al., 2014). Therefore, in addition to generating precursors that eventually differentiate and fuse to myofibers during tissue homeostasis and regeneration, they need to self-renew and return to quiescence in order to ensure the maintenance of the stem cell compartment (Shea et al., 2010). These two functions are achieved via symmetric and asymmetric cell divisions, through which a satellite cell gives rise to two stem cells, or to one stem and one precursor cell, respectively (Conboy, Karasov, & Rando, 2007; Kuang, Kuroda, Le Grand, & Rudnicki, 2007; Shinin, Gayraud-Morel, Gomes, & Tajbakhsh, 2006). Experiments in isolated myofibers have demonstrated that, during these two types of cell division, the orientation of the dividing cells with respect to the longitudinal axis of the fiber varies. During asymmetric divisions, the diving cells are perpendicular to the fiber in an apical-basal orientation (Kuang et al., 2007).

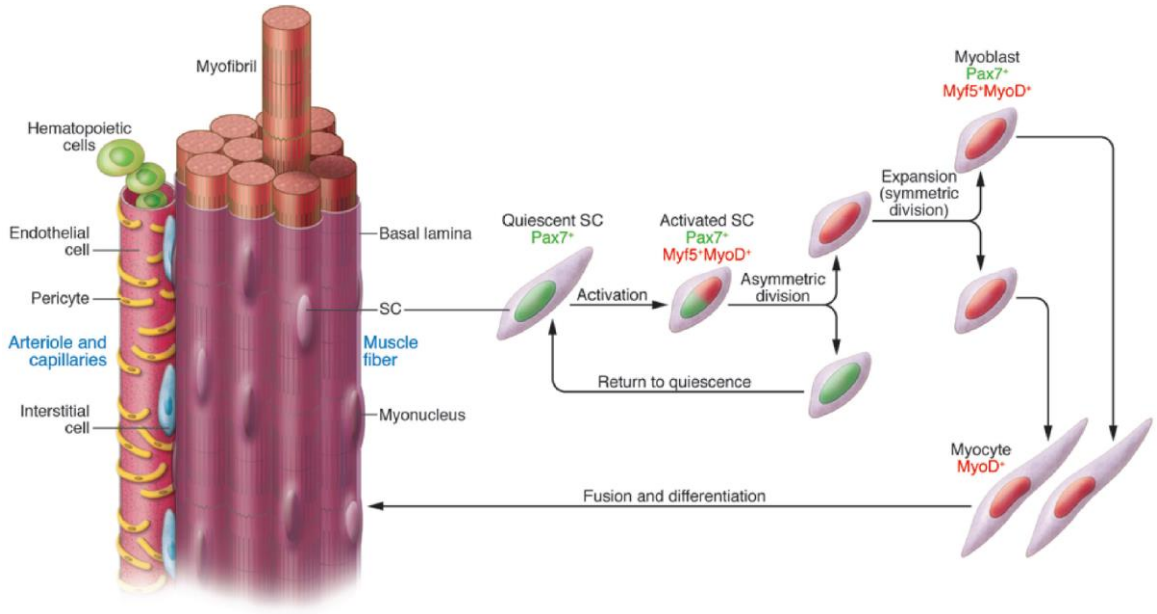

Figure 1. 7: Model of asymmetric divisions during satellite cell activation.

The quiescent satellite cells expressing Pax7 (green) are located underneath the basal lamina that surrounds myofibers. When they are activated and start to proliferate, they express the transcription factors Myf5 and MyoD (red). They divide giving rise to one daughter cell with high Pax7 expression, which returns to quiescence, and one daughter cell that downregulates Pax7 and becomes a committed progenitor, further dividing to generate numerous myoblasts. Those will ultimately exit cell cycle and undergo terminal differentiation, fusing to the fiber in order to provide more myonuclei. Modified from (Tedesco, Dellavalle, Diaz-Manera, Messina, & Cossu, 2010).

A subset of satellite cells expressing higher levels of Pax7 shows non-random segregation of DNA strands during cell division. This occurs possibly to minimize the risk of mutations in the stem cell pool during DNA replication. During asymmetric divisions, they segregate their template, older DNA strands into the daughter cell that will retain high Pax7 expression and eventually return to quiescence and continue to be a stem cell (Conboy et al., 2007; Rocheteau, Gayraud-Morel, Siegl-Cachedenier, Blasco, & Tajbakhsh, 2012; Shinin et al., 2006).

1.3.2 Regenerative potential of transplanted satellite cells

Pax7+ mouse satellite cells with regenerative capacity in transplantation studies have been isolated by mechanically and enzymatically disrupting the skeletal muscle tissue. This is followed by FACS purification using different markers or combinations of them. Some of those are the surface markers CXCR4 and β1 integrin (Cerletti et al., 2008), syndecan-4 (K. K. Tanaka et al., 2009), CD34 and α7 integrin (Sacco, Doyonnas, Kraft, Vitorovic, & Blau, 2008) or VCAM1 (Brohl et al., 2012). Transplantable mouse satellite cells have also been directly isolated by FACS from transgenic mice carrying a Pax3-GFP reporter (Montarras et al., 2005). Mouse myofibers with their associated satellite cells have been isolated through enzymatic tissue digestion and dissection (Rosenblatt, Lunt, Parry, & Partridge, 1995). This method of isolation has enabled intramuscular transplantation of myofiber-associated mouse satellite cells in mice, whereby the grafted cells gave rise to multiple donor-derived satellite cells in the grafted tissue. These cells maintained their regenerative capacity throughout serial transplantations (Collins et al., 2005). Freshly isolated mouse satellite cells suitable for grafting have also been obtained by physically stripping them from myofibers dissected by enzymatic digestion (Boldrin, Neal, Zammit, Muntoni, & Morgan, 2012; Boldrin, Zammit, Muntoni, & Morgan, 2009).

However, enzymatic treatments digest the proteins that form the basal lamina, therefore disrupting the satellite cell niche, which is an essential contributor to the biology of satellite cells. The importance of the niche in maintaining satellite cell quiescence, stemness and regenerative potential is evidence by the fact that satellite cells in culture rapidly downregulate the expression of Pax7 and upregulate markers of differentiation (reviewed in (Briggs & Morgan, 2013)). Loss of stemness in culture results in a much reduced engraftment efficiency of cultured satellite cells in comparison with that of freshly isolated cells (Montarras et al., 2005). This inability for *ex vivo* expansion, together with their availability only in low numbers is a major hurdle in the therapeutic use of satellite cells. Disruption of the lamina also eliminates the possibility to study the biology of satellite cells in their natural microenvironment.

Isolation of human muscle fiber fragments (HMFFs) containing satellite cells in their niche from human muscle biopsies without any enzymatic treatment preserves the basal lamina around the fiber fragment intact. In those conditions, human satellite cells not only maintain their Pax7 expression for prolonged periods of time, but also extensively proliferate. The can give rise to 20-50 times more Pax7 positive cells after 5-10 days before they start to differentiate. Transplantation of HMFFs into the irradiated tibialis anterior muscles of humanized NOG mice demonstrated the robust engraftment capacity and contribution to muscle fibers of these cultured human satellite cells. Therefore, loss of stemness can be circumvented by *ex vivo* culture of satellite cells in their non-disrupted niche (Marg et al., 2014).

Human and mouse satellite cells are known to remain viable in the tissue for several days after the death of an individual. In the tissue devoid of continuous nutrients and oxygen supply, they are presumed to have a selective advantage and enter a deep quiescent state that further enhances their regenerative capacity upon transplantation, demonstrated by their robust engraftment following transplantation into mouse muscle (Latil et al., 2012). Also, in contrast to other non-myogenic cell types contained in muscle biopsies, like fibroblasts, human satellite cells can survive for up to several weeks in biopsy specimens stored at 4°C. This hypothermic treatment (HT) results in almost 100% myogenic cells once fiber fragments are dissected as described previously and put into culture. Moreover, fiber fragments containing satellite cells subjected to this procedure engrafted more efficiently in irradiated NOG muscles and repopulated the satellite cell compartment (Marg et al., 2014). These results are encouraging for the applicability of human satellite cells in muscle regenerative therapies. Specially, the possibility of

long-term storage of biopsy specimens, with its additional benefits, facilitates the handling and transport of biopsies, improving availability in both autologous and allogeneic settings.

However, an unresolved issue in satellite cell therapy is the inability of these cells to transverse the blood vessels and engraft in skeletal muscle if delivered by any ways other than transplantation directly into the muscle (reviewed in (Briggs & Morgan, 2013; Yin et al., 2013)). Therefore, the current expectations for satellite cell transfer include only those conditions where a clinical benefit could be achieved by injecting stem cells into groups of muscles that are sufficiently accessible for this kind of local delivery.

1.3.3 Clinical trials of myoblast transplantation for muscular dystrophy

A number of clinical trials have assessed the safety and efficacy of transplanting allogeneic, *ex vivo* expanded myoblasts in patients affected by DMD or BMD. Unfortunately, the expectations of clinical improvement were not met, and the trials performed so far had limited success in terms of engraftment and reconstitution of dystrophin expression in the grafted muscles (Briggs & Morgan, 2013; Tedesco et al., 2010).

Périé et al. have recently published the results of a 2-year follow-up of a phase I/IIa trial on autologous myoblast transplantation for the treatment of dysphagia in oculopharyngeal muscular dystrophy (OPMD) patients (Perie et al., 2014). In OPMD, only a subset of muscles (extraocular and pharyngeal) is affected. The patients received an intramuscular injection of *ex vivo* expanded myoblasts isolated from their unaffected muscles into the pharyngeal muscles. This resulted in a cell dose-dependent improvement in swallowing. This study is still ongoing under the ClinicalTrials.gov Identifier NCT00773227.

Another phase I/II trial for allogeneic myoblast transfer into the extensor carpi radialis muscle of DMD patients (NCT02196467) is currently in the recruitment phase. Clinical trials using myoblasts have also been conducted for heart failure and stress urinary incontinence (Tedesco et al., 2010).

1.3.4 Contribution of other cell types to skeletal muscle regeneration

Several other cell types have myogenic potential both *in vitro* (when co-cultured with myoblasts, spontaneously or if induced to differentiate by other means) and *in vivo* during development or regeneration (Tedesco et al., 2010; Yin et al., 2013).

However, despite the contribution of other stem cell types to skeletal muscle regeneration naturally or in transplantation studies, satellite cells are essential to adult muscle regeneration. Ablation of Pax7 expressing cells in two independent studies using diphtheria toxin completely abolished muscle regeneration following myotoxin injury. Moreover, transplantation of other cells with known myogenic potential could not rescue the regeneration defect of the muscles devoid of satellite cells (Lepper, Partridge, & Fan, 2011; Sambasivan et al., 2011). This finding is of utmost importance when considering the potential benefits and outcomes of stem cell transfer to treat skeletal muscle disorders.

1.3.4.1 Bone marrow stem cells

Bone marrow-derived cells delivered by systemic of intramuscular injection can engraft and give rise to myonuclei in dystrophic mice following muscle injury. However, their contribution to new myonuclei is reportedly very inefficient (Bittner, Schofer, et al., 1999; Ferrari et al., 1998). Two phase I clinical trials for autologous transplantation of bone marrow-derived mononuclear cells in DMD (NCT02241434) and LGMD (NCT02245711) patients are currently on the recruitment phase.

1.3.4.2 Muscle side population (SP) cells

Muscle SP cells are a heterogeneous population of interstitial cells with myogenic potency *in vitro* and *in vivo* when transplanted into regenerating mouse muscles. They are characterized by the absence of CD45 and c-kit and the expression of Sca-1, ABCG2 and Pax7. Some cells expressing those three markers and additionally syndecan-4 have also been found in sublaminar positions around myofibers. They are thought to be a distinct population of satellite cells (Asakura, Seale, Girgis-Gabardo, & Rudnicki, 2002). They have been shown to engraft and restore expression of dystrophin in irradiated muscles of *mdx* mice following systemic delivery (Gussoni et al., 1999).

1.3.4.3 PW1+ interstitial cells (PICs)

PICs are interstitial cells marked by PW1 expression and found in skeletal muscle. Although they do not originate from Pax3 expressing embryonal progenitors, they are myogenic *in vitro* and *in vivo*. They can give rise to myonuclei and repopulate the satellite cell compartment following transplantation into regenerating mouse muscles (Mitchell et al., 2010). A subpopulation of PICs resident in muscle that expresses PDGFRα has adipogenic instead of myogenic potential (Pannerec, Formicola, Besson, Marazzi, & Sassoon, 2013). PW1 is also expressed in other somatic stem and progenitor cells in mice (Besson et al., 2011), including satellite cells (Pannerec et al., 2013). Expression of PW1 has also been associated with the myogenic potency of mesoangioblasts (Bonfanti et al., 2015).

1.3.4.4 Mesoangioblasts

Mesoangioblasts are large vessel-associated cells that originate from the embryonic dorsal aorta. They can differentiate into several mesodermal tissues like bone, cartilage, smooth, cardiac and skeletal muscle *in vivo* when transplanted into mice. They express CD34, c-Kit and Flk-1 and can be isolated, cultured and expanded for prolonged time periods *in vitro* (De Angelis et al., 1999; Minasi et al., 2002). They are capable of extensive engraftment and muscle regeneration following intramuscular or systemic transplantation into mice (Diaz-Manera et al., 2010; Galvez et al., 2006; Guttinger, Tafi, Battaglia, Coletta, & Cossu, 2006; Sampaolesi et al., 2006; Sampaolesi et al., 2013).

Encouraging preclinical results have been achieved in a mesoangioblast-based gene therapy approach for LGMD2E (caused by mutations in the DGC component α-sarcoglycan). In this study, intra-arterial injection of patient derived mesoangioblasts transduced with a lentiviral vector carrying α-sarcoglycan into α-sarcoglycan$^{-/-}$ mice gave rise to a large number of α-sarcoglycan+ myofibers (Sampaolesi et al., 2003). Dystrophin-null mesoangioblasts have also been genetically engineered to carry a human artificial chromosome (HAC) containing the complete human dystrophin locus with its own regulatory sequence. Systemic transplantation of these corrected mesoangioblasts led to robust engraftment, dystrophin reconstitution and amelioration of the dystrophic phenotype in *mdx* mice (Tedesco et al., 2011).

Owing to their robust regenerative capacity, the possibility of expanding and genetically manipulating them *ex vivo* and their ability to reach many groups of muscles when injected systemically, they hold great promise for cell therapy of skeletal muscle disorders.

1.3.4.5 Pericytes

Similar to mesoangioblasts, they are vessel-associated cells, although pericytes are generally found juxtaposed to small vessels. They are thought to regulate the blood flow in capillaries (Kutcher & Herman, 2009). They can differentiate into adipocytes, chondrocytes, osteoblasts and skeletal muscle cells (Dellavalle et al., 2011; Dellavalle et al., 2007; M. J. Doherty et al., 1998;

Farrington-Rock et al., 2004). Human control pericytes have been shown to engraft as myonuclei or satellite cells following intra-arterial delivery into *scid-mdx* mice. They also restored dystrophin expression in myofibers, leading to a functional phenotypic recovery of dystrophic muscles (Dellavalle et al., 2007). Dystrophin reconstitution in *scid-mdx* mice has also been achieved by transplantation of genetically engineered pericytes obtained from DMD patients and transduced *ex vivo* with a lentiviral vector carrying a human mini-dystrophin transgene (Dellavalle et al., 2007).

1.3.4.6 CD133+ cells (also called AC133)

Human cells with myogenic potential expressing the CD133 surface marker can be found in peripheral blood and in the muscle interstitium. They can be expanded *ex vivo* and participate in muscle regeneration, forming myonuclei when delivered to mouse muscle directly or via the blood circulation (Negroni et al., 2009; Torrente et al., 2004). Alike mesoangioblasts, they could restore dystrophin expression and repopulate the satellite cell compartment following transplantation into *scid-mdx* mice (Torrente et al., 2004).

Ex vivo engineered patient-derived CD133+ cells have also been shown to restore dystrophin expression and promote functional recovery of *scid-mdx* mouse muscles (Benchaouir et al., 2007). A recent study also identified CD133 expressing cells underneath the basal lamina of myofibers in control and dystrophic muscles (Meng et al., 2014). These human muscle-derived CD133+ cells can robustly engraft following transplantation into irradiated and regenerating muscles of severely immunocompromised mice. Moreover, transplanted CD133+ cells generate functional satellite cells capable of giving rise to a large number of donor-derived myofibers after subsequent rounds of muscle injury.

However, as occurs with satellite cells, their *in vivo* myogenic potential is reduced after prolonged *ex vivo* culturing, limiting their availability for therapy (Meng et al., 2014). A phase I clinical trial reported the safety of autologous transplantation of muscle-derived CD133+ cells in DMD patients (reviewed in (Torrente et al., 2007)) but so far no clinical studies have assessed the safety or efficacy of allogeneic or genetically engineered CD133+ cell transfer.

1.3.4.7 ES or iPS-derived myogenic cells

Embryonic stem (ES) cells and induced pluripotent stem (iPS) cells have been used in muscle regeneration studies. Transplantation of either undifferentiated cells or cells previously derived into myogenic-like precursors *in vitro* resulted in functional engraftment in the host mouse muscles (Bhagavati & Xu, 2005; Chang et al., 2009; Darabi, Pan, et al., 2011; Darabi & Perlingeiro, 2014; Darabi, Santos, et al., 2011; Filareto, Darabi, & Perlingeiro, 2012). It is well established, however, that the transplantation of ES or iPS cells without previous differentiation into committed progenitors *in vitro* involves risk of tumorigenesis, as one of the defining characteristics of pluripotent stem cells is their ability to form teratomas *in vivo* (Takahashi et al., 2007; Takahashi & Yamanaka, 2006).

A proof-of-concept preclinical study demonstrated the feasibility of delivering a therapeutic micro-utrophin transgene into iPS cells generated from double dystrophin/utrophin knock-out mice prior to their *in vitro* differentiation into myogenic cells. Intramuscular or systemic transplantation of these genetically modified myogenic cells resulted in very efficient long-term engraftment, repopulation of the satellite cell compartment and transgene expression in myofibers of the grafted animals (Filareto et al., 2013).

1.4 Therapeutic approaches for dysferlinopathy

Extensive efforts have been made to understand the disease and develop feasible therapeutic approaches. Those are evidenced by the substantial increase in the number of publications about dysferlin and dysferlinopathy within the last decade (The Jain Foundation website: http://www.jain-foundation.org/about-us/progress-metrics/number-labs-and-publications).

Unfortunately, however, no effective treatment is available for patients. The recent advances in cell transplantation for skeletal muscle disease and dysfunction, and the clinical translation of some of them, hold great hopes for the treatment of muscular dystrophy. Given that dysferlinopathy is bound to a single causative gene, the advancement of gene therapy has also been regarded as a necessary and promising step in the search for a specific treatment.

1.4.1 Cell transplantation

The first report of cell transplantation with a therapeutic aim into a dysferlin deficient mouse model was by Leriche-Guerin et al. in 2002. They found expression of human dysferlin, recognized specifically by the Ham3/17B2 antibody, in 40–50% of fibers one month after intramuscular transplantation of human myoblasts from healthy donors into SCID mice. The same study reported dysferlin reconstitution in 20–30% of fibers following transplantation of mouse myoblasts expressing β-galactosidase into SJL mice immunosuppressed with FK506 (Leriche-Guerin et al., 2002).

A study published shortly after detected modest engraftment and expression of dysferlin and human-specific dystrophin 12 weeks after intravenous injection of $1*10^6$ human umbilical cord blood (HUCB) derived cells a source of myogenic progenitors into immunosuppressed SJL mice (Kong, Ren, Kraus, Finklestein, & Brown, 2004).

A modest reconstitution of dysferlin protein *in vivo* has been achieved by intramuscular transplantation of mesoangioblasts isolated from adult wild-type mice into the muscles of dysferlin-null Bla/J mice (Diaz-Manera et al., 2010). The donor-derived cells were present in the muscles 36 h and 12 days after grafting albeit surrounded by an inflammatory infiltrate, but were no longer detected 3 weeks after transplantation, probably due to immune rejection. On the contrary, injection of mesoangioblast into muscles or the femoral artery of Scid/blAJ mice resulted in successful engraftment and large areas of donor-derived fibers after one month in all target muscles. Interestingly, cardiotoxin treatment of the host's muscles prior to grafting increased the number of donor-derived fibers. However, the presence of numerous donor-derived fibers only rescued dysferlin protein levels to ~20% of wild-type and did not lead to a significant improvement of locomotor parameters. It did, nevertheless, partially rescue the membrane repair defect of myofibers.

Bone marrow transplantation (BMT) has also been explored as a therapeutic alternative for dysferlinopathy, leading to dysferlin expression in monocytes of transplanted A/J mice. However, BMT failed to restore dysferlin expression in skeletal muscle (Flix et al., 2013).

1.4.2 Gene transfer

Adeno-associated viral (AAV) vectors of various serotypes have been widely used for gene transfer into skeletal muscle due to their natural tropism. However, their packaging size is limited to 4.7 kb. That narrows their utility for delivery of large transgenes, like the coding sequence of many genes mutated in muscular dystrophies. They are also non-integrating vectors and would therefore need to be repeatedly administered (D. Wang, Zhong, Nahid, & Gao, 2014).

The large size of the dysferlin cDNA (6.2 kb) is a hurdle for packaging into viral vectors of widespread use in gene therapy. However, the discovery of a naturally occurring truncated dysferlin protein including the last two C2 and the TM domains with partially retained function (Krahn et al., 2010) raised the possibility of mini-gene transfer using AAV vectors, successfully used for delivery of mini- and micro-dystrophin in DMD models (Jarmin, Kymalainen, Popplewell, & Dickson, 2014). This ~73 kDa protein was found in a female dysferlinopathy patient with late disease onset and mild phenotype totally lacking full-length dysferlin. The patient had a homozygous deletion of exons 2-40 in the dysferlin gene and mRNA. Expression of minidysferlin resulted from usage of a cryptic TSS 22 bp downstream of the native TSS. This enabled rescue of the reading frame and use of the natural stop codon of *DYSF*. Minidysferlin was robustly expressed and localized at the sarcolemma and the T-tubules in muscles of A/J mice following transfer via AAV. Its expression led to a functional rescue of membrane repair in myofibers of AAV-injected muscles (Krahn et al., 2010).

However, it was later shown that expression of minidysferlin in skeletal muscle of dysferlin null B6.A/J-*Dysf*^{prmd} mice, although rescuing the membrane repair deficit in isolated myofibers, does not ameliorate dystrophic features *in vivo*, nor does it protect sarcolemmal integrity from exercise-induced injury. In fact, when expressed at levels higher than those physiological for dysferlin in wild-type muscle, minidysferlin has a detrimental effect, resulting in worsening of the dystrophic features (Lostal et al., 2012). The same study assessed the possibility of therapeutic overexpression of myoferlin in dysferlin deficient skeletal muscle with similar results to those observed for minidysferlin.

AAV vectors are known to undergo intermolecular concatemerization when present episomally in cells. This intrinsic property of AAV vectors has been exploited to deliver transgenes that exceed the cargo size of one vector. This can be achieved either by *trans*-splicing of non-overlapping transgene segments, or by homologous recombination of overlapping 5' and 3'sequences to generate a full-length transgene. Each segment is encapsidated in one vector and following coinfection of one cell with both vectors, the complete transgene is reconstituted (Duan, Yue, & Engelhardt, 2001).

The dual vector strategy has allowed restoration of full-length dysferlin protein in mice via *trans*-splicing or recombination using rAAV2/1 and rAAV2/9 (Lostal et al., 2010), and AAV5 (Grose et al., 2012), respectively. Very recently, a further developed recombination-based dual AAVrh74 vector approach was used to successfully deliver full-length dysferlin into mice and non-human primates. In this study, up to ~90% of myofibers were positive for dysferlin 6 months after intramuscular delivery and ~70% after regional vascular delivery into the lower limbs of 129-Dysf$^{-/-}$ mice. Systemic delivery via the tail vein of Bla/J mice also lead to protein restoration in the tibialis anterior, gastrocnemius, quadriceps, triceps, and diaphragm muscles 3 months after injection. Expression of dysferlin rescued membrane repair in isolated myofibers from treated muscles, in addition to improving specific force of diaphragm muscles of mice subjected to systemic vector delivery. Although dysferlin protein was only detected in the muscles injected with both 5' and 3' vectors, detectable levels of virus were also found in all other tested tissues by PCR amplification of the viral genomes (Sondergaard et al., 2015).

The study also examined the safety of intramuscular injection of dual AAV5 and AAVrh.74 vectors in a small cohort of rhesus macaques. Those were previously confirmed to have low baseline levels of T cells and antibodies against the viral capsid and dysferlin. The treatment resulted in robust overexpression of dysferlin exclusively in the injected muscles after 3 and 6 months. The authors reported absence of histological signs of toxicity or inflammation in the treated muscles and no aberrant responses to the capsid or transgene. These results thus appear

very encouraging for a potential clinical applicability, although repeated administrations of AAV vectors would likely induce an immune response against the viral capsid.

Transfer of full-length dysferlin driven by EF1α promoter into dysferlin deficient myoblasts has been previously performed *in vitro* using a *piggyBac* transposon vector. The myoblasts were derived from human iPS cells of MM patients by directed differentiation via inducible expression of MyoD1. *piggyBac*-mediated delivery lead to detection of dysferlin protein in western blot samples of engineered myotubes, and to rescue of membrane resealing (A. Tanaka et al., 2013).

1.4.3 Combined gene and cell therapy

The efficacy of engineered CD133+ cells for the treatment of dysferlinopathy has also been assessed in a dysferlin deficient mouse model (Meregalli et al., 2013). In the study, blood CD133+ cells from dysferlinopathy patients were transduced with a lentiviral vector carrying the full-length human dysferlin cDNA driven by the human PGK1 promoter. The genetically engineered cells were injected into notexin treated or untreated tibialis anterior muscles of Scid/blAJ mice. Transplantation resulted in ~30% human nuclei per section in notexin treated muscles one month after cell injection and detectable expression of dysferlin mRNA and protein in all injected muscles. However, dysferlin was only found in a patchy distribution in less than 10% of total myofibers. The low number (~40 per section) of dysferlin expressing fibers was attributed to poor engraftment into the muscle compartment or insufficient expression of dysferlin from the donor-derived cells, since transplantation of modified CD133+ cells from healthy individuals yielded similar results (Meregalli et al., 2013). Nevertheless, low levels of dysferlin expression appeared to suffice for a partial rescue of the membrane repair capacity of fibers from transplanted muscles, similar to what was previously reported (Diaz-Manera et al., 2010).

1.4.4 RNA based therapies

Exon skipping in patient derived dysferlinopathic myoblasts led to successful mRNA targeting and removal of dysferlin exon 32, establishing a basis for the further development of therapeutic dysferlin exon skipping approaches (Wein et al., 2010). Those may be applicable to patients with mutations in parts of the protein susceptible to being removed albeit maintaining a protein sequence with preserved functionality, at least partially. However, the usefulness of exon skipping for dysferlinopathy is still to be proven and requires a better understanding of dysferlin protein structure and function. As such, the dispensability of protein modules needs to be addressed in more depth.

Exon skipping by antisense oligonucleotides (AONs) has also been used for restoring proper splicing of *DYSF* in cells from two patients with a point mutation in intron 44 (c.4886+1249 (G>T)) (Dominov et al., 2014). The mutation gave rise to aberrant pre-mRNA splicing and inclusion of a 177 nt sequence between exons 44 and 45 (pseudoexon 44.1, PE44.1), generating an in-frame insertion of 59 additional amino acids within the C2F domain. The insertion was thought to disrupt protein function, since the two patients had only one additional disease causing mutation in the other allele. The use of AONs targeting possible exonic splice enhancer (ESE) sequences of the novel pseudoexon resulted in blocking of the aberrant splicing and production of normal mRNA, increasing dysferlin expression in patient-derived myotubes (Dominov et al., 2014).

Another approach that has successfully been used for dysferlin protein restoration is spliceosome-mediated RNA *trans*-splicing (SmaRT). In a therapeutic context, this method aims to replace the mutated part of the pre-mRNA by manipulating the splicing process. This is achieved

by providing a suitably designed pre-*trans*-splicing molecule (PTM) coding for the corresponding part of the wild-type mature transcript. The PTM is targeted to the endogenous pre-mRNA by a so-called binding domain (BD), complementary to the intron following the mutant exon if a 3' exchange is desired. Using the PTM's splice site, the splicing machinery can replace the endogenous pre-mRNA segment by the PTM-encoded sequence, resulting in a repaired mRNA (Puttaraju, Jamison, Mansfield, Garcia-Blanco, & Mitchell, 1999).

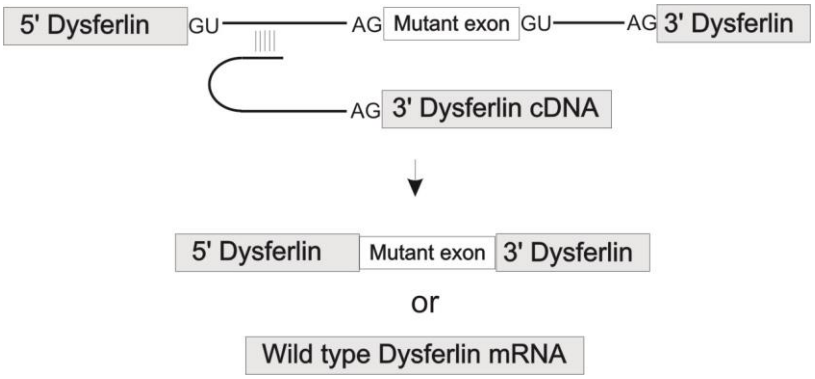

Figure 1. 8: Spliceosome-mediated RNA *trans*-splicing to restore mutated dysferlin mRNA.

A PTM molecule coding for the wild-type 3' moiety of dysferlin is targeted by its BD to an intron of the endogenous dysferlin mRNA upstream of the mutation. The splicing machinery will process the pre-mRNA to produce either the endogenous mature transcript (carrying the mutation) or the SmaRT product, where the 3' moiety of the endogenous mRNA has been exchanged by the PTM molecule thereby restoring the mutation. Courtesy of Dr. Attila Szvetnik.

Using SmaRT, Philippi et al. succeeded to replace the complete 3' moiety of dysferlin mRNA downstream of exons 31 to 37 through exon 55. *Trans*-splicing enabled restoration of dysferlin protein in patient derived myotubes transduced with lentiviral vectors carrying the therapeutic PTMs. It also resulted in protein rescue *in vivo* when the PTMs were delivered via rAAV2/1 into the tibialis anterior muscle of dysferlin-null (B6.129-*Dysf*^{tm1Kcam}/J) mice. However, the protein could only be detected at low levels at the sarcolemma of up to ~6% of fibers in the treated muscles (Philippi et al., 2015).

1.4.5 Relocation of mutated dysferlin

Many dysferlinopathy patients have missense mutations causing protein aggregation and misfolding (Wenzel et al., 2006), formation of amyloid deposits (Spuler et al., 2008), and protein degradation by the endoplasmic reticulum-associated protein degradation machinery (ERAD) (Fujita et al., 2007). Thus, another possible therapeutic avenue is to prevent aggregation and partially restore the correct localization and function of mutated dysferlin. For this purpose, Schoewel et al. used short dysferlin peptides fused at their N-terminus with the transactivator of transcription (TAT) cell-penetrating peptide from the human immunodeficiency virus type 1 to allow transmembrane permeation and cytosolic targeting. Short (10-15mer) peptides with sequence identical to the mutated protein segment and harboring the specific mutations caused a partial re-location of mutated dysferlin from the ER-proximal aggregates to the sarcolemma. This relocation possibly accounts for a functional improvement in membrane repair following sarcolemmal injury in myotubes derived from two patients harboring missense mutations

(Schoewel et al., 2012). These mutations were previously shown to cause dysferlin protein misfolding and aggregation in addition to absence of sarcolemmal dysferlin (Wenzel et al., 2006).

The complete mechanism by which short peptides specifically recapitulating the mutations have a positive effect on mutated dysferlin is still poorly understood. Treatment with the corresponding peptides was shown to result in a downregulation of ER stress markers in the patient-derived myotubes and a release of mutated dysferlin from the aggregates, thereby allowing for a partial relocation to the membrane and functional rescue (Schoewel et al., 2012). The feasibility and effectivity of this approach are yet to be tested *in vivo*.

1.4.6 Rescue of mutated dysferlin from degradation

Some missense mutations in dysferlin render the protein susceptible to proteasomal degradation thereby reducing its cellular levels and, consequently, leading to functional deficits caused by the absence of dysferlin (Azakir, Di Fulvio, Kinter, & Sinnreich, 2012). Augmenting the levels of mutated dysferlin by inhibiting protein degradation has been shown to rescue the membrane repair and fusion deficits in muscle cells derived from patients with the *DYSF* Arg555Trp, Gly426Arg or Gly299Arg missense mutations (Azakir et al., 2012; Azakir, Erne, Di Fulvio, Stirnimann, & Sinnreich, 2014). This showed that the mutant protein, if rescued from degradation, can retain part of its functionality and therefore be exploited as a therapeutic substrate in patients harboring similar mutations.

Those results encouraged an open-label single-arm clinical study evaluating the effect of the FDA–approved proteasome inhibitor bortezomib in dysferlinopathy patients. The study was performed on three 26-30-year old brothers with combined MM and LGMD2B phenotype, homozygous for the *DYSF* Arg555Trp missense mutation and with very low levels of dysferlin protein in muscle. They were administered a single dose of bortezomib by intravenous or subcutaneous injection, both separated by at least 12 days. Both types of administration resulted in an increase in dysferlin expression in muscle and in monocytes, reaching a maximum of ~30% of control levels in muscle at 36 to 48 hours after injection, and decreasing thereafter. The treatment restored sarcolemmal staining of dysferlin as well as membrane repair in cultured patient derived myotubes. The therapeutic effects did not appear to be exclusive to bortezomib, since the *in vitro* results were confirmed with two other newer-generation proteasome inhibitors (Azakir et al., 2014).

1.4.7 Increasing dysferlin expression

The dysferlin promoter contains a vitamin D response element (VDRE) consensus DR3-type sequence (T. T. Wang et al., 2005). Treatment with vitamin D3 increased dysferlin mRNA and protein in a dose-dependent manner in mobilized peripheral blood monocytes (PBM) and myotubes derived from asymptomatic carriers with a single *DYSF* mutation that caused reduced levels of dysferlin (less than 75% of controls). This effect is mediated by two distinct pathways: binding of the vitamin D3 receptor to the dysferlin promoter and activation of MEK/ERK signaling (De Luna et al., 2012). The *in vitro* results were confirmed in an open-label randomized clinical trial, where asymptomatic carriers were treated during one year with orally administered vitamin D3. The treatment resulted in a significant increase in dysferlin expression in PBM after 1 year of follow-up in the D3-treated group. Despite the adverse effects resulting from excessive D3 intake observed in a previous study (Jacobsen, Hronek, Schmidt, & Schilling, 2011), the authors reported no adverse-events as well as normal levels of blood calcium, creatinine, and urea during treatment and follow-up.

However, although no data is available on the administration of vitamin D3 to dysferlinopathy patients, the treatment failed to increase protein levels *in vitro* in patient-derived myotubes lacking expression of dysferlin (De Luna et al., 2012). Thus, vitamin D3 treatment may represent an encouraging alternative for patients with mutations that affect dysferlin protein levels while at least partially retaining protein functionality, or in combination with therapies directed at rescuing the function of mutated dysferlin.

1.5 The *Sleeping Beauty* transposon system

Transposons are mobile DNA sequences that can relocate within the genome through a process called transposition. There are two main classes of transposable elements depending on their molecular mechanism of transposition:

- Class I or retrotransposons operate through a "copy and paste" mechanism. They require an RNA intermediate that is retrotranscribed to generate an additional dsDNA molecule, copy of the original transposon. This new transposon sequence is then inserted into a new position thereby amplifying the number of copies per genome. Retrotransposons account for approximately 42% of the human genome (Lander et al., 2001). Many of them are still actively "jumping" and are a considerable source of inter and intra-individual polymorphisms by generating genomic variability transmittable to the germline or by transposing in somatic tissues (Babatz & Burns, 2013; Carreira, Richardson, & Faulkner, 2014; Richardson, Morell, & Faulkner, 2014; Venter et al., 2001).
- Class II or DNA transposons, on the contrary, operate through a "cut and paste" mechanism that does not require an RNA intermediate. They are directly excised from one genomic location and inserted into another. There are certain mechanisms that allow amplification of DNA transposons during DNA replication or repair but these processes are very infrequent. DNA transposons have come to form about 3% of the human genome but they are inactive (Lander et al., 2001).

Sleeping Beauty (SB) is a DNA transposon member of the Tc1/mariner family and originates from fish genomes. It was reactivated through molecular reconstruction based on the alignment of fossil sequences of the salmonid transposon subfamily that had been inactivated throughout evolution via accumulation of mutations. The reconstructed sequence showed for the first time active jumping of a DNA transposon in contemporary mammalian genomes (Ivics, Hackett, Plasterk, & Izsvak, 1997). After the reactivation of SB in 1997, several other DNA transposons were similarly reconstructed and shown to be transposition-competent in vertebrate genomes, like the *Frog Prince* (Miskey, Izsvak, Plasterk, & Ivics, 2003), *harbinger* (Sinzelle et al., 2008), *TcBuster* and SPIN(ON) elements (Li et al., 2013).

The structure of SB in its native conformation consists of two inverted terminal repeats (ITRs) at both ends of the transposon sequence, each containing two binding sites for the transposase. The two ITRs flank an ORF that encodes the transposase protein, whose expression is driven by its own regulatory sequence (Ivics et al., 1997).

However, the transposon and transposase can be separated, providing a flexible genetic tool that allows delivery of engineered transposon sequences from a DNA vector, most frequently a plasmid, into the target genome. In this configuration, the SB transposase can mobilize any sequence of interest that is flanked by the transposon ITRs (Grabundzija, Izsvak, & Ivics, 2011;

Ivics et al., 1997). The transposase can be provided in *trans* as an expression vector, mRNA or recombinant protein.

Since SB was developed, both transposon and transposase have been subject to modifications in order to enhance their activity (Baus, Liu, Heggestad, Sanz, & Fletcher, 2005; Zayed, Izsvak, Walisko, & Ivics, 2004). The most active variant of the transposase is SB100X, generated through a mutational screen on the original SB transposase (Mates et al., 2009). SB100X is highly active in gene transfer in numerous somatic and stem or progenitor cell types (Mates et al., 2009; Xue et al., 2009).

In addition to SB, the DNA transposon *piggyBac*, derived from the cabbage looper moth *Trichoplusia ni*, is also capable of highly efficient gene transfer in human cells (J. E. Doherty et al., 2012; Grabundzija et al., 2010; X. Huang et al., 2010) and has been widely exploited as a genome manipulation tool (Di Matteo et al., 2012).

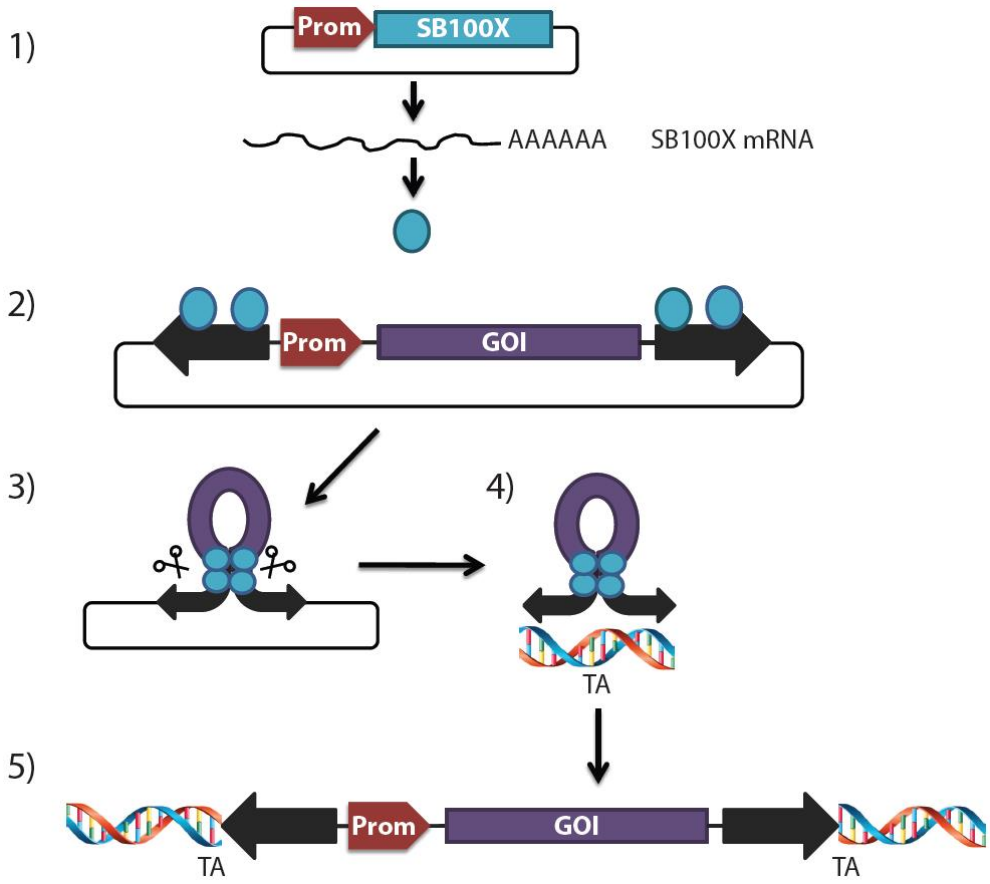

Figure 1. 9: Mechanism of transposition of SB in a *trans* configuration.

When both components of the system are introduced into a cell and the transposase is expressed (1), it is able to recognize and bind the ITRs of the transposon sequence (2). It then catalyzes the excision of the transposon carrying the gene of interest (GOI) from its donor location (3), most frequently a plasmid for gene transfer applications, and it mediates its integration into the target genome (4). Most transposases of the Tc1/mariner superfamily, including SB and its hyperactive variant SB100X, integrate transposon cassettes into TA dinucleotides generating a target site duplication upon insertion (5).

1.5.1 SB in gene therapy

The SB system has been widely used for delivery of therapeutic transgenes in a variety of preclinical models and is currently being used in clinical trials for cancer immunotherapy and age-related macular degeneration (AMD).

1.5.1.1 Preclinical studies using *ex vivo* gene transfer with SB

SB has been tested for gene therapy of Huntington disease, where delivery of transposons encoding siRNA molecules successfully reduced the levels of huntingtin in cultured human cells (Chen, Kren, Wong, Low, & Steer, 2005). Transfer of the Fanconi anemia complementation group C (FAC) gene into patient-derived lymphoblastoid cells using SB vectors resulted in correction of the DNA repair defects characteristic of FAC deficiency and provided a proof-of-concept for gene therapy of Fanconi anemia type C using SB (Hyland et al., 2011). *Ex vivo* gene therapy of sickle cell anemia (SCA) via transfer of a therapeutic β-Globin transgene into bone-marrow derived hematopoietic stem cells (HSCs) from a SCA patient resulted in a decrease of sickling in mature red blood cells derived in vitro from HSCs (Sjeklocha, Wong, Belcher, Vercellotti, & Steer, 2013).

SB has also been used in proof-of-concept studies for *ex vivo* gene therapy of muscular dystrophies. Conditionally immortalized mouse myoblasts from dystrophin deficient mice were stably transfected with a SB vector carrying a micro-dystrophin transgene. However, intramuscular transplantation of these engineered myoblasts into a mouse of model of dystrophinopathy (*mdx nu/nu*) resulted only in a moderate engraftment and expression of micro-dystrophin in myofibers of grafted muscles (Muses, Morgan, & Wells, 2011b). Much better *in vivo* results were achieved through SB-mediated delivery of a micro-utrophin transgene into iPS cells derived from a utrophin/dystrophin double knock-out (dKO) mouse line. Those were subsequently differentiated *in vitro* into myogenic progenitors by transiently induced expression of Pax3. The corrected cells were capable of engraftment and micro-utrophin expression in myofibers following both intramuscular and intravenous injection into dKO mice. Expression of micro-utrophin was also sufficient to restore the formation of the DGC in donor-derived myofibers and the treated muscles showed improved force parameters (Filareto et al., 2013).

Gene therapy not only includes transfer or repair of defective genes but also introduction of transgenes that protect against disorders, like for example conferring resistance to tumors. Human primary peripheral blood and umbilical cord blood T cells engineered to carry a chimeric antigen receptor (CAR) for human CD19 and CD20 were effective in lysing CD19+ leukemia and lymphoma cells *in vitro* and reduced tumor growth following grafting into pre-irradiated NOD/SCID mice (X. Huang et al., 2008).

1.5.1.2 SB-mediated gene transfer *in vivo*

In vivo gene transfer of fumarylacetoacetate hydrolase (FAH) with SB vectors through hydrodynamic tail vein injections has proven successful in restoring FAH function in the liver and correcting the phenotype of mouse models of tyrosinemia type 1, a lethal liver disease (Montini et al., 2002; Pan, Ma, Zhang, Fan, & Li, 2012; Wilber et al., 2007). *In vivo* SB-mediated gene delivery of human beta-glucuronidase or alpha-L-iduronidase in mouse models of mucopolysaccharidosis types I and VII has also resulted in phenotypic correction (Aronovich et al., 2007; Aronovich et al., 2009).

SB-based *in vivo* delivery of coagulation factor VIII (FVIII) through hydrodynamic tail vein injections resulted in phenotype amelioration in mouse models of hemophilia A (Kren et al., 2009; L. Liu, Mah, & Fletcher, 2006; Ohlfest et al., 2005).

Coupling of SB-based vectors with nanoparticles or with viral platforms has been exploited in order to enhance the efficiency of *in vivo* delivery. Selective targeting of distinct cell types in the liver via intravenously delivered ligand-coated nanocapsules carrying therapeutic SB vectors restored expression of FVIII specifically in liver sinusoidal endothelial cells of hemophilia A mice and resulted in partial phenotypic recovery (Kren et al., 2009).

Transfer of FVIII into the liver of mouse (Hausl et al., 2010; Yant et al., 2000) and dog (Hausl et al., 2010) models of hemophilia B has also been achieved by coupling the therapeutic SB transposon cassettes with adenoviral vectors. The coupling with viruses facilitates cell entry in systemic delivery approaches. The hybrid vectors benefit from the tropism of the viral capsid but maintain the genomic integration profile of SB transposon. Some other examples of the use of SB transposon vectors in combination with viral vectors include coupling with integrase-defective lentiviral vectors (Moldt et al., 2011; Staunstrup et al., 2009; Vink et al., 2009), baculovirus (Luo et al., 2012; Turunen, Laakkonen, Alasaarela, Airenne, & Yla-Herttuala, 2014) and additional studies using adenovirus (Yant et al., 2002; Zhang, Muck-Hausl, et al., 2013; Zhang, Solanki, et al., 2013). SB transposon cassettes have also been combined with the minicircle technology for production of bacterial-backbone free DNA vectors by recombination (Sharma et al., 2013).

1.5.1.3 Clinical trials using SB

The first clinical trials using SB transposon were initiated in the USA at the MD Anderson Cancer Center in Houston, Texas (Williams, 2008), focusing on adoptive T-cell immunotherapy for cancer. They are based on the delivery of CARs against CD19 into peripheral blood mononuclear cells (PBMCs) from cancer patients in order to prompt recognition and cytotoxicity against CD19+ malignant B cells. The first patients have already been treated with an autologous transplant of modified tumor-specific T cells expressing a CD19-directed CAR (Kebriaei et al., 2012). This study is currently underway and the results are expected with great excitement.

SB mediated transfer of pigment epithelium-derived factor (PEDF) into retinal and iris pigment epithelial cells *in vitro* enabled long-term expression and secretion of PEDF (Johnen et al., 2012). These results stablished a basis for a current gene therapy clinical trial coordinated by the European consortium TargetAMD. This trial aims to use *ex vivo* SB-mediated gene transfer of PEDF to treat the exudative form of age-related macular degeneration (AMD). In this disease, a neovascularization of the choroid results in damage to the retinal pigment epithelium (RPE) cell layer in the eye, ultimately causing death of the photoreceptor cells and blindness. PEDF is an anti-angiogenic molecule naturally secreted by RPE cells that prevents blood vessel growth. Increased expression of PEDF therefore protects against choroidal neovascularization and provides a treatment alternative for AMD patients. Although RPE cells in AMD patients are already damaged, iris pigment epithelial (IPE) cells are viable and much more abundant and accessible. They are functionally similar to RPE cells and can be transplanted in the subretinal space, where they can form a monolayer and functionally substitute for damaged or lost RPE cells. IPE cells will be extracted from the patients' iris, nucleofected with a SB vector to stably transfer PEDF and re-implanted into the subretinal space within the same surgery.

1.5.1.4 Biosafety of SB for gene therapy

Gene therapy clinical trials based on transfer of autologous HSC engineered *ex vivo* with retroviral vectors have resulted in the development of leukemia due to insertional oncogenesis in X-linked severe combined immunodeficiency (SCID-X1) (Deichmann et al., 2007; Hacein-Bey-Abina et al., 2008; Hacein-Bey-Abina et al., 2003; Howe et al., 2008), chronic granulomatous

disease (CGD) (Stein et al., 2010) and Wiskott-Aldrich syndrome (WAS) patients (Braun et al., 2014).

Retroviral vector integrations causing *trans*-activation of proto-oncogenes in the engineered HSCs due to the non-random vector insertion pattern (Deichmann et al., 2007; Schwarzwaelder et al., 2007) and the high activity of the retroviral enhancer elements (Howe et al., 2008) were the cause of the adverse events, which resulted in the death of some patients. On the other hand, some patients were successfully treated from the hematopoietic malignancies and recovered from the underlying genetic disorders thanks to the HSC gene therapy treatment (Hacein-Bey-Abina et al., 2008).

Clinical trials of autologous HSC-gene therapy using newer generation gamma-retroviral and lentiviral vectors with lower enhancer activity have so far resulted in much better outcomes regarding vector genotoxicity in WAS (Aiuti et al., 2013), metachromatic leukodystrophy (Biffi et al., 2013) and SCID-X1 patients (Hacein-Bey-Abina et al., 2014), although long-term studies on leukemogenesis still need to follow.

Opposite to HSC-gene therapy trials using early generation retroviral vectors, clinical trials for adoptive cancer immunotherapy based on viral-mediated gene transfer into T cells have not resulted in oncogenic transformation (June, Blazar, & Riley, 2009). This is likely due to the fact that, in contrast to HSC, which need to repopulate multiple hematopoietic lineages upon engraftment, mature T cells are non-dividing and thus probably resistant to transformation (Cattoglio et al., 2010; Newrzela et al., 2008; Recchia et al., 2006).

It is therefore clear that, besides efficacy, biosafety considerations regarding genotoxicity are of utmost importance in the design and selection of appropriate vectors for each kind of gene therapy scenario. In addition, minimizing the risks is desirable for any trial.

In this regard, SB benefits from a very close-to-random genomic integration profile and does not preferentially integrate into transcriptionally active sites, coding regions or regulatory regions of genes. It is therefore less prone to induce genotoxicity in comparison to integrating viral vectors (e.g. HIV-derived lentivirus, MLV or retrovirus) or other transposon systems like *piggyBac* (X. Huang et al., 2010; Moldt et al., 2011; Staunstrup et al., 2009; Vigdal, Kaufman, Izsvak, Voytas, & Ivics, 2002; Yant et al., 2005; Zhang, Muck-Hausl, et al., 2013). That makes SB safer than all other integrating vectors currently used for therapeutic gene transfer. It is also important to note that SB derived from fish genomes and is evolutionarily very different from human Tc1/mariner elements. SB transposase proteins do not bind class II transposon sequences in the human genome (reviewed in (Hackett, Largaespada, Switzer, & Cooper, 2013)). Furthermore, SB ITRs have very little enhancer/promoter activity and are thus unlikely to coax *trans*-activation of nearby transcriptional units by themselves (Dalsgaard et al., 2009; Walisko et al., 2008).

It may seem paradoxical that SB has also been used for somatic mutagenesis screens in mice in order to find candidate cancer genes. However, those studies have used genetically predisposed mouse lines harboring underlying cooperative mutations. Alternatively, multi-copy transposon insertions have been used to produce multiple genetic alterations in the same cell upon transposon re-mobilization. Also, the transposon cassettes used for mutagenesis screens were specifically designed to induce oncogenic transformation upon insertion into host genes (Hackett et al., 2013)

Nevertheless, the risk of genotoxicity cannot be completely eliminated when using non-targeted transgene integrations. Obviously, the ideal scenario for gene therapy is the targeted correction of mutations in the endogenous gene using site specific nucleases in combination with homology directed DNA repair (HDR). The realization of gene editing as a feasible treatment alternative is a topic of intense investigation and new technological developments in the last years

have brought into picture a large number of applications in gene therapy. However, safety issues regarding especially off-target events, which could result in the disruption of undesirable loci, are still an important concern and need to be addressed before clinical trials are earnestly contemplated.

1.5.1.5 Cargo capacity, cost-effectiveness and transgene silencing

Although large transgenes are delivered less efficiently (Izsvak, Ivics, & Plasterk, 2000; Swierczek, Izsvak, & Ivics, 2012) no upper size limit has been established for SB system. It has been used to deliver sequences of up to ~100 kb when combined with bacterial artificial chromosomes (BACs) for human ES cell transgenesis (Rostovskaya et al., 2012).

Unlike transgenes contained within some viral long terminal repeats (LTRs) that are rapidly subject to silencing upon integration, the SB transposon ITRs do not trigger transgene silencing following genomic insertion. Silencing events can nevertheless occur and are influenced by the site of insertion and the cargo sequence. The latter can be prevented by careful cassette design and avoidance of viral promoters/enhancers (Garrison, Yant, Mikkelsen, & Kay, 2007).

Last, regarding large-scale production of clinical-grade vectors, SB has the advantage of being a plasmid-based system. Therefore the lower manufacturing costs and production time as well as the higher certainty about lot homogeneity likely represent an important advantage against the manufacture of clinical-grade viral vectors.

2 Aim of the study

We sought to develop an *ex vivo* cell-based gene therapy approach to treat dysferlinopathy using a non-viral vector system for full-length dysferlin transfer. We selected SB transposon as a gene delivery tool due to its biosafety features and gene transfer efficacy. Our concrete goal was to restore dysferlin expression in dysferlin-deficient mouse myoblasts *ex vivo* and to transplant them into a mouse model of dysferlinopathy in order to reconstitute the protein in skeletal muscle *in vivo*.

We also aimed to investigate culture models that would enable the *ex vivo* expansion and genetic manipulation of human satellite cells in order to render them flexible and effective for cell-based gene therapies in patients.

3 Materials and Methods

3.1 List of antibodies

Antibody	Species	Company	Cat. No.	Stock conc.	Working dilution
dysferlin C-terminus	mouse (monoclonal)	Novocastra	NCL-Hamlet	180 µg/ml	1:1000 WB
dysferlin N-terminus	rabbit (monoclonal)	abcam	ab124684	0.5 mg/ml	1:200 IF cells / 1:100 tissue
fast MyHC	mouse (monoclonal)	Novocastra	NCL-MHCf	n.s.	1:500 WB
PAN-actin	mouse (monoclonal)	Dianova	DLN-07272	200 ug/ml	1:2000 WB
alpha-tubulin	mouse (monoclonal)	Sigma-Aldrich	T5168	-	1:3000 WB
Pax7	mouse (monoclonal)	DSHB	PAX7	SN, 1:1 glycerol	1:10 IF tissue
laminin	rabbit (polyclonal)	Sigma-Aldrich	L9393	0.69 mg/ml	1:200 IF tissue
human Lamin A/C	rabbit (monoclonal)	Epitomics	ab 108595	-	1:2000 IF tissue
anti-mouse-HRP	goat (polyclonal)	Thermo Scientific	31432	0.8 mg/ml	1:5000 WB
anti-rabbit-HRP	goat (polyclonal)	Thermo Scientific	31462	0.8 mg/ml	1:5000 WB
anti-mouse-IRDye800	donkey (polyclonal)	Rockland Immunochemicals	610-732-124	1 mg/ml	1:5000 WB
anti-rabbit-Cy3™	donkey (polyclonal)	Jackson Immunoresearch	711-165-152	1.5 mg/ml	1:500 IF
anti-mouse-AlexaFluor®555	donkey (polyclonal)	life technologies	A31570	2 mg/ml	1:500 IF
anti-rabbit-AlexaFluor®647	donkey (polyclonal)	life technologies	A31573	2 mg/ml	1:500 IF

Western blot (WB), immunofluorescence (IF), supernatant (SN).

3.2 Plasmid vectors & cloning

The SB100X expression vector was previously described (Mates et al., 2009). The pT2-CAG-GFP and pT2-EF1α-GFP were available in the laboratory. The SB-based reporter vector pT2-CAG-IRES-GFP (pLICU1) (map in page 89) was kindly provided by Angélica García Pérez, (laboratory of Dr. Zsuzsanna Izsvák).

The SB-based reporter vectors for assaying promoter activities in H2K A/J myoblasts were constructed as follows: for cloning of pT2-Spc5-12-GFP, the Spc5-12 promoter sequence (Li, Eastman, Schwartz, & Draghia-Akli, 1999) was extracted from pAAV-Spc5-12-huDys-co (map in page 89, kindly provided by Prof. George Dickson, Royal Holloway, University of London, UK) with XbaI. It was later inserted into pT2-CAG-GFP previously digested with SpeI + NheI in order to remove the CAG promoter and isolate the fragment containing the plasmid backbone with the SB ITRs and the GFP CDS + poly(A) signal.

For cloning of pT2-SV40-GFP, the SV40 promoter sequence was extracted from pGEM-T-SV40 (plasmid map in page 89) (kindly provided by Julia Rugor, laboratory of Dr. Zsuzsanna Izsvák) with EagI + NheI. The 256 bp fragment was inserted into pT2-CAG-GFP previously digested with NotI + NheI in order to remove the CAG promoter.

The SB-based vectors for full-length dysferlin transfer were constructed as follows: for cloning of pT2-2Spc5-12-hDYSF_v1-GFP, the *hDYSF_v1* coding sequence (accession #DQ267935) was extracted from the pDONR221:15803 plasmid (provided by The Jain Foundation) with SpeI + NotI and cloned into an empty transposon-based plasmid (containing the SB ITRs) previously digested with XbaI + NotI (resulting vector - pT2-hDYSF_v1). The Spc5-12 promoter sequence was extracted from pAAV-Spc5-12-huDys-co with XbaI. Two copies of the ~400 bp sequence were inserted in tandem in a 5' to 3' orientation into pT2-hDYSF_v1 digested with SpeI (resulting vector - pT2-2Spc5-12-hDYSF_v1). The IRES-GFP-poly(A) sequence was PCR-amplified from pLICU1 with Pfu Ultra II Fusion DNA polymerase (Agilent) using the forward 5'-ATCTGCGGCCGCTAGCCAATTCCGCCCCTC-3' and reverse 5'-TCTTGCGG-CCGCTGTACAACTAGTCGATCCCTCTTAAGTACCAC-3' primers. The resulting PCR fragment was digested with NotI and inserted into pT2-Spc5-12-hDYSF_v1 previously digested with NotI.

For cloning of pT2-Spc5-12-hDYSF_v1-GFP, the Spc5-12 promoter was extracted from pAAV-Spc5-12-huDys-co with XbaI and a single copy of the sequence was inserted into pT2-hDYSF_v1 (resulting vector - pT2-Spc5-12-hDYSF_v1). The sequence containing the single Spc5-12 promoter and the 5' region of *hDYSF_v1* was extracted from pT2-Spc5-12-hDYSF_v1 with EcoRV + XbaI. The ~4.6 kb fragment was inserted into pT2-2Spc5-12-hDYSF_v1-GFP, which had been previously digested with EcoRV + XbaI in order to remove the matching sequence containing the double Spc5-12 promoter.

For cloning of pT2-Spc5-12-hDYSF_c-GFP, the 5' region of *hDYSF_c* was extracted from the pDONR221:15803 plasmid (kindly provided by The Jain Foundation) containing the *hDYSF_c* (original) transcript variant (accession #NM_003494*). The resulting 643 bp fragment was inserted into pT2-Spc5-12-hDYSF_v1-GFP previously digested with PmeI + XbaI in order to remove the 5' region of *hDYSF_v1*.

3.3 Cell culture

H2K A/J and control (wt) myoblasts (Cohen et al., 2012) were kindly provided by Dr. Terence Partridge, from the Children's National Medical Center, Washington DC, USA. Primary human myoblasts were obtained from the laboratory of Prof. Simone Spuler. If not stated otherwise, cells were cultured in a humidified CO_2 incubator at 37°C with 5% CO_2.

3.3.1 Culture and differentiation of H2K myogenic cells

H2K myoblasts were cultured on dishes coated with 0.1% gelatin from porcine skin (Sigma-Aldrich) diluted in sterile PBS. For coating, enough gelatin was poured onto the dish in order to

cover the entire surface. The gelatin-containing plates were incubated at 33°C for at least 30 min. After this time, the excess of gelatin was removed by aspiration and the media and cells were immediately added to the dish. H2K myoblasts were routinely tested for mycoplasma by PCR as described in (Young, Sung, Stacey, & Masters, 2010) and all experiments shown here were done with mycoplasma-free cells.

To allow proliferation, H2K myoblasts were cultured at 33°C and 10% CO_2 in Dulbecco's Modified Eagle's Medium (DMEM) with 4.5g/L D-Glucose, GlutaMAX™ and pyruvate (Gibco™, life technologies) containing 1x Antibiotic-Antimycotic (Gibco™, life technologies), 20% fetal calf serum (FCS, PAA), 2% chick embryo extract (CEE, US Biological, C3999) and 200 U/ml of γ-interferon (Merck Millipore, IF005). Cells were passaged every 2-3 days using 0.05% trypsin-EDTA (Gibco™, life technologies) and were not allowed to reach a confluence higher than 70% to avoid differentiation. For maintenance of H2K myoblasts in proliferative conditions, all culture steps, including trypsinization, were performed at 33°C.

For differentiation, cells were cultured and passaged for 7 days at 37°C and 5% CO_2 in proliferation media without γ-interferon. For differentiation, the media was switched to DMEM containing 1x Antibiotic-Antimycotic, 5% horse serum (HS, Gibco™, life technologies) and 2% CEE.

3.3.2 Transfection of H2K A/J myoblasts

H2K A/J myoblasts were transfected with a Neon® Transfection System (life technologies) in sterile conditions. For determining the optimal electroporation settings, the Neon® 24-well optimization protocol was used first. The protocols number 6 (1100 mV, 30 ms, 1 pulse) and 19 (1050 mV, 30 ms, 2 pulses) were selected due to their optimal ratio between transfection efficiency and cell viability and were used for assaying the activity of various promoters in H2K A/J myoblasts (Figure 4. 1). Afterwards, all experiments were performed with protocol number 19 (1050 mV, 30 ms, 2 pulses). For electroporation, cells were washed with PBS, detached with trypsin, collected in DMEM media containing 20% FCS and counted. They were centrifuged and resuspended in PBS for a second wash in order to remove all traces of media. They were aliquoted in sterile tubes according to the number of cells needed for each transfection (each sample was transfected with the corresponding plasmid or mix of plasmids) and were centrifuged again. They were resuspended in buffer R (Neon® Transfection System, life technologies) containing plasmid DNA and electroporated according to the manufacturer's instructions. Immediately after electroporation, cells were plated in gelatin-coated dishes containing H2K myoblast proliferation media.

3.3.3 Routine flow cytometry

Routine flow cytometry to monitor expression of GFP was performed using a FACSCalibur™ flow cytometer (BD Biosciences) using appropriate settings to detect GFP. When the measurements were performed in different days, the instrument settings needed to be modified slightly to optimally adapt to the analyzed cell populations. However, when a comparison is shown (e.g. percentage and mean fluorescence intensity at day 2 post-transfection in Figure 4. 1 or percentage of GFP expressing cells at day 3 and at day 11 in Figure 4. 4) the measurements were obtained in the same day with the exact same settings. Analysis of the flow cytometry data was performed with the Cellquest Pro™ (BD Biosciences) and FlowJo softwares.

3.3.4 Sorting of stably transfected H2K A/J myoblasts

Sorting of GFP expressing H2K A/J myoblasts was done with a FACSAria™ flow cytometer (BD Biosciences). Pre-sorting cell preparation was done under sterile conditions. Sorting was performed in non-sterile conditions since a sterility-compatible cell sorting station was not available at the institute. For sorting, the cells were washed with PBS, trypsinized and collected in DMEM containing 20% FCS. They were centrifuged and resuspended in PBS containing 2% FCS and 100 µg/ml Primocin™ (InvivoGen) to avoid contamination by Gram+ and Gram- bacteria, mycoplasmas and fungi. After sorting, they were collected in DMEM containing 20% FCS and 100 µg/ml Primocin™. They were kept on ice until plating. For at least three days after sorting, they were cultured in proliferation media containing 100 µg/ml Primocin™ instead of 1x Antibiotic-Antimycotic.

3.3.5 Human muscle biopsies

Muscle biopsies were obtained during hip surgery from individuals without neuromuscular disorders or for diagnostic purposes after due approval by the Charité Internal Review Board. The skeletal muscle tissue was dissected and transferred into solution A (30 mM HEPES, 130 mM NaCl, 3 mM KCl, 10 mM d-glucose, and 3.2 µM Phenol red) for storage at 4°C until isolation of HMFFs or primary myoblasts was performed.

3.3.6 Culture and differentiation of human primary myoblasts

Primary human myoblasts were isolated and purified in the laboratory of Prof. Simone Spuler as described previously (Schoewel et al., 2012). The muscle biopsy specimens were minced and subsequently digested in a solution containing 254 U/ml Collagenase CLS II (Biochrom AG), 100 U/ml Dispase II (Roche) and trypsin/EDTA at 37°C for 45 minutes. Cells were grown in skeletal muscle growth medium (SMGM, Promocell) supplemented with 10% FCS (Lonza), 2.72 mM GlutaMAX™ and gentamicin (400 µg/ml) (Gibco™, life technologies). Myoblasts were purified using anti-CD56 ab-coated magnetic beads (Miltenyi Biotech). Differentiation into myotubes was induced in DMEM containing 2% horse serum.

3.3.7 Isolation and culture of HMFFs

HMFFs were prepared in the laboratory of Prof. Simone Spuler as described in (Marg et al., 2014). Muscle biopsy specimens were mechanically dissected using miniature forceps under a stereomicroscope (Leica Microsystems) and carefully loosened to obtain bundles of fibers or single fibers. Those were cut with miniature scissors to obtain HMFFS of ~3 mm in length. HMFFs were cultured on ibiTreat 8-well µ-Slides (ibidi, 80826) in SMGM supplemented as described in 3.3.3.

3.3.8 Transfection of HMFFs

HMFFs were co-transfected with 900 ng of a GFP reporter SB transposon-based vector (pT2-CAG-GFP) and 90 ng of an expression vector for SB100X in SMGM. The plasmids were diluted in 100 µl Opti-MEM® (Gibco™, life technologies) and 3 µl X-tremeGENE™ HP transfection reagent (Roche). The mix was incubated for 25 minutes at R.T., mixed well and added to the HMFFs on a 12-well culture dish. The medium was replaced by fresh SMGM 24 h after transfection. Images of the transfected fiber fragments shown in Figure 4. 24 were taken 2 and 7 days after transfection.

3.4 SDS-page and immunoblot

For protein purification, cells were plated on 6-well plates. Prior to or after differentiation into myotubes, they were lysed on ice with RIPA buffer (50 mM Tris-HCl, 150 mM NaCl, 0.1% NP-40, 0.1% SDS, 0.1% sodium deoxycholate and protease inhibitors). The protein concentration was determined using a BCA Protein Assay Kit™ (Pierce) and following the standard protocol according to the manufacturer's instructions. For each sample, 10 µg of protein diluted in sample buffer (0.25 M Tris-HCl, 50% Glycerol, 5% SDS, 0.05% bromophenol blue and 10% freshly added β-mercaptoethanol) were loaded onto an 8% poly-acrylamide gel. Proteins were separated in denaturing conditions and transferred to a PVDF membrane using a wet electroblotting system (Bio-Rad) in Tris-glycine buffer containing 10% methanol and 0.1% SDS. Following transfer, the membrane was incubated for 1 h at R.T. in TBST solution containing 5% dry milk powder (blocking buffer). After blocking, the membrane was incubated with the corresponding primary antibodies diluted in blocking buffer (anti-dysferlin NCL-Hamlet, 1:1000, overnight at 4°C / anti-fast MyHC 1:500, 1 h at R.T. / anti-PAN-actin 1:2000, 1 h at R.T.). Three washes of 10 min with TBST were performed after incubation with the primary antibody. Incubation with horse radish peroxidase (HRP)-conjugated secondary antibodies against mouse IgG (Thermo Scientific, 31432) and rabbit IgG (Thermo Scientific, 31462) diluted 1:5000 in blocking buffer was performed at R.T. for 1 h. Afterwards, the membrane was washed 5 times as described previously, incubated with Amersham™ ECL™ Prime Western Blotting Detection Reagent (GE Healthcare, RPN2232) for 5 min and imaged using a STELLA 3200 system (Raytest). Images were processed using Adobe Photoshop CS5. Modifications were applied to the full image (all the lanes). Since the molecular weight of dysferlin and fast MyHC is very similar (237 kDa and 223 kDa, respectively), immunolabeling with the anti-fast MyHC antibody was done following incubation of the membrane with stripping buffer (60 mM Tris-HCl, 2% SDS and 0.7% β-mercaptoethanol) for 30 minutes at 60°C and re-blocking (Figure 4. 6-A).

The western blot in Figure 4. 6–B was performed using a gradient 8-16% Tris-Glycine Gel (life technologies EC60485BOX). Transfer was done onto a nitrocellulose membrane using a semi-dry electroblotting instrument (BioRad) for 45 min at 18 V. The membrane was incubated overnight at 4°C with primary antibodies against dysferlin (NCL-Hamlet, 1:500) and alpha-tubulin (Sigma-Adrich T5168, 1:3000) diluted in blocking buffer. The membrane was incubated 1 h at R.T. with a secondary antibody against mouse IgG labelled with IRDye800 (Rockland Immunochemicals 610-732-124). It was developed with a chemiluminescence western blot imager (LI-COR).

3.5 Mouse experiments

B6.Cg-*Dysf*^{prmd}*Prkdc*^{scid}/J (Scid/blAJ) mice homozygous for the *dysf*^{prmd} and *prkdc*^{scid} alleles were purchased from The Jackson Laboratory (Bar Harbor, Maine, USA) and inbred in our SPF animal facility. NOD.Cg-*Prkdc*^{scid} *Il2rg*^{tm1Sug}/JicTac (NOG) were purchased from Taconic Biosciences (Bomholtvej, Denmark) before each experiment. Mouse experiments were performed under the license numbers G0016/13 and G0035/14. Mice were kept in a temperature and humidity controlled SPF animal facility with a 12 h light/dark cycle and free access to food and water in accordance with the German animal protection laws.

3.5.1 Focal irradiation

Focal irradiation of mouse hind limbs prior to transplantation of H2K myoblasts and HMFF was performed as described in (Marg et al., 2014). All mice were treated with a single X-radiation

dose using a CyberKnife image-guided robotic radiosurgery system (Accuray Inc.). Female 6-week-old NOG mice were anesthetized with ketamine-xylazine in PBS (9 mg/ml ketamine, 1.2 mg/ml xylazine) with an i.p. dose of 160 µl/20 g of body mass. To reproducibly guide the radiation robot to the mouse hind limbs, an acrylic glass block with surface fiducial markers was constructed. A computed tomography (CT) scan, with 0.75-mm slice thickness, was conducted using a dedicated CT scanner (Siemens Emotion) to calculate the digitally reconstructed radiographs (DRRs). The CT scan served to design the proper radiation protocol according to the desired dose of 18 Gy and distribution in the three-dimensional target area (the mouse's hind limb), sparing the adjacent body parts. The anesthetized mice were placed on the acrylic block, which had attached fiducial markers for superimposing the live positioning images with the previously calculated radiograms. The radiation procedure of each hind limb was conducted within approximately 5 minutes.

3.5.2 Transplantation of H2K myoblasts into Scid/blAJ mice

For transplantation, cultured H2K myoblasts were washed with PBS, detached with trypsin and collected in DMEM containing 20% FCS. They were centrifuged and resuspended in DMEM containing 2% FCS. Female 11-15-week old Scid/blAJ mice were injected intraperitoneally (i.p.) with a solution containing ketamine-xylazine (9 mg/ml ketamine, 1.2 mg/ml xylazine) in sterile PBS at a dose of 160 µl/20 g of body mass. Once anesthesia was effective, the area below the knee was shaved and disinfected with isopropanol. 30 µl of cell suspension were injected with a syringe coupled to a 26 gauge hypodermic needle in an approximately 20 degrees angle roughly in the middle of the tibialis anterior muscle. In muscles that were additionally subjected to cardiotoxin injury, injection of 40 µl of 10 µM cardiotoxin (Latoxan) dissolved in sterile PBS was performed 1-2 minutes after cell injection.

3.5.3 Transplantation of HMFFs into NOG mice

Mice were injected i.p. with a solution containing ketamine-xylazine (9 mg/ml ketamine, 1.2 mg/ml xylazine) in sterile PBS at a dose of 160 µl/20 g of body mass. Once anesthesia was effective, the area below the knee was shaved and disinfected with isopropanol. A longitudinal incision of approximately 4 mm was performed in the tibialis anterior muscles with a scalpel, and HMFFs containing 4–8 muscle fibers were placed inside the muscle in parallel to the mouse's fibers. The muscles were closed without sutures and the overlying skin was sutured with polyglycolic acid threads (MARLIN violett HR22, USP 4/0, EP 1.5 threads; Catgut GmbH).

3.5.4 Freezing of mouse muscles and preparation of cryosections

Mice were sacrificed by neck dislocation at the indicated time points. The tibialis anterior muscles were dissected with the aid of tweezers and scissors and cut in two halves (proximal-I and distal-II) with a blade following a transversal plane. Each half was separately embedded in gum tragacanth (10% Gum Tragacanth (Merck Millipore, 1.08405.0500), a few granules of Crystal Thymol (Synopharm, 222575-0003) and 5% glycerin in dH_2O) and mounted on cork plates with the cutting surface facing the top. The embedded muscles were first immersed in chilled isopentane for ~12 s for cryopreservation and afterwards immediately transferred to liquid nitrogen. Frozen muscles were then kept at -80°C for long-term storage. The frozen muscles were sectioned with a Leica CM3050S Cryostat.

3.6 Immunofluorescence and histological stains

The histological stains (H&E, Gomori's trichrome, NADH and acid phosphatase) were performed by Kornelia Gräning in the laboratory of Prof. Simone Spuler.

3.6.1 Dysferlin immunostaining in cultured myoblasts and myotubes

For immunofluorescence staining, H2K myoblasts were plated and induced to differentiate on 8-well µslides (ibidi, 80826). Prior to fixation, they were washed with PBS at R.T. for 5 min. They were fixed for 5 min in 100% methanol at -20°C, washed with PBS at R.T. and blocked with 1% BSA/PBS for 1 h at R.T. They were incubated overnight with an antibody against the N-terminal part of dysferlin (abcam, ab124684) diluted 1:200 in 1% BSA/PBS. The wells were washed 3 times with PBS for 5 min at R.T. and incubated with a Cy3™-conjugated secondary antibody against rabbit IgG (Jackson ImmunoResearch, 711-165-152) diluted 1:500 in PBS for 1 h at R.T. Nuclei were counterstained with 4',6-diamidino-2-phenylindole (DAPI, Sigma-Aldrich, D9564, 0.1µg/ml) diluted 1:5000 in PBS for 10 min at R.T. The wells were then washed 4 times in PBS, sealed with parafilm and kept with sufficient PBS at 4°C until imaging.

3.6.2 Dysferlin immunostaining in mouse muscle cryosections

6 µm transversal cryosections were air dried for at least 30 min at R.T. They were fixed for 5 min in acetone at -20°C, allowed to dry and blocked with 1% BSA/PBS for 1 h at R.T. They were incubated overnight at 4°C with an antibody against the N-terminal part of dysferlin (abcam ab124684) diluted 1:100 in 1% BSA/PBS. The sections were washed 3 times with PBS for 5 min at R.T. and incubated with a Cy3™ -conjugated secondary antibody against rabbit IgG (Jackson ImmunoResearch, 711-165-152) diluted 1:500 in PBS for 1 h at R.T. Nuclei were counterstained with Hoechst 33258 diluted 1:5000 in PBS for 10 min at R.T. The sections were then washed 4 times in PBS and once in ddH_2O for 5 min, and mounted on glass slides with Aqua Poly/Mount (Polysciences, Inc).

3.6.3 Pax7/laminin immunostaining in mouse muscle cryosections

6 µm transversal cryosections were air dried for at least 30 min at R.T. They were fixed for 5 min in 4% para-formaldehyde (PFA) diluted in PBS, washed with PBS for 5 min, allowed to dry for ~10 min and blocked with 5% BSA plus 3% donkey serum in PBS for 45 min at R.T. They were incubated overnight with antibodies against Pax7 (mouse, DSHB supernatant diluted 1:1 in sterile glycerol) diluted 1:10 and laminin (rabbit, Sigma-Aldrich, L9393) diluted 1:200 in 1% BSA/PBS. The sections were washed 3 times with PBS for 5 min at R.T. and incubated in darkness with secondary antibodies against mouse IgG (AlexaFluor®555, life technologies) diluted 1:500 and rabbit IgG (AlexaFluor®647, life technologies) diluted 1:500 in PBS for 1 h at R.T. Nuclei were counterstained with Hoechst 33258 diluted 1:5000 in PBS for 10 min at R.T. The sections were then washed 4 times in PBS and once in ddH_2O for 5 min, and mounted on glass slides with Aqua Poly/Mount (Polysciences, Inc).

3.6.4 Human lamin A/C immunostaining in mouse muscle cryosections

Immunofluorescence stating of human lamin A/C on cryosections of muscles grafted with HMFFs and image acquisition were performed by Dr. Andreas Marg according to the protocol published in (Marg et al., 2014). 6 µm muscle cryosections from grafted muscles were fixed in 3.7% formaldehyde and incubated in 5% goat serum diluted in PBS for 45 min. The sections were incubated with an anti-human lamin A/C antibody (rabbit, Epitomics, ab 108595) diluted 1:2000

for 4-16 hours at 4°C. The sections were washed with PBS and incubated with a Cy3™-conjugated secondary antibody against rabbit IgG diluted 1:1000 in 1% BSA in PBS for 45 minutes at R.T.

3.6.5 H&E staining in mouse muscle cryosections

Hematoxylin & Eosin (H&E) staining allows visualization of nuclei in blue, connective tissue in lighter pink, normal myofibers in dark pink and basophilic fibers in blue. 6 µm transversal cryosections were fixed in 10% buffered formalin for 1 minute, washed with dH_2O, stained with filtered Gill's II Hematoxylin solution (Merck, 1.05175.0500, modified according to GILL II) for 1 minute and washed again with dH_2O. Afterwards, they were rinsed consecutively with acid alcohol (0.8% glacial acetic acid in 80% methanol), dH_2O, 2.5% saturated lithium carbonate (Merck, 1.05680.0250) diluted in dH_2O, 80% and 100% methanol. They were stained with 0.5% alcoholic Eosin Y (Fa. Waldeck, 2C284) diluted in 50% ethanol for 3 minutes. The stained sections were subsequently dehydrated in ethanol, cleared in xylene, and mounted with Vitro-Clud® (Langenbrinck).

3.6.6 Gomori's trichrome staining in mouse muscle cryosections

Gomori's one-step trichrome staining (Engel & Cunningham, 1963) allows visualization of myofibers in greenish blue, collagen in light green, nuclei in red, myelin in foamy red, axons in blue and the intermyofibrillar network in dark red. 6 µm transversal cyosections were stained for 5 minutes with Gill's Hematoxylin solution (Merck, modified according to GILL II), washed with dH_2O, stained with filtered Gomori's trichrome solution (Sigma-Aldrich, HT10316) for 10 minutes and differentiated in 0.2% acetic acid until clear. The stained sections were subsequently dehydrated in 95% and 100% ethanol, cleared in xylene, and mounted with Vitro-Clud® (Langenbrinck).

3.6.7 NADH staining in mouse muscle cryosections

The β-Nicotinamide adenine dinucleotide (NADH) tetrazolium reductase (NADH-TR) reaction stains the intermyofibrillar matrix, which appears as a reticular network. Normal type I fibres show high enzymatic activity and appear darker, whereas type II fibres show low enzymatic activity, displaying a lighter stain. 6 µm transversal cryosections were placed for 30 minutes at 37°C in incubating solution containing 0.5 mg/ml NADH (Sigma-Aldrich, N9410-15VL), 0.1% nitrotetrazolium blue chloride (Sigma-Aldrich, N6876), 15 mM NaCl and 10 mM phosphate buffer in dH_2O. The sections were subsequently rinsed with 30% - 60% - 30% acetone, once with dH_2O and mounted with Kaiser's glycerol gelatine (Merck).

3.6.8 Acid phosphatase staining in mouse muscle cryosections

Acid phosphatase stain ((Burstone, 1958), modified by Barks, 1960) allows visualization of muscle fibers in light green, whereas lysosomes and lipofuscin deposits, which have acid phosphatase activity, appear in red. 6 µm transversal cryosections were kept in incubating solution (see composition below) for 60-70 minutes at 37°C. The sections were then washed in dH_2O for 5-10 minutes and counterstained in filtered 2% Methyl Green Stain (Newcomer Supply 12253) for 3-5 minutes. The stained sections were subsequently dehydrated in 95% and 100% ethanol, cleared in xylene, and mounted with Vitro-Clud® (Langenbrinck).

Incubating solution (pH 4.7-5.0):

- 1.6 ml diazonium salt solution (1:1, 4% sodium nitrite in dH_2O (Merck, 1.06549.0100) : 4% pararosaniline (Sigma-Aldrich, P-1528) in 2N HCl)
- 5 ml veronal acetate (2% sodium acetate-$3H_2O$ + 3% sodium barbiturate (Sigma-Aldrich, B5934) in dH_2O)
- 1 ml substrate solution (1% naphthol ASB1 phosphate (Sigma-Aldrich, N2250) in dimethyl formamide (AppliChem, A3676.0500))
- 13 ml dH_2O

3.7 Image acquisition and processing

All image-containing figures were built in Adobe Illustrator CS5 and image graphics were added in Adobe Illustrator CS5.

3.7.1 Histological stains on cryosections

Images from histological stains on mouse muscle cryosections were acquired with a Leica DM LB2 microscope (Leica Microsystems) and processed with Adobe Photoshop CS5. All modifications were applied to the whole image.

3.7.2 Immunofluorescence stains on cultured cells and cryosections

Images from immunofluorescence stains on cultured cells and mouse muscle cryosections were acquired with a Zeiss LSM 700 confocal microscope and processed with Zen 2012 (both from Carl Zeiss). Modifications were applied to the whole image.

3.7.3 Analysis of the number of dysferlin positive fibers

Images of dysferlin immunostaining on cryosections from grafted muscles were first processed in Zen 2012 to obtain slightly overexposed images in order to visualize all dysferlin positive fibers. The resulting processed images were opened in ImageJ and the dysferlin positive fibers were counted manually with the cell counter plugin. The criteria for inclusion or exclusion of positively stained structures in the counting procedure are shown below.

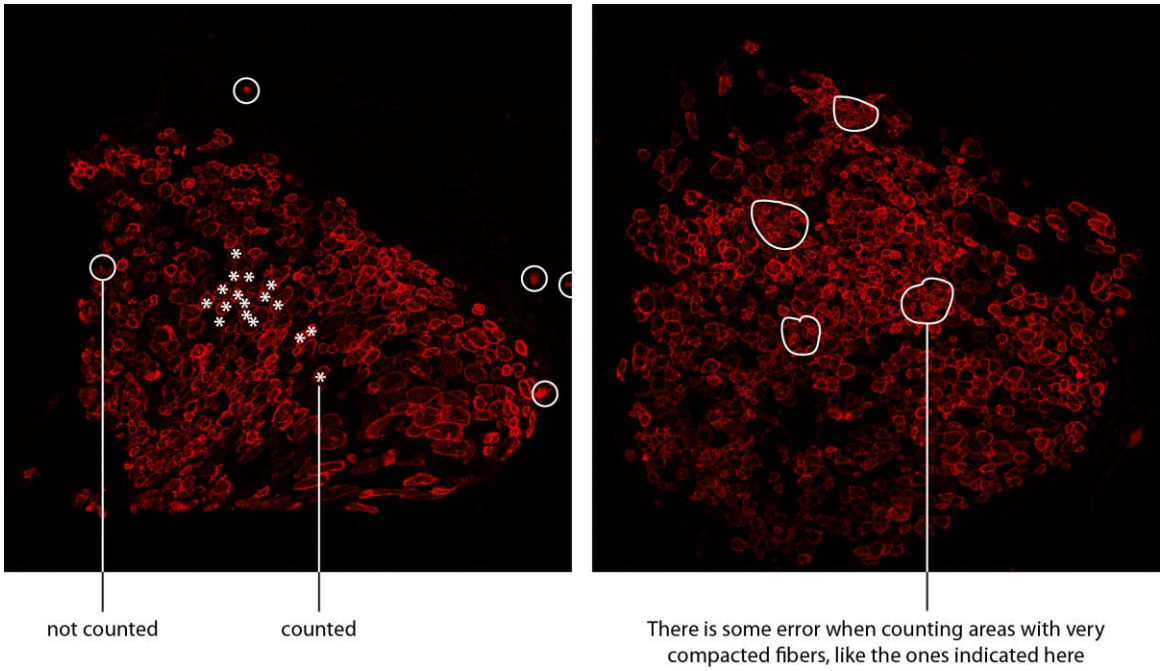

Figure 3. 1: Analysis of the number of dysferlin positive fibers in grafted muscles.

Examples of images used for counting dysferlin positive fibers in cryosections of grafted Scid/blAJ muscles. Left image: the asterisks indicate examples of clearly distinguishable stained fibers included in the analysis. The circles indicate examples of stained structures not recognized as fibers due to their morphology and thus not included in the analysis. Right image: some examples of areas with very compacted stained fibers are encircled. In those areas the identification of single fibers is occasionally difficult and thus some error can be expected in counting.

4 Results

4.1 Assessment of promoter activities in H2K myoblasts

The choice of a suitable promoter to drive transgene expression in target cells or tissues is a critical step in the design of expression cassettes for gene transfer in *in vivo* or *ex vivo* settings. In order to decide on an appropriate cassette design for full-length dysferlin expression in myogenic cells, I tested the efficiency of various promoters in driving the expression of a reporter gene in H2K A/J myoblasts. For that purpose, I constructed two vectors carrying a reporter gene under the control of the Simian virus 40 regulatory region sequence (SV40 promoter) or the synthetic promoter c5-12 (Spc5-12) (Li et al., 1999). These two promoters were chosen because of their small sequence length. Although SB transposon does not have a strict cargo size limitation, the length of the transposon sequence influences the efficiency of transposition and sequences larger than 8 kb are delivered less efficiently (Izsvak et al., 2000). Full-length dysferlin cDNA, as mentioned previously, spans 6.2 kb. Minimizing the size of the promoter was thus important to restrict the overall length of the transposon cassette and enhance genomic integration upon co-transfection with SB100X transposase. The vectors contained a TurboGFP transgene (improved variant of the GFP protein from the copepod *Pontellina plumata*) driven by the corresponding promoter and followed by a poly(A) signal, all flanked by the SB transposon ITRs.

The Spc5-12 promoter was constructed by random assembly of evolutionarily conserved sites responsible for tissue specificity of adult skeletal muscle promoters (serum response element of skeletal α-actin promoter, MEF-1, MEF-2 and TEF-1 binding sites) and was previously shown to drive strong transgene expression *in vitro* in myoblasts and myotubes (Li et al., 1999) and *in vivo* in mouse myofibers (Foster et al., 2008; Koo et al., 2011). Additionally, I utilized two SB transposon-based vectors available in the laboratory, where TurboGFP was driven by either the constitutive human elongation factor 1 alpha (EF1α) promoter or the hybrid viral CMV immediate enhancer/β-actin (CAG) promoter. All the vectors had the same backbone and only the promoter sequence was different. After optimizing electroporation using the 24-well optimization protocol for adherent and suspension cell lines of the Neon® Transfection System, I selected two electroporation protocols (Figure 4. 1) for further experiments using H2K A/J myoblasts. I transfected $5*10^5$ H2K A/J myoblasts with 500 ng of transposon plasmid (pT2-CAG-GFP, pT2-EF1α-GFP, pT2-SV40-GFP and pT2-Spc5-12-GFP). Three days after transfection, I performed FACS analysis to determine the percentage and mean fluorescence intensity values of GFP expressing cells as readout of promoter activity. The values are indicated in Table 4. 1.

	Non-transfected		pT2-CAG-GFP		pT2-SV40-GFP		pT2-Spc5-12-GFP		pT2-EF1α-GFP	
	%	**FI**	**%**	**FI**	**%**	**FI**	**%**	**FI**	**%**	**FI**
1100mV 30ms 1 pulse	0	-	43,79	325,22	13,41	32,43	35,71	96,36	20,82	49,51
1050mV 30ms 2 pulses	0	-	64,44	950,47	40,43	69,51	57,16	248,87	55,88	126,08

Table 4. 1: Promoter activities in H2K A/J myoblasts.

The values indicate the percentage (%) of GFP expressing cells and the mean fluorescence intensity (FI) of the GFP positive population assessed by FACS three days after transfection of H2K A/J myoblasts.

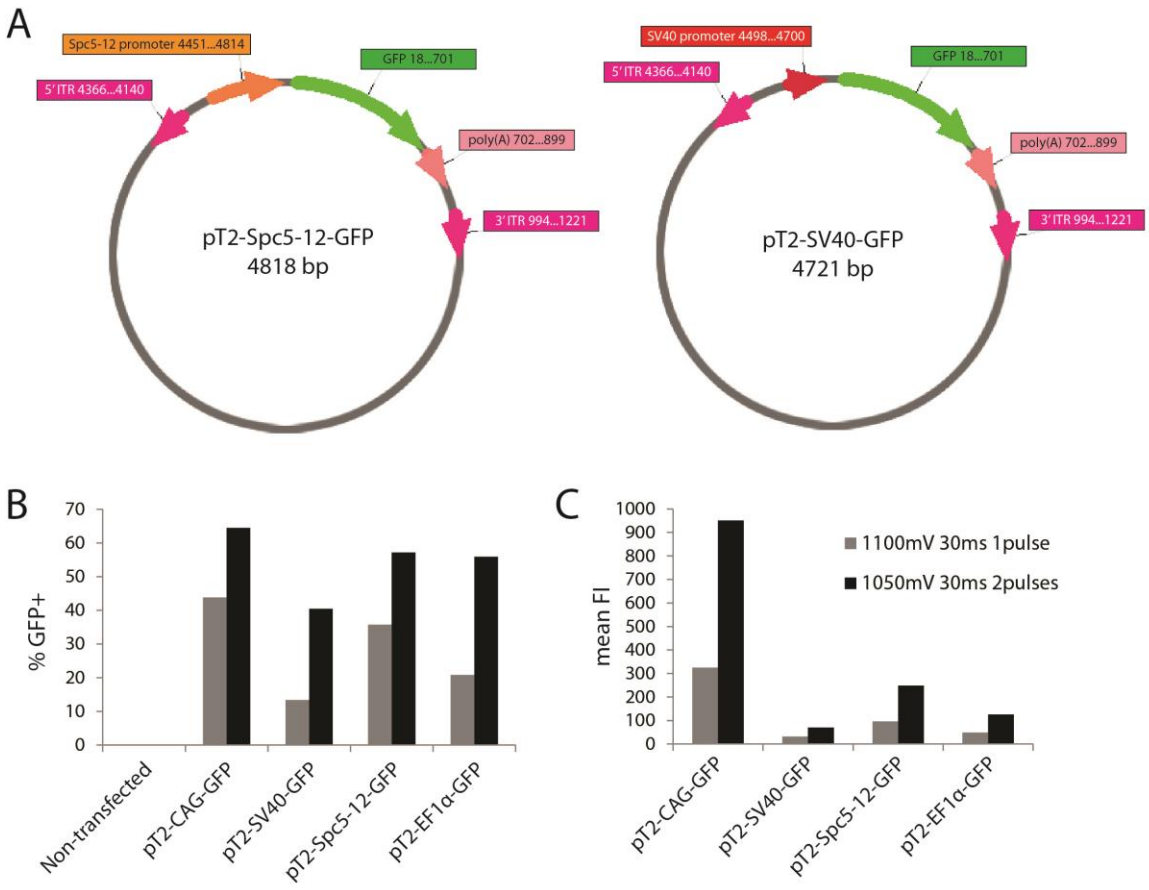

Figure 4. 1: Cloning of SB transposon-based reporter constructs and assessment of promoter activities in H2K A/J myoblasts.

(A) pT2-Spc5-12-GFP and pT2-SV40-GFP vectors. Green arrows indicate the GFP CDS. Orange and red arrows indicate the Spc5-12 and SV40 promoters, respectively. Light pink arrows following the GFP CDS indicate the SV40 poly(A) signals. Dark pink arrows flanking the expression cassette in opposite orientations indicate the SB transposon 5' and 3' ITRs. SB transposon vectors containing a transgene cassette flanked by the SB ITRs are named as pT2. (B) Percentage of GFP expressing cells and (C) mean fluorescence intensity of the GFP+ cell population assessed by FACS three days after transfection of H2K A/J myoblasts with the GFP reporter vectors using two different electroporation protocols.

Based on the results obtained with the reporter vectors we considered the Spc5-12 promoter most suitable for driving expression of full-length dysferlin in our *ex vivo* gene transfer approach. The favorable criteria were its tissue specificity, high level of activity in H2K A/J myoblasts and short sequence (<400 bp) compared with the EF1α and CAG promoters (> 1kb).

4.2 Construction of vectors for dysferlin gene transfer

I constructed SB-transposon based vectors for transfer of full-length *hDYSF_c* (original) and *hDYSF_v1* cDNAs into dysferlin null myoblasts to restore expression of dysferlin. I constructed bicistronic vectors where full-length dysferlin was followed by a TurboGFP CDS, which served as a reporter to positively select by FACS the cells carrying integrated transposon cassettes and therefore stably expressing dysferlin. GFP was preceded by an Internal Ribosome Entry Site (IRES) sequence to allow simultaneous translation of both cistrons.

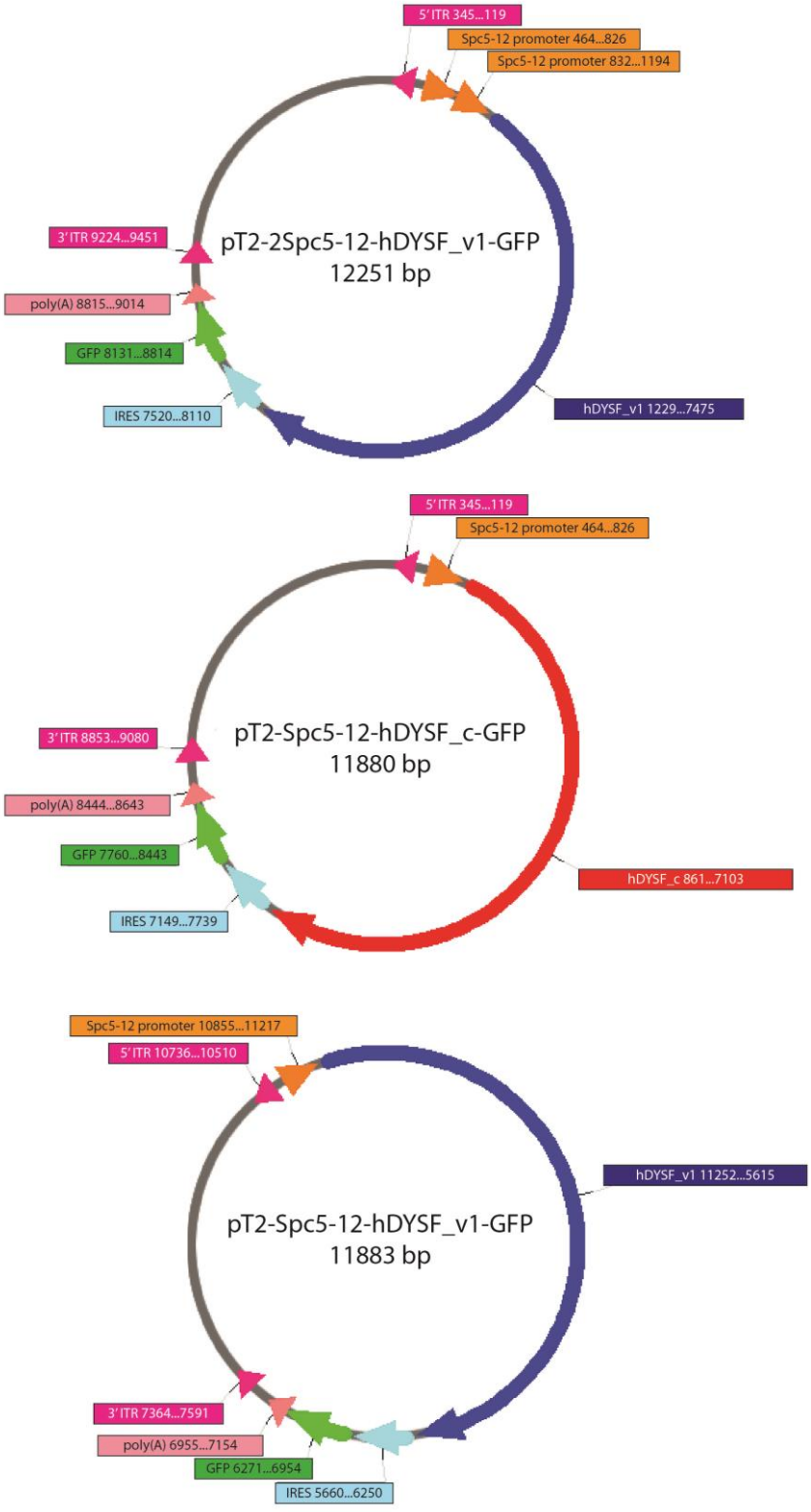

Figure 4. 2: Bicistronic SB transposon-based vectors for transfer of full-length dysferlin.

Orange arrows indicate the Spc5-12 promoter. Dark blue and red arrows indicate the human *DYSF_v1* and *DYSF_c* cDNAs, respectively. Light blue arrows indicate the IRES sequence. Green arrows indicate the GFP CDS. Light pink arrows indicate the SV40 poly(A) signals. Dark pink arrows indicate the SB transposon ITRs. The vector names and sizes in base pairs (bp) are indicated in the figure.

Expression of the unique ORF was under the control of Spc5-12 regulatory sequence. A vector resulting from an insertion of two copies of the Spc5-12 promoter in the same orientation during the cloning process was also used to compare the efficiency of transgene expression (Figure 4. 2).

hDYSF_c and *hDYSF_v1* are the first (~73%) and second (~13%) most abundant mRNA isoforms in human skeletal muscle, respectively (Pramono et al., 2009). However, the relative levels of the corresponding protein isoforms are not known because of the lack of antibodies that can specifically recognize either isoform. Some insights into the functional differences have been provided by studies on the crystal structure and the Ca^{2+} and phospholipid binding properties of the two alternative C2A domains. However, not much is known about the real implications of these C2A domain variants for the function of dysferlin in different tissues or contexts.

4.3 Transfer of full-length dysferlin into H2K A/J myoblasts

We selected H2K A/J myoblasts (Cohen et al., 2012) as a dysferlin deficient cell model to establish the proof-of-concept study of *ex vivo* SB-based full-length dysferlin gene transfer. H2K A/J (Figure 4. 3) are conditionally immortalized mouse myoblasts derived from a mouse strain generated by crossing the dysferlin-null A/J mouse line with the *H-2K*^{b}tsA58 (immortomouse) line (Jat et al., 1991). This immortomouse line harbors an expression cassette for the tsA58 thermosensitive SV40 large T antigen under the control of the ubiquitous *H-2K*^{b} promoter, whose transcriptional activity is enhanced by Interferon-γ (IFN-γ). tsA58 is degraded at temperatures higher than 33°C. Therefore, when cultured in permissive conditions (33°C and in the presence of IFN-γ), cells derived from the immortomouse strain are immortalized.

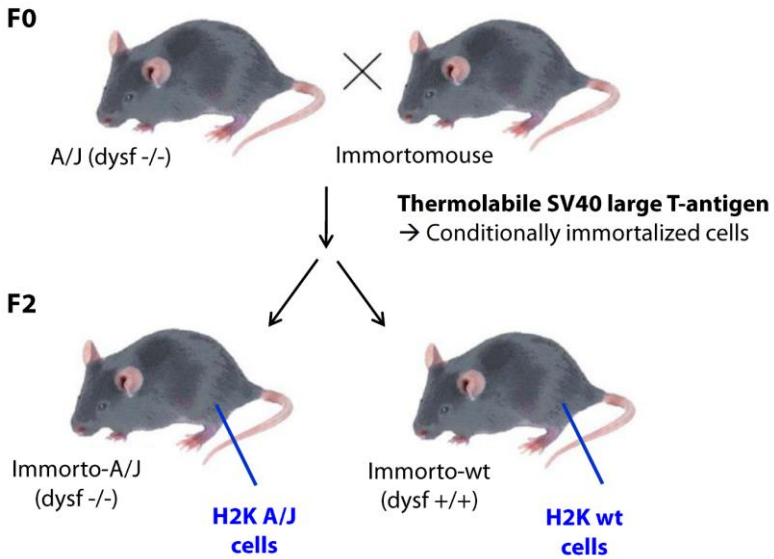

Figure 4. 3: Derivation of dysferlin-null (A/J) and control (wt) H2K myoblasts.

The conditionally immortalized myoblasts are derived from the F2 generation of crosses between the *H-2K*^{b}tsA58 immortomouse strain and the dysferlin-null A/J strain (homozygous for the *dysf*^{prmd} knock-out allele). Muscle satellite cells are isolated from control (immorto-wt) and dysferlin-null (immorto-A/J) mice of the F2 generation harboring the *H-2K*^{b}tsA58 allele and homozygous for the dysferlin wild-type (dysf+/+) or the *dysf*^{prmd} (dysf-/-) allele, respectively. The cells are expanded *ex vivo* in permissive conditions and their myoblast progeny is conditionally immortalized by the expression of the tsA58 thermolabile SV40 large T antigen.

However, if switched to non-permissive conditions (higher temperatures and absence of IFN-γ) they can no longer proliferate indefinitely. H2K cells are also suitable for mouse transplantation studies because, due to the higher body temperature of mice, they are unable to form tumors *in vivo* (Jat et al., 1991). H2K myogenic cells derived from immortomice have been previously shown to have an extensive proliferative capacity *in vitro* when grown in permissive conditions (Morgan et al., 1994). They undergo myogenic differentiation when cultured in fusion media under non-permissive conditions and can robustly engraft when transplanted into injured mouse muscle (Morgan et al., 1994; Muses, Morgan, & Wells, 2011a).

4.3.1 Selection of stably transfected cells

The next step was to deliver full-length dysferlin into dysferlin-null H2K A/J myoblasts using the SB system. I first determined the time course during which GFP+ events not due to stable transposon integrations could no more be detected in the absence of SB100X. For this purpose I transfected H2K A/J myoblasts with pT2-2Spc5-12-hDYSF_v1-GFP in the presence or absence of an expression vector for SB100X transposase. As a control, I used a reporter vector where the GFP CDS was preceded by an IRES sequence and driven by the CAG promoter. I monitored the GFP signal in the transfected populations by flow cytometry for 14 days. 11 days after transfection, GFP+ events in the cells not transfected with SB100X were barely detected, indicating that all positive events were due to stable integrations of the transgene cassettes (Figure 4. 4). It must be noted that random genomic integrations of the plasmid not mediated by the transposase can occur at a low frequency.

Next, I transfected H2K A/J myoblasts with the three full-length dysferlin transfer vectors (pT2-2Spc5-12-hDYSF_v1-GFP, pT2-Spc5-12-hDYSF_v1-GFP and pT2-Spc5-12-hDYSF_c-GFP, vector details in Figure 4. 2). As control, I transfected cells with the above mentioned reporter vector in order to have a control population of engineered cells expressing only GFP. I electroporated H2K A/J myoblasts with equimolar amounts of transposon vectors (~500 ng of dysferlin transfer vectors and 250 ng of reporter vector per $5*10^5$ cells) and a 1:10 mass ratio (transposase:transposon) of an expression vector for SB100X transposase (pCMV(cat)-T7-SB100X). 7-11 days after transfection, I selected the stably transfected cells by FACS based on their GFP signal. The percentage and intensity of GFP were low in cells transfected with the dysferlin transfer vectors in comparison with cells transfected with the reporter. This could be due to the large size of the dysferlin transfer vectors, which likely limits transfection rates. Additionally, the inefficiency of the IRES to enable translation of the second cistron when preceded by a very large cistron could also impact the detection of transfection events. It was therefore necessary to enrich the populations throughout various rounds of cell sorting (Figure 4. 5-B).

I obtained cell populations highly enriched in GFP expressing cells for pT2-2Spc5-12-hDYSF_v1-GFP and pT2-Spc5-12-hDYSF_c-GFP. I also selected cells stably transfected with the reporter vector (pLICU1). I was not able to enrich any of the samples transfected with pT2-Spc5-12-hDYSF_v1-GFP due to their very low percentage of GFP+ cells (Figure 4. 5-A).

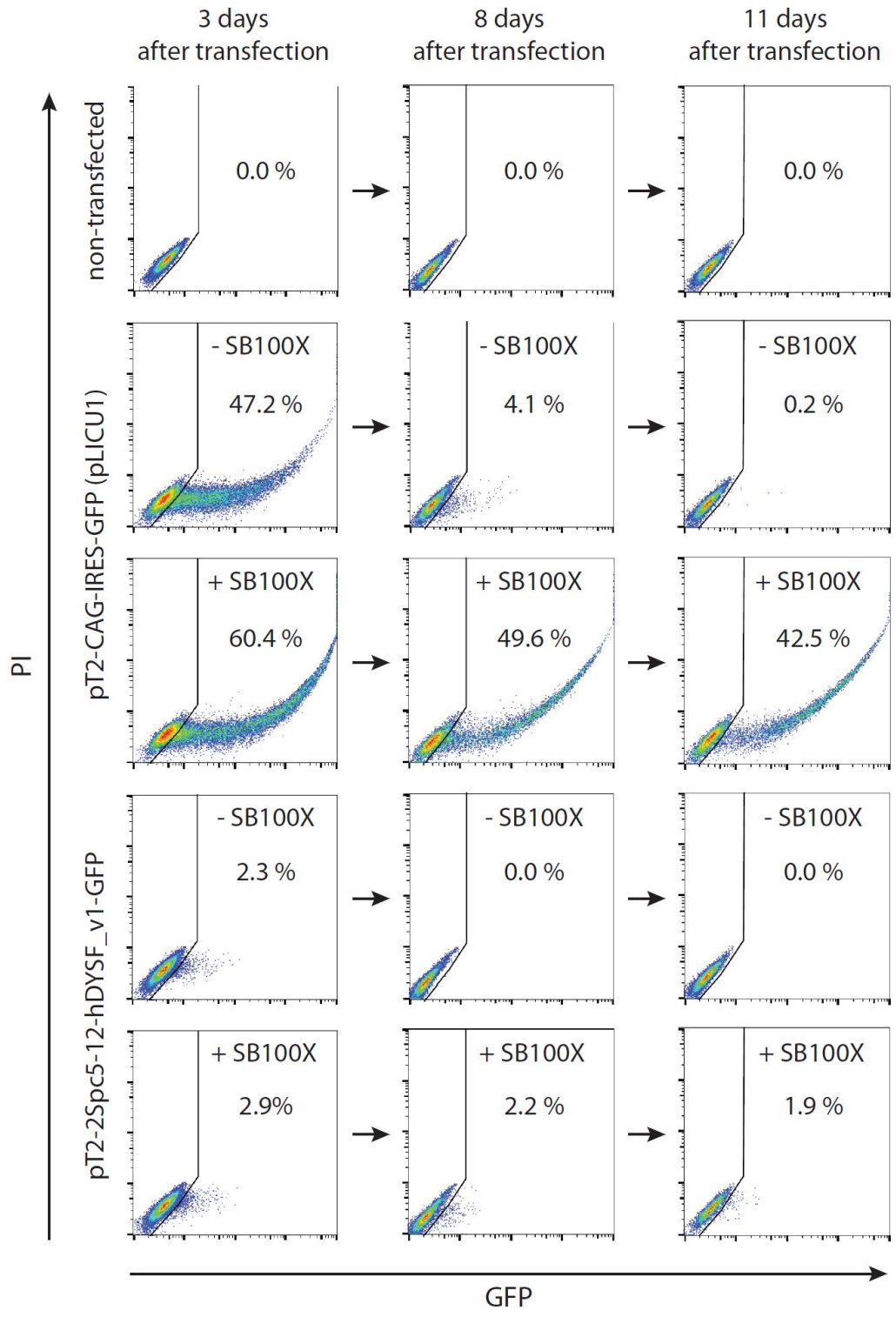

Figure 4. 4: SB transposition in H2K A/J myoblasts.

H2K A/J myoblasts were transfected with pT2-CAG-iresGFP (pLICU1) and pT2-2Spc5-12-hDYSF_v1-GFP in the presence or absence of an expression vector for SB100X transposase. GFP expression was monitored by FACS during a time course of 14 days. At day 11 after transfection, GFP+ cells could not be detected in samples transfected only with the transposon vectors without SB100X.

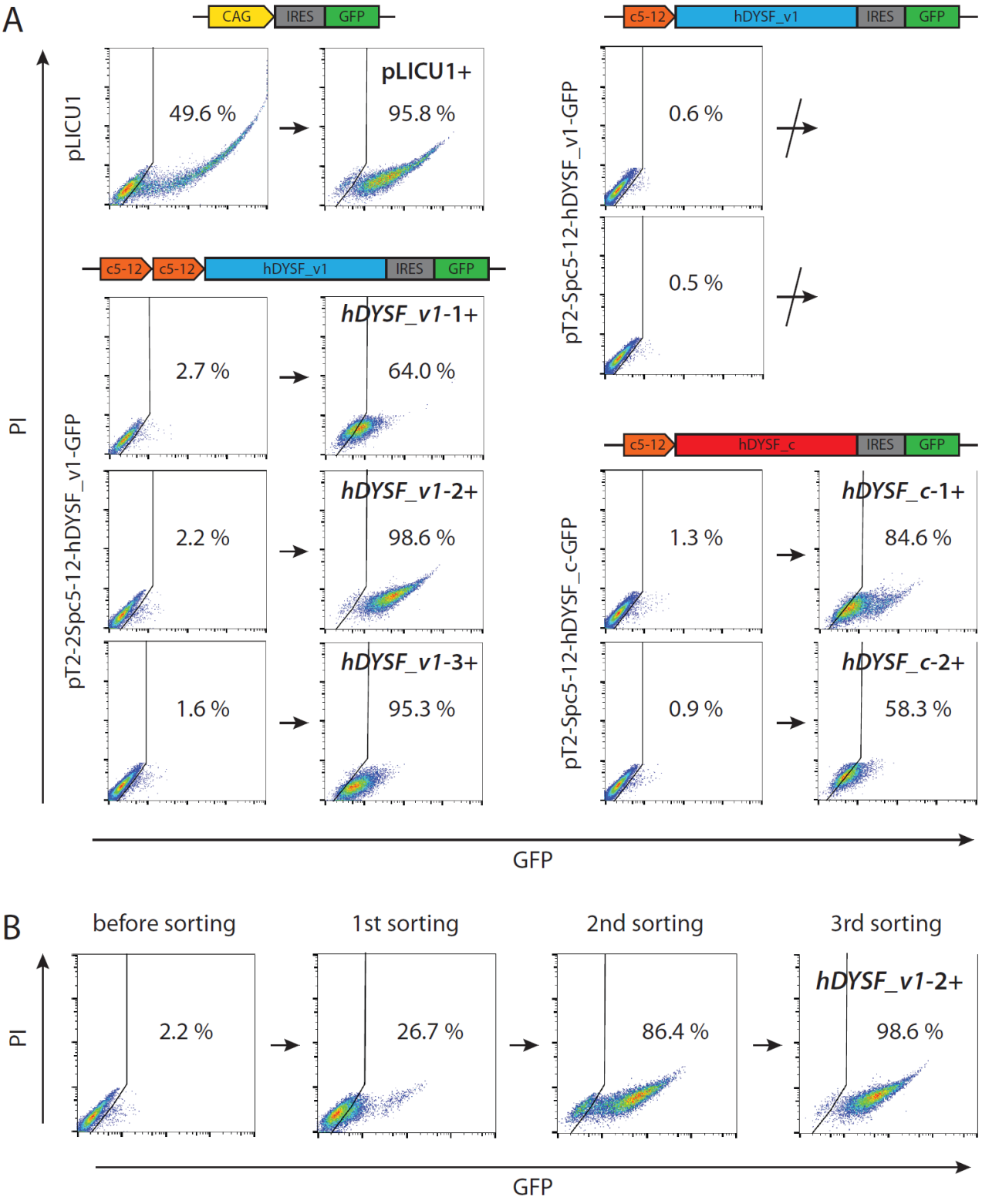

Figure 4. 5: Sorting of stably transfected H2K A/J myoblasts.

(A) For each vector, the transfected cell populations before sorting (7-8 days after transfection) are shown on the left and the same populations after enriching for GFP expressing cells throughout 2-4 sorting steps are shown on the right. The sample IDs of the cell populations after sorting are indicated in bold letters on the corresponding plots. (B) Example illustrating the subsequent sorting steps for selection of GFP expressing H2K A/J myoblasts transfected with pT2-2Spc5-12-hDYSF_v1-GFP and SB100X transposase (sample ID: *hDYSF_v1*-2+).

4.3.2 Analysis of dysferlin protein expression in the cells enriched for reporter expression

Next, we analyzed the H2K A/J myoblasts selected by FACS based on their GFP signal for expression of transgenic dysferlin. We performed immunoblot on protein lysates with an antibody against C-terminal dysferlin. I confirmed expression of dysferlin_v1 and dysferlin_c in the corresponding sorted populations. Expression of transgenic dysferlin driven by Spc5-12 promoter was stronger in differentiated myotubes (Figure 4. 6-A). As expected, dysferlin was absent in protein lysates from non-corrected H2K A/J myoblasts transfected only with SB100X and pLICU1 and sorted for GFP expressing (pLICU1+) and non-expressing (pLICU1-) cells (Figure 4. 6).

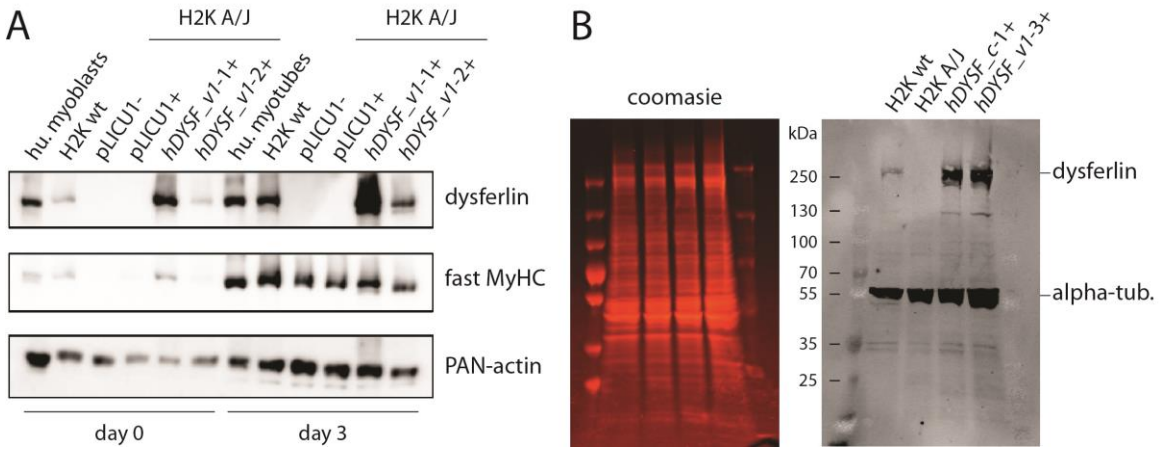

Figure 4. 6: Analysis of dysferlin expression in selected H2K A/J myoblasts and myotubes.

(A) Western blot of corrected H2K A/J myoblasts and myotubes (*hDYSF_v1*-1+ and *hDYSF_v1*-2+). Human primary and mouse H2K wt myoblasts were used as control for endogenous dysferlin expression. Unmodified H2K A/J myoblasts (pLICU1-) or myoblasts harboring only a GFP reporter (pLICU1+) were used as negative control for dysferlin expression. Protein lysates were collected at day 0 (before switching from proliferation to fusion media) and at day 3 of differentiation. The membrane was hybridized with an antibody against C-terminal dysferlin. Fast myosin heavy chain was used as a marker of differentiation. Actin was used as a loading control. (B) Western blot of corrected H2K A/J myotubes (*hDYSF_c*-1+ and *hDYSF_v1*-3+). The membrane was hybridized with an antibody against C-terminal dysferlin. Alpha-tubulin was used as a loading control.

4.3.4 Dysferlin localization in "corrected" myoblasts and myotubes

Next, I analyzed the localization of dysferlin in "corrected" myotubes. Proper localization cannot be fully assessed *in vitro* because dysferlin is predominantly a myofiber protein. However, it is also expressed at a lower level *in vivo* and *in vitro* in satellite cells and myoblasts prior to and during differentiation (De Luna et al., 2004). There, dysferlin is present both at the membrane and the developing T-tubule network in forming myotubes and myofibers (Y. Huang et al., 2007; Klinge et al., 2010; Klinge et al., 2007). I performed an immunofluorescence staining to visualize dysferlin in H2K wt, dysferlin-null and corrected H2K A/J myotubes. As seen in Figure 4. 7, dysferlin staining appeared stronger in the two populations of corrected myoblasts analyzed than in wild-type myotubes, and was absent in non-corrected H2K A/J myotubes, confirming the results obtained by western blot. In wild-type myotubes, dysferlin was visible primarily at the membrane with a faint cytoplasmic stain.

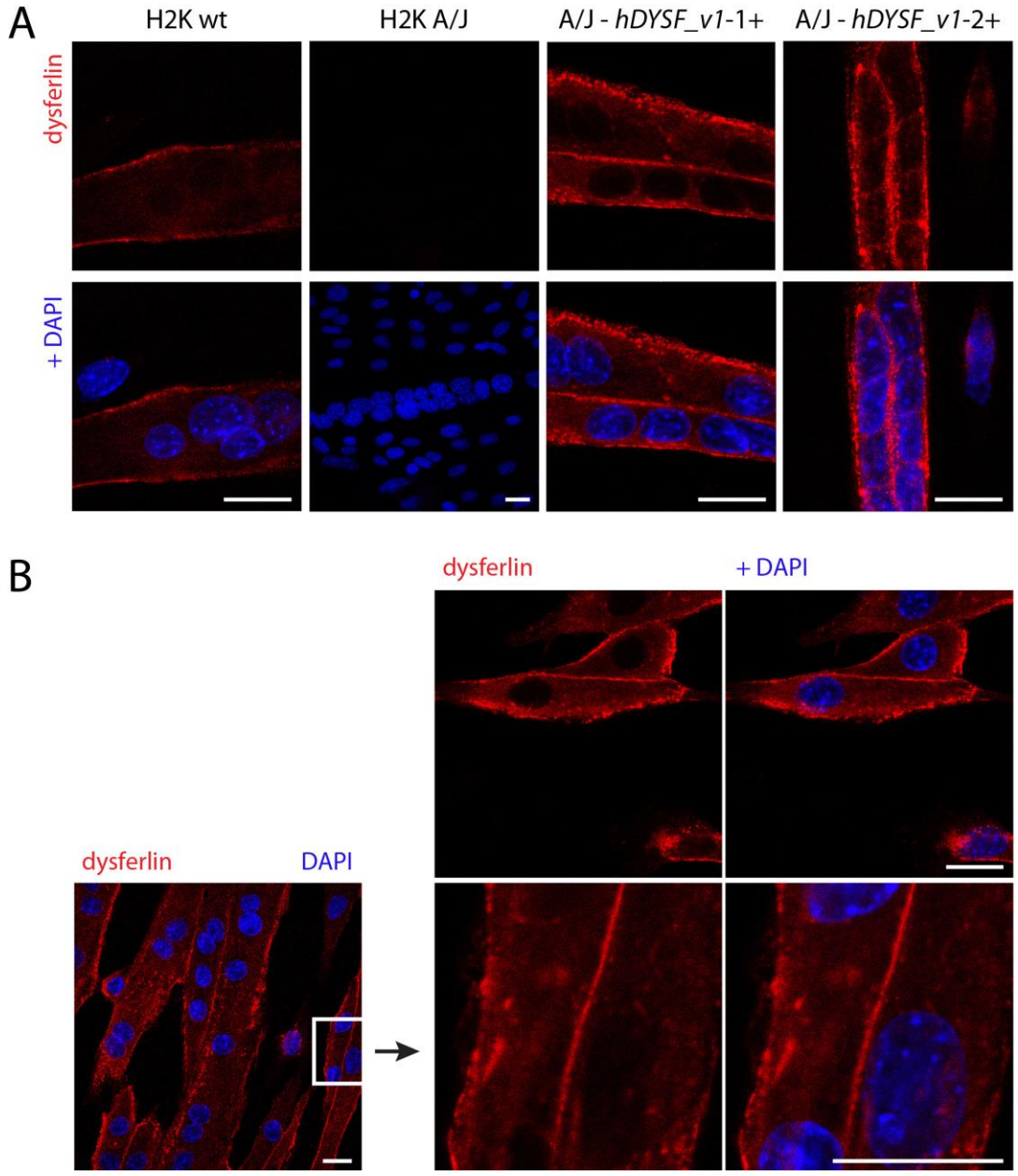

Figure 4. 7: Dysferlin localization in corrected H2K A/J myotubes.

(A) Confocal microscopy images showing dysferlin expression in H2K control (wt), dysferlin-null (A/J) and corrected (*hDYSF_v1*-1+ and *hDYSF_v1*-2+) myotubes. Cells were immunostained with an antibody against dysferlin (red). Nuclei were counterstained with DAPI (blue). Scale bars: 20 µm. (B) Higher magnification depicting in detail the localization of dysferlin in corrected H2K A/J cells (*hDYSF_v1*-1+). Dysferlin is enriched in the membrane of some myotubes and differentiating myoblasts. It is also strongly detected in the cytoplasm of all cells. Scale bars: 20 µm.

In corrected myotubes, dysferlin was strongly detected both at the membrane and in the cytoplasm of myoblasts and myotubes (Figure 4. 7). Also, it was enriched at the membrane of some cells. This localization pattern is similar to that described for wild type dysferlin, suggesting that transgenic dysferlin may be functional.

4.4 Development of a local irradiation protocol for mice

Engraftment of donor cells following myoblast transplantation is usually enhanced by induction of a regenerative environment in the recipient muscle. The transplanted cells are then recruited to the ongoing muscle regeneration process and can contribute to the repair of damaged myofibers or to the generation of new myofibers. However, if the endogenous satellite cells are fully functional, as is the case in several muscle disorders, they compete with the cells of donor origin, reducing their contribution to myofibers and their colonization of the satellite cell compartment (Briggs & Morgan, 2013). The latter is required for a long term therapeutic effect. Some of the acute injury models commonly used to induce a regenerative response in muscle, such as snake-venom derived myotoxins or concentrated salt solutions like $BaCl_2$, damage the myofiber structure (Duchen, Excell, Patel, & Smith, 1974; Stringer, Kainer, & Tu, 1971) but are harmless to the nerve terminals (Duchen et al., 1974) and the satellite cells (Boldrin et al., 2012). On the other hand, muscle irradiation has long been used as a method to prevent muscle regeneration in mouse models (Weller, Karpati, Lehnert, & Carpenter, 1991). Whilst inactivating the satellite cells present in the muscle, irradiation does not have evident short-term effects on the postmitotic myonuclei and seemingly preserves myofiber integrity (Morgan, Hoffman, & Partridge, 1990; Morgan, Pagel, Sherratt, & Partridge, 1993). We and others have reported that engraftment and contribution to muscle formation of cells transplanted into mouse skeletal muscle is greatly enhanced by inactivation of endogenous satellite cells by radiation (Boldrin et al., 2012; Boldrin et al., 2009; Gross & Morgan, 1999; Marg et al., 2014; Meng et al., 2014; Ross et al., 2012).

We aimed to develop a local and precise irradiation protocol for mice in order to affect only the muscles target for transplantation and spare the rest of the body. For this purpose we used a Cyberknife image-guided robotic linear accelerator generally used for highly precise radiosurgery procedures in patients. For treatment planning, we performed a computed tomography (CT) scan of one C57BL/6 mouse of approximately the same age and weight as the recipient mice for the transplantation experiments. According to the CT, an irradiation protocol was established to deliver a three-dimensional total dose of 18 Gy to the mouse hind limb with minimal dispersion into neighboring tissues. This radiation dose was previously reported as optimal for engraftment of donor myoblasts (Boldrin et al., 2012). The maximum, minimum and average doses in the target zone, as well as the percentage spreading of the radiation dose into surrounding areas are indicated in Figure 4. 8.

24h after radiation, irradiated and non-irradiated tibialis anterior muscles of C57BL/6 mice were challenged with cardiotoxin. Extensive regeneration, indicated by a majority of centrally nucleated fibers, was visible in control muscles only injected with cardiotoxin. However, irradiation resulted in a complete failure to regenerate muscles 8 days after cardiotoxin-induced acute injury. This indicates that the endogenous satellite cells were robustly inactivated by the irradiation procedure. No effects of radiation were visible in the non-cardiotoxin-injured muscles 9 days after the focal delivery of 18 Gy (Figure 4. 8).

A

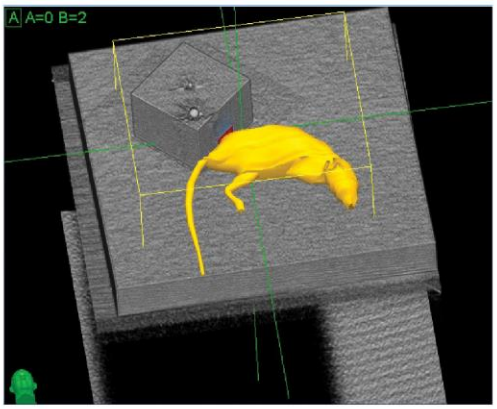

B

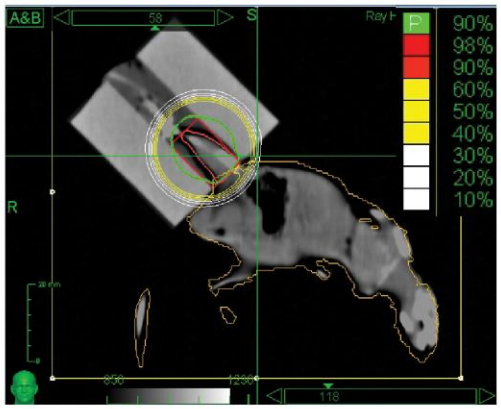

C

	Minimum	Average	Maximum
Dose (mouse leg)	15.5 Gy	18.5 Gy	19.2 Gy

D

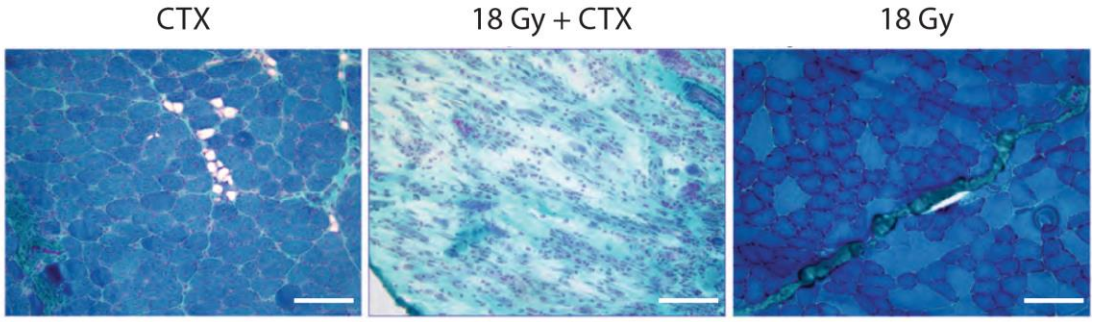

Figure 4. 8: Local irradiation of mouse hind limbs for inactivation of endogenous satellite cells.

(A) Computer screenshot showing the positioning of the mouse in an acrylic glass block with fiducial markers on the surface to guide the radiation robot and (B) the distribution of the radiation dose in the target (red) and proximal (green to white) areas. (C) Maximum, minimum and average three-dimensional radiation dose in the target area (the mouse hind limb). (D) Gomori's trichrome stain of tibialis anterior muscle cryosections from mice subjected to 18 Gy radiation only or followed 24h later by injection of cardiotoxin. Muscle histology showed that irradiated muscles failed to regenerate after acute injury. Muscles were collected for histological analysis 9 days after irradiation (D is modified from (Marg et al., 2014)). Scale bars: 100 µm.

4.5 Transplantation of corrected myoblasts into Scid/blAJ mice

After confirming restoration of dysferlin expression in H2K A/J myoblasts *in vitro*, we further wanted to assess their capacity to reconstitute dysferlin protein *in vivo* in a mouse model of dysferlinopathy. For this purpose, I performed transplantation of the corrected myoblasts into the tibialis anterior muscle of dysferlin-null Scid/blAJ (B6.Cg-*Dysf*^{prmd}*Prkdc*^{scid}/J) mice (Farini et al., 2012). We chose this mouse line because of its immunocompromised phenotype, which would allow us to perform non-allogeneic grafts without the need for chemically induced immune suppression.

The success of myoblast transplantation depends on the survival and engraftment of the transplanted cells, their contribution to myofibers and their ability to repopulate the satellite cell niche (Briggs & Morgan, 2013). As mentioned previously, various injury regimes have been routinely used to enhance engraftment of donor-derived cells in skeletal muscle. Some of those

treatments, like injection of cardiotoxin or notexin, induce acute damage to the myofibers resulting in degeneration and necrosis (Duchen et al., 1974; Stringer et al., 1971). Acute damage inflicted by injection of myotoxins induces muscle regeneration and presumably boosts the participation of the transplanted cells in the repair and *de novo* formation of myofibers, thereby augmenting the number of donor-derived fibers. However, if the endogenous satellite cells are not functionally impaired, they are likely to hinder the contribution of the donor derived cells to muscle regeneration and compete for the colonization of the niche during maturation of the newly formed fibers. The same competition for the satellite cell niche exists in non-injured muscle with viable satellite cells (Briggs & Morgan, 2013). Alternatively, the satellite cell niche can be modulated by ablation of the endogenous stem cells (e.g. by radiation) and their replacement by donor-derived cells. It has been described that this process is time sensitive, since long-term disruption of the niche, for example by inactivating the endogenous satellite cells through radiation, renders it permanently non-functional. This can be prevented by repopulation of the nice by donor-derived satellite cells in a short time window after irradiation (Boldrin et al., 2012).

Studies performed in different mouse strains and using diverse types of myogenic cells as a source of grafting material have shown that different injury regimes may be suitable for each kind of experimental setup, mouse strain and cell type (Briggs & Morgan, 2013).

That prompted us to explore various injury models in order to identify the best suited for transplantation of H2K myoblasts in the skeletal muscle of Scid/blAJ mice (Figure 4. 9). This included 1) injection of cardiotoxin, 2) local irradiation and 3) both.

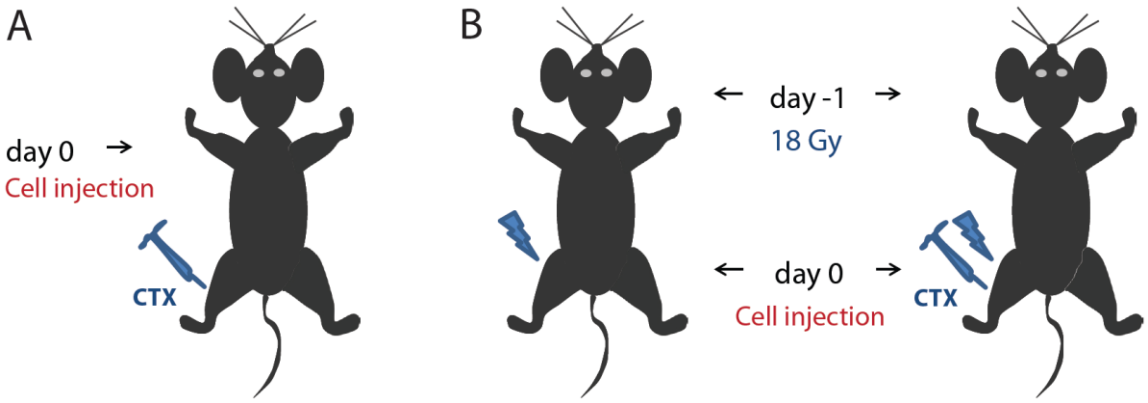

Figure 4. 9: Transplantation scheme and injury regimes for grafting of H2K myoblasts into Scid/blAJ mice.

(A) The host tibialis anterior muscles were injected with cardiotoxin simultaneously to cell injection. Muscles were collected 14 days after transplantation (n = 5). (B) The host tibialis anterior muscles were irradiated with 18 Gy one day prior to transplantation (n = 8). On the same day of transplantation, half of the muscles were injected with cardiotoxin (n = 4) and half were not (n = 4). The muscles were collected for analysis 3 weeks (n = 4) or 6 weeks (n = 4) after transplantation. In total, each group (injury model + time point of analysis) consisted of 2 mice.

4.5.1 Engraftment of corrected H2K A/J myoblasts and dysferlin reconstitution in grafted muscles of Scid/blAJ mice

We first aimed to determine the number of donor myoblasts sufficient for robust engraftment in the host muscles. I performed a series of transplants in five 11-12-week-old female Scid/blAJ mice, where either $1*10^5$ or $3*10^5$ myoblasts were injected into a single tibialis anterior muscle simultaneously with cardiotoxin. Both left and right tibialis anterior muscles of five mice were

injected with either myoblasts or only carrier solution. All muscles were injected with cardiotoxin. Two muscles were injected with $1*10^5$ and three muscles with $3*10^5$ corrected H2K A/J myoblasts (*hDYSF_v1*-2+). As a control for this first series of grafts I also transplanted $1*10^5$ or $3*10^5$ H2K wild-type myoblasts into two muscles each. As a control, another muscle was injected with carrier solution without cells. I collected and cryopreserved the muscles 14 days after transplantation. I prepared cryosections of the collected muscles and performed immunofluorescence staining to detect dysferlin in myofibers, which would indicate successful engraftment of donor myoblasts and restoration of dysferlin protein in the host muscles. I found >100 dysferlin positive fibers in cryosections of one muscle injected with $3*10^5$ corrected H2K A/J myoblasts (Figure 4. 10). Only 2-3 dysferlin positive fibers were found in cryosections of another muscle injected with $3*10^5$ corrected myoblasts. No dysferlin positive fibers were found in muscles injected with $1*10^5$ corrected myoblasts, with wild type myoblasts, or with carrier solution.

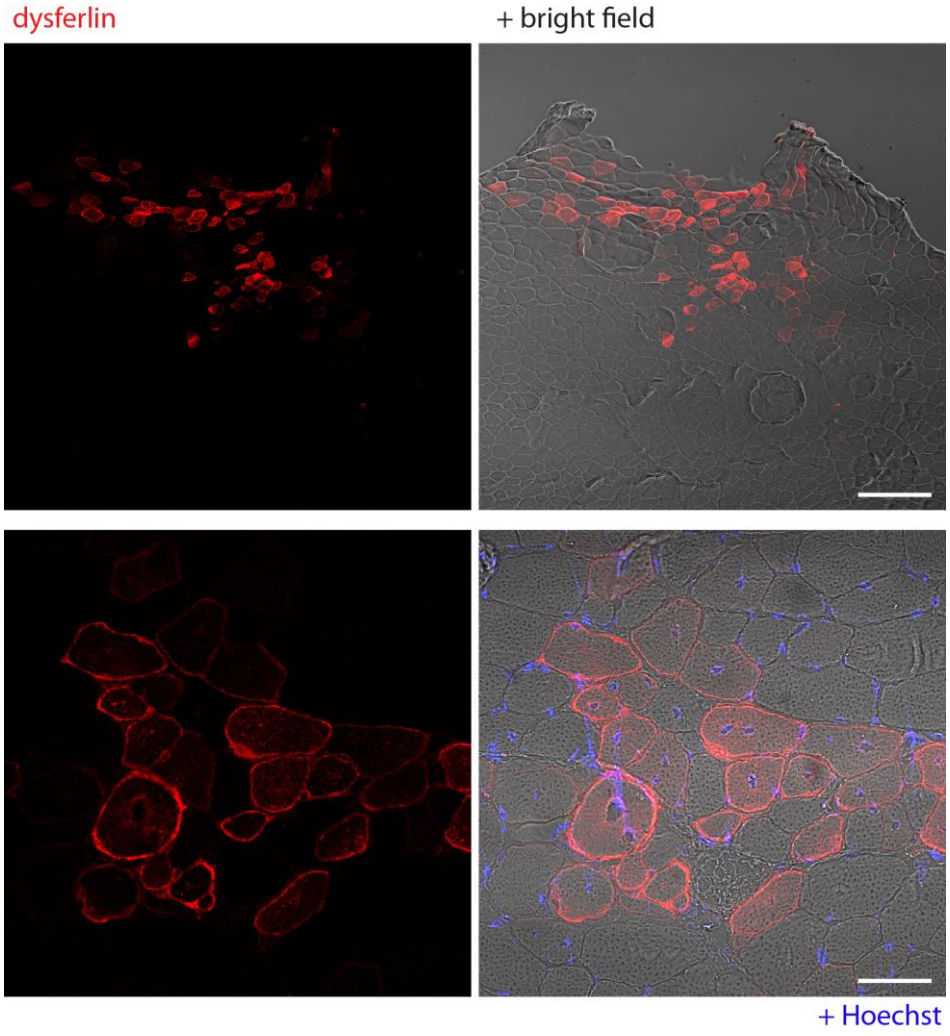

Figure 4. 10: Engraftment of corrected H2K A/J myoblasts and expression of dysferlin in grafted Scid/blAJ muscles injured with cardiotoxin.

Confocal microscopy images of cryosections prepared from one grafted tibialis anterior muscle immunostained with an antibody against dysferlin (red). Nuclei were counterstained with Hoechst (blue). The muscles were collected 14 days after transplantation and cardiotoxin injection. Scale bars: 200 µm (top) and 50 µm (bottom).

Next, I performed a second series of transplants in mice that had been locally irradiated with a dose of 18 Gy as described in Figure 4. 8**,** one day before transplantation. Given that dysferlin positive fibers were only found in muscles injected with a higher number of donor myoblasts in the previous transplant series, I injected $3*10^5$ corrected myoblasts (*hDYSF_v1*-2+) into pre-irradiated tibialis anterior muscles of 12-15-week-old female Scid/blAJ mice (n = 8). Half of the mice (4/8) received a cardiotoxin injection in their grafted tibialis anterior muscles simultaneously to cell transplantation. Two muscles (2/8) that had received a transplant without injection of cardiotoxin and two muscles (2/8) that received both cardiotoxin and donor cell injections were collected and cryopreserved 3 weeks after transplantation. The remaining four muscles (two with and two without cardiotoxin injection) were collected and cryopreserved 6 weeks after transplantation.

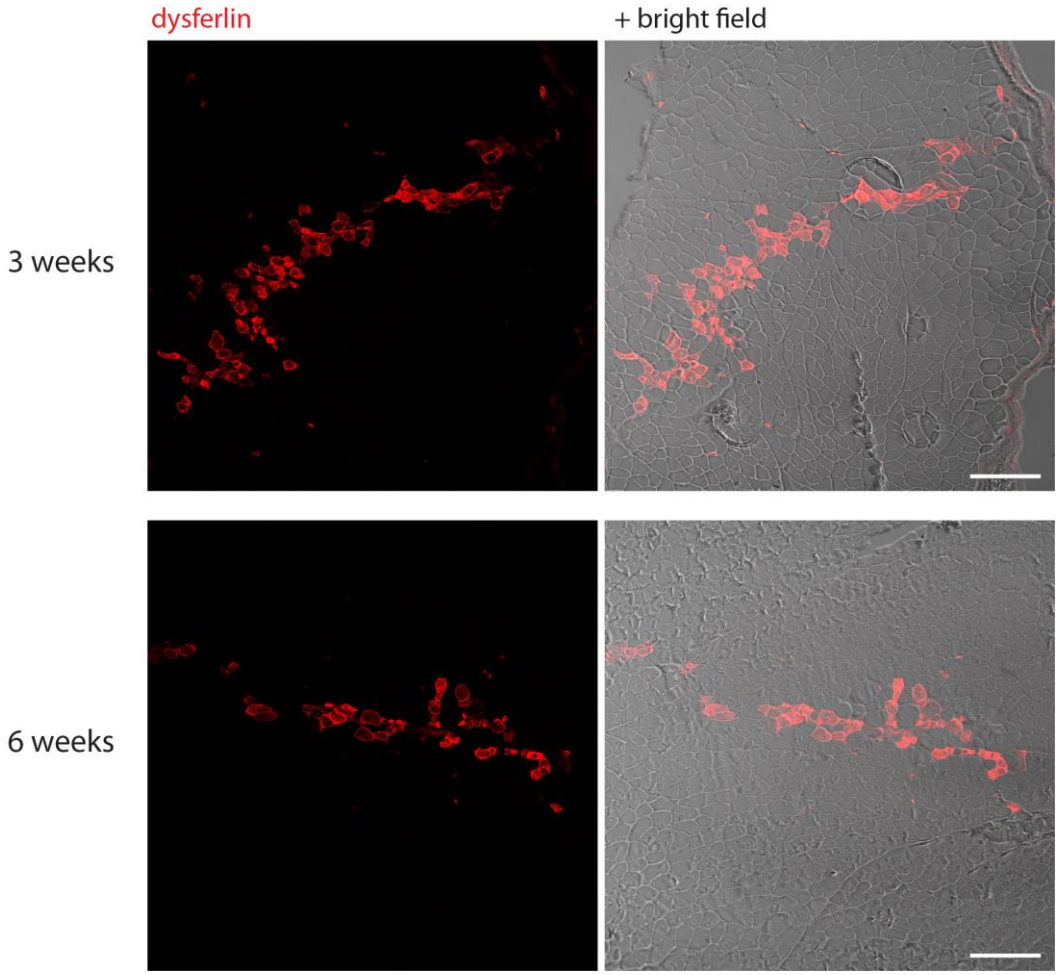

Figure 4. 11: Engraftment of corrected H2K A/J myoblasts in pre-irradiated muscles of Scid/blAJ mice.

Confocal microscopy images of cryosections prepared from grafted tibialis anterior muscles and immunostained with an antibody against dysferlin (red). Nuclei were counterstained with Hoechst (blue). Dysferlin positive fibers are distributed in longitudinally arranged groups, likely along the wound created by the injection trajectory, in muscles collected 3 weeks (top images) and 6 weeks (bottom images) after transplantation. Scale bars: 200 µm.

Next, we prepared cryosections of the collected muscles and performed immunostaining to detect dysferlin. In muscles pre-irradiated but not injected with cardiotoxin, we found ~30-90

and ~50 dysferlin positive fibers 3 and 6 weeks after transplantation, respectively (Figure 4. 11). The dysferlin positive fibers were distributed in longitudinally arranged groups in all muscle samples. This distribution may correspond to the regenerating area in the wound created by the injection trajectory through the muscle. Detailed analysis of the number of dysferlin positive fibers per stained cryosection and the distribution along the length of the grafted muscles can be found in Figure 4. 13.

Interestingly, the engraftment of the transplanted cells and the number of donor-derived myofibers were greatly enhanced by applying a double injury regime. With this model, ablation of the recipient muscles' endogenous satellite cells was accompanied by the induction of regeneration in response to acute damage. In all grafted muscles pre-irradiated with 18 Gy and injected with cardiotoxin, donor-derived fibers covered a large area of the cryosections both 3 and 6 weeks after transplantation. We found up to 1102 dysferlin positive fibers in cryosections from muscles collected after 3 weeks and up to 1029 after 6 weeks (Figure 4. 12). Detailed numbers of dysferlin positive fibers per stained cryosection can be found in Figure 4. 13.

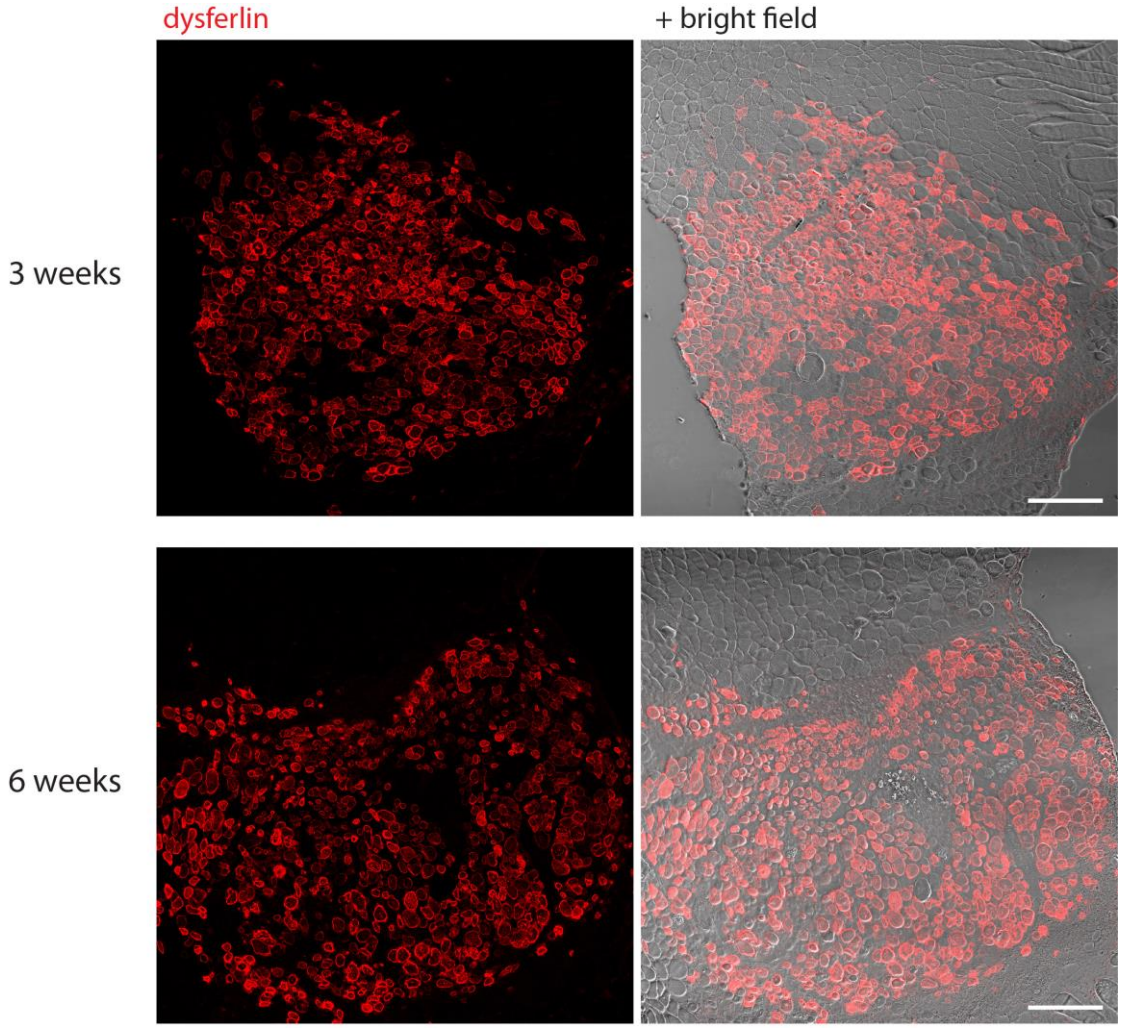

Figure 4. 12: Engraftment of corrected H2K A/J myoblasts in muscles pre-irradiated and injected with cardiotoxin.

Confocal microscopy images of cryosections prepared from grafted tibialis anterior muscles and immunostained with an antibody against dysferlin (red). Dysferlin positive fibers cover a large area of the cryosections from grafted muscles collected both 3 weeks (top images) and 6 weeks (bottom images) after transplantation. Scale bars: 200 µm.

The number of dysferlin positive fibers was consistent in all muscles grafted following the same injury regime, and was much higher in muscles that had been pre-irradiated and injured with cardiotoxin simultaneously to cell transplantation (Figure 4. 13 and Table 4. 2). We analyzed the distribution of dysferlin positive fibers along the length of the grafted muscles. The injection point was roughly in the middle of the muscle. We found that a large number of dysferlin expressing myofibers spread throughout several hundreds of µm in muscles that were co-injected with cardiotoxin (Figure 4. 13-B and Figure 4. 14). The maximum transversal area covered was approx. 1000 x 800 µm (mouse ID = 9). We found dysferlin expressing fibers spreading up to ~5 mm throughout the longitudinal axis of grafted muscles.

Mouse ID	Treatment[A]	Time (weeks)	Max. dysf+ fibers[B]
1	CTX	2	111
2	CTX	2	3
3	CTX	2	0
4	CTX	2	0
5	CTX	2	0
6	CTX + 18Gy	6	387
7	CTX + 18Gy	6	1029
8	CTX + 18Gy	3	477
9	CTX + 18Gy	3	1102
10	18 Gy	3	89
11	18 Gy	3	32
12	18 Gy	6	51
13	18 Gy	6	49

Table 4. 2: Transplantation of corrected H2K A/J myoblasts in Scid/blAJ mice.

[A]Cardiotoxin injection (CTX) and/or 18 Gy irradiation; [B]maximum number of dysferlin positive fibers in a single cryosection of the corresponding muscle (detected in confocal microscopy images of cryosections stained with an antibody against dysferlin).

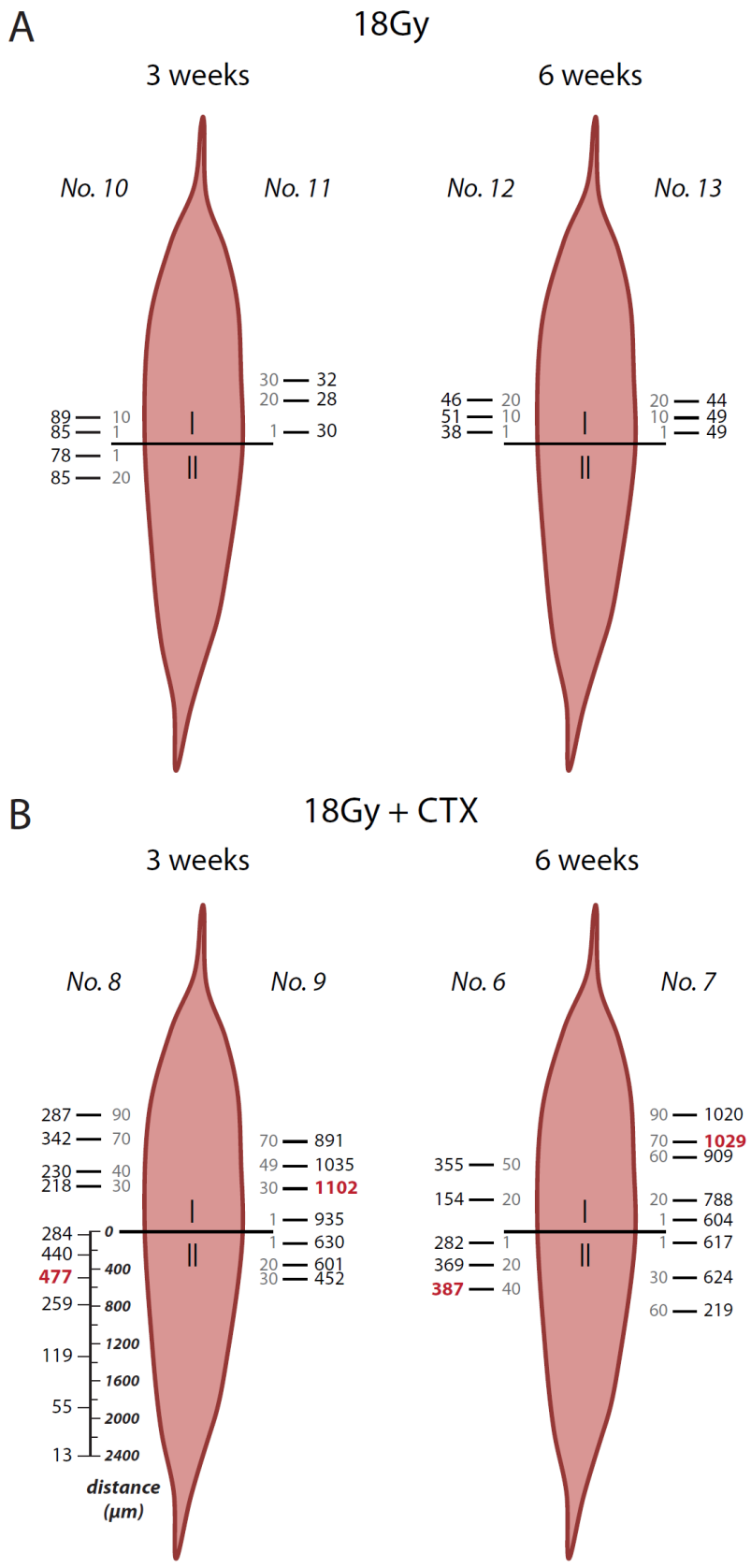

Figure 4. 13: Counts of dysferlin positive fibers in cryosections of grafted muscles.

Total number of dysferlin positive fibers in cryosections of grafted tibialis anterior muscles (A) pre-irradiated with 18 Gy or (B) pre-irradiated and injured with cardiotoxin simultaneously to cell injection. 6 µm cryosections were prepared from each muscle and stained with an antibody against dysferlin. The dysferlin positive fibers were counted on the confocal microscopy images of cryosections immunostained with an antibody against dysferlin. For freezing, the muscles were divided in two halves (I/II) along a transversal plane, and cryosections were prepared from each half starting from the middle of the muscle towards the tendon. The drawing represents the tibialis anterior muscle. The numbers of the cryosections analyzed from each muscle are indicated in grey. The position of the cryosections along the drawing intends to represent their physical distribution in the muscle (not in scale). The numbers of dysferlin positive fibers found in each individual cryosection are indicated in black. Each vertically aligned group of [cryosection – number of dysf+ fibers] corresponds to one grafted tibialis anterior muscle of one mouse (n = 2 per injury regime and time point of analysis). The mouse ID is indicated on top of each column. One muscle (No.8, II) was sectioned until the end and the distribution of dysferlin positive fibers along the muscle is shown as a function of the real distance in µm. I: proximal half of the muscle. II: distal half of the muscle. Red: largest number of dysferlin positive fibers found in one cryosection of the corresponding muscle.

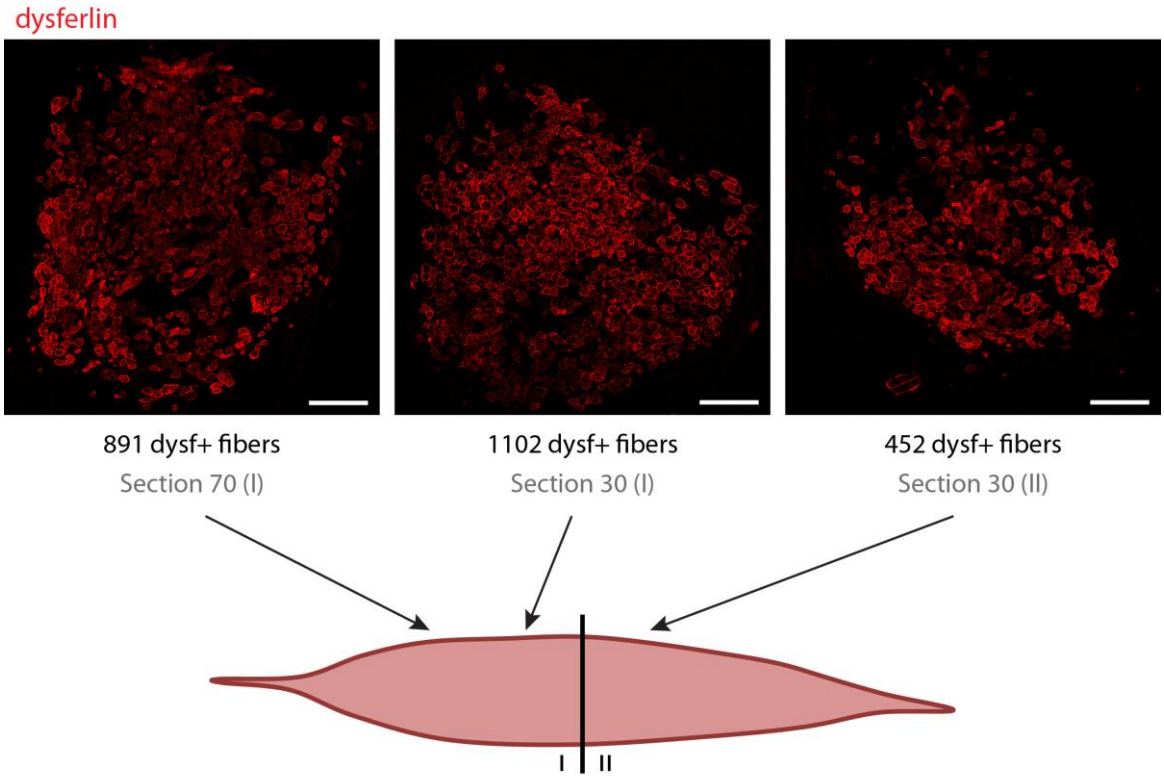

Figure 4. 14: Distribution of donor-derived myofibers along the grafted muscles.

Confocal microscopy images of cryosections from one muscle (treated with 18 Gy + cardiotoxin injection) 3 weeks after transplantation. The cryosections were immunostained with an antibody against dysferlin (red). The drawing represents the tibialis anterior muscle. The numbers of the cryosections corresponding to each image are indicated in grey. The numbers of dysferlin positive fibers found in each cryosection are indicated in black above the cryosection number. I: proximal half of the muscle. II: distal half of the muscle. Scale bars: 200 µm.

We decided to further compare the expression level of dysferlin in donor-derived myofibers of grafted muscles to the endogenous level of dysferlin protein in mouse wild type muscles. For that purpose, I simultaneously stained cryosections of grafted tibialis anterior muscles and from C57BL/6J quadriceps muscles with an antibody against dysferlin and imaged them with the same confocal microscope and settings. I found the levels of dysferlin to be much higher in donor-derived myofibers from muscles grafted with corrected H2K A/J myoblasts than in myofibers of wild type muscles (Figure 4. 15-A).

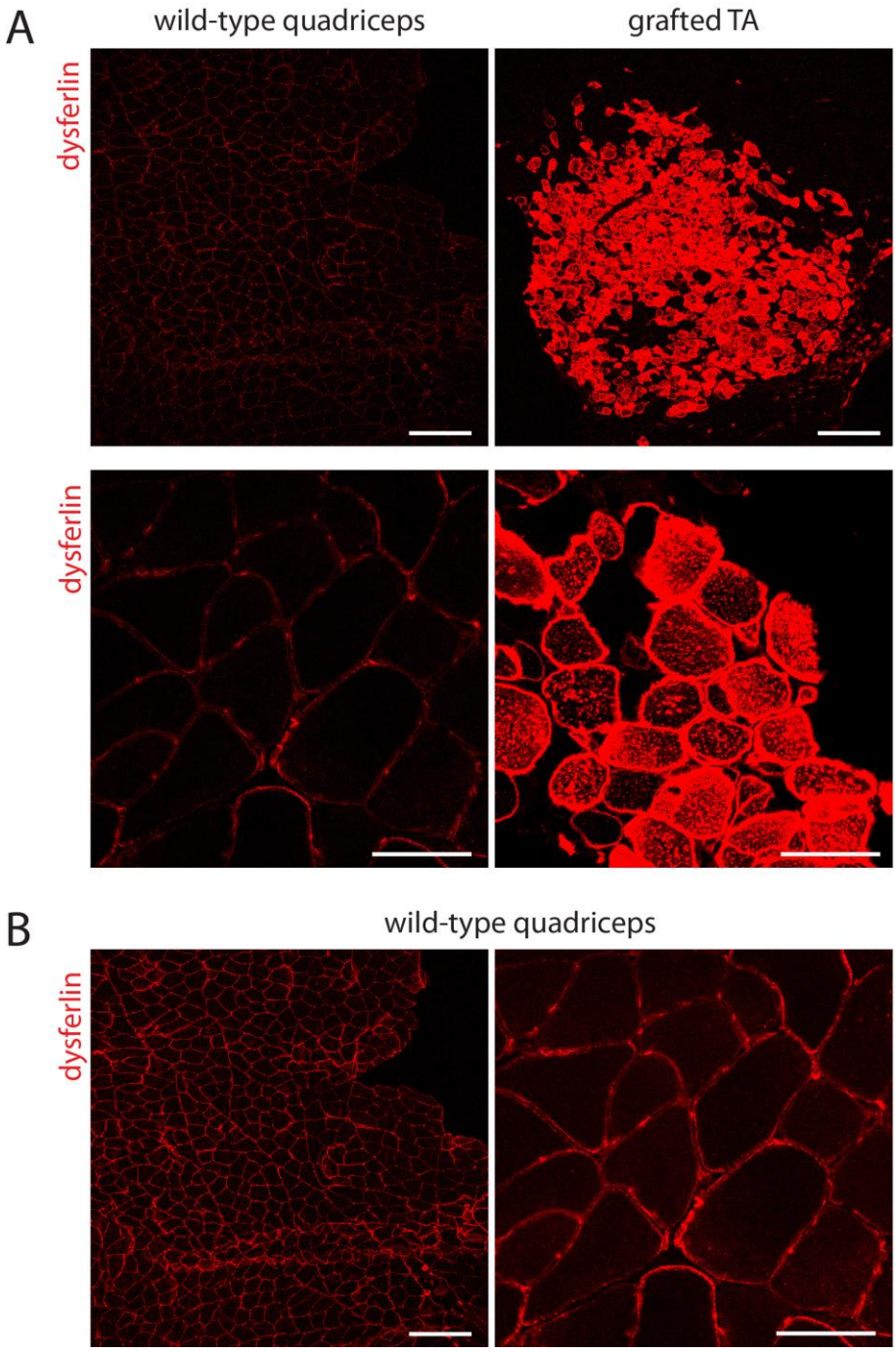

Figure 4. 15: Dysferlin expression level in donor-derived myofibers of grafted muscles.

(A) Confocal microscopy images of cryosections from quadriceps muscles of a C57BL/6J mouse and one grafted tibialis anterior muscle of a Scid/blAJ mouse (treated with 18 Gy + cardiotoxin injection) 3 weeks after grafting of corrected myoblasts. The cryosections from the control and grafted muscles were simultaneously stained with an antibody against dysferlin (red) and the images were obtained with the same microscope and settings for both the lower and the higher magnifications. Scale bars: 200 µm (top images) and 50 µm (bottom images). (B) Confocal microscopy images of cryosections from quadriceps muscles of a C57BL/6J mouse (same areas as in A) obtained with different microscopy settings to better visualize the pattern of dysferlin protein (red) immunostaining in wild type mouse muscles. Scale bars: 200 µm (left) and 50 µm (right).

4.5.2 Dysferlin localization in donor-derived myofibers

A proper localization is crucial for the function of any protein. In skeletal muscle *in vivo*, dysferlin localizes at the sarcolemma (Anderson et al., 1999) and the T-tubule network (Ampong et al., 2005; Y. Huang et al., 2007; Kerr et al., 2013; Klinge et al., 2010; Klinge et al., 2007; Piccolo et al., 2000; Roche et al., 2011) of myofibers. The function of sarcolemmal dysferlin has been classically associated with the repair of membrane wounds (Bansal et al., 2003). On the other hand, potential roles for dysferlin in T-tubulogenesis during muscle regeneration and in the maintenance of the T-tubule structure in mature fibers have been described more recently (Kerr et al., 2013; Klinge et al., 2010). Importantly, the localization pattern of dysferlin observed in muscle sections may vary depending on the fixation and immunostaining procedures (Roche et al., 2011).

I examined the localization of human dysferlin in donor derived myofibers from grafted muscles of Scid/blAJ mice, and found it predominantly enriched at the membrane of most dysferlin expressing myofibers. Some of the fibers with a sarcolemmal staining of dysferlin also presented a fainter cytoplasmic stain in the form of irregularly distributed puncta (Figure 4. 16 and Figure 4. 17). However, in some of the fibers we could observe a cytoplasmic stain in a regular reticular pattern (Figure 4. 17) characteristic of intracellular dysferlin.

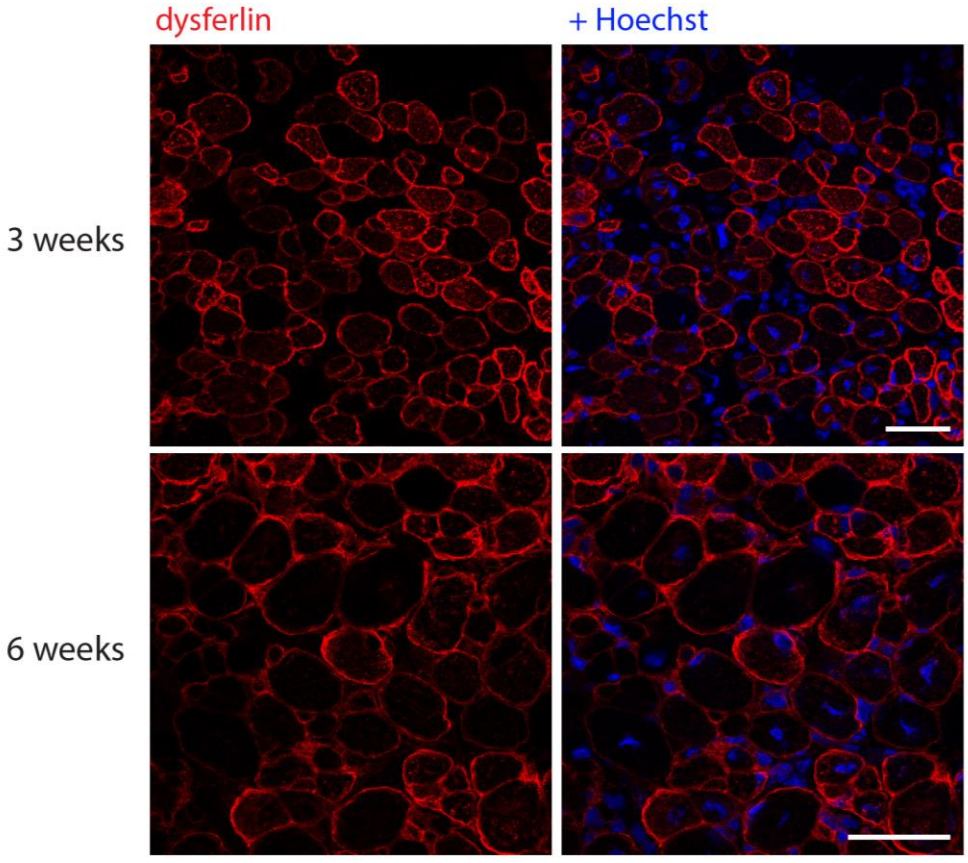

Figure 4. 16: Dysferlin localization in grafted muscles.

Confocal microscopy images of cryosections from grafted tibialis anterior muscles of Scid/blAJ mice (18 Gy + injection of cardiotoxin) 3 and 6 weeks after injection of corrected H2K A/J myoblasts. The cryosections were immunostained with an antibody against dysferlin (red). Nuclei were counterstained with Hoechst (blue). Scale bars: 50 µm.

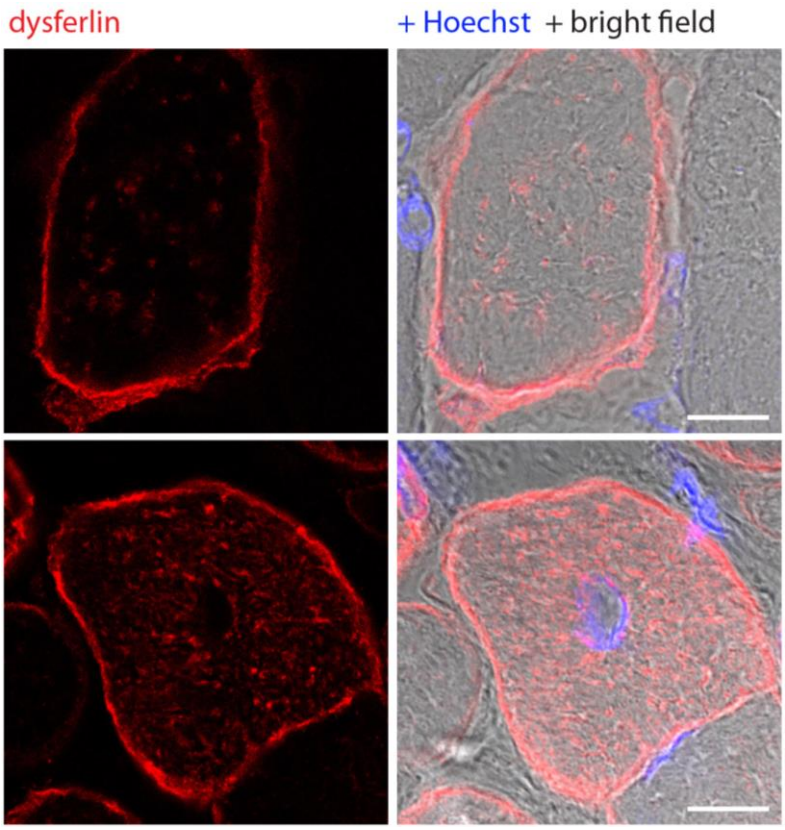

Figure 4. 17: Distinct patterns of dysferlin localization in donor-derived myofibers.

High magnification confocal microscopy images of dysferlin (red) immunostaining in donor-derived myofibers from muscles grafted with corrected H2K A/J myoblasts. In all fibers dysferlin was enriched at the sarcolemma. Some of the fibers presented an irregular punctate cytoplasmic stain (top images) and others presented a cytoplasmic stain in a regular reticular pattern characteristic of intracellular dysferlin (bottom images). The cryosections were immunostained with an antibody against dysferlin (red). Nuclei were counterstained with Hoechst (blue). Scale bars: 10 µm.

We hypothesized that the finding of dysferlin in irregular intracellular puncta in some fibers could be due to an inability of our staining method to properly label cytoplasmic dysferlin or to the presence of protein aggregates due to the high level of dysferlin in donor-derived myofibers.

4.5.3 Histological features of grafted muscles

Next, we examined the histological features of the grafted muscles. It should be noted that the onset of symptoms in Scid/blAJ mice is approximately at 5 months of age. The examined mice were 11-15 weeks old at the time of transplantation and the muscles were collected for analysis 3-6 weeks later. Therefore, the pathological features characteristic of dysferlin deficient skeletal muscle should be very mild or not yet apparent in those mice.

Grafted muscles injured only with cardiotoxin and collected after 2 weeks displayed the typical characteristics of regenerating muscles, with a majority of centrally nucleated fibers. Donor derived, dysferlin expressing myofibers did not have any distinctive histological features from non-donor-derived fibers (Figure 4. 18-B and Figure 4. 19).

The dysferlin positive fibers found in grafted muscles subjected only to 18 Gy radiation were easily identified in the histological stains due to their distribution in clusters along what appeared to be the injection trajectory. Moreover, they presented distinctive histological characteristics from non-donor-derived myofibers and had features of regeneration such as central nucleation with big nuclei, small size, irregular architecture and stronger NADH stain. In contrast, the surrounding areas of non-donor derived fibers had barely any centrally nucleated fibers and were not histologically different from non-grafted muscles irradiated with 18 Gy (Figure 4. 18-B and Figure 4. 19).

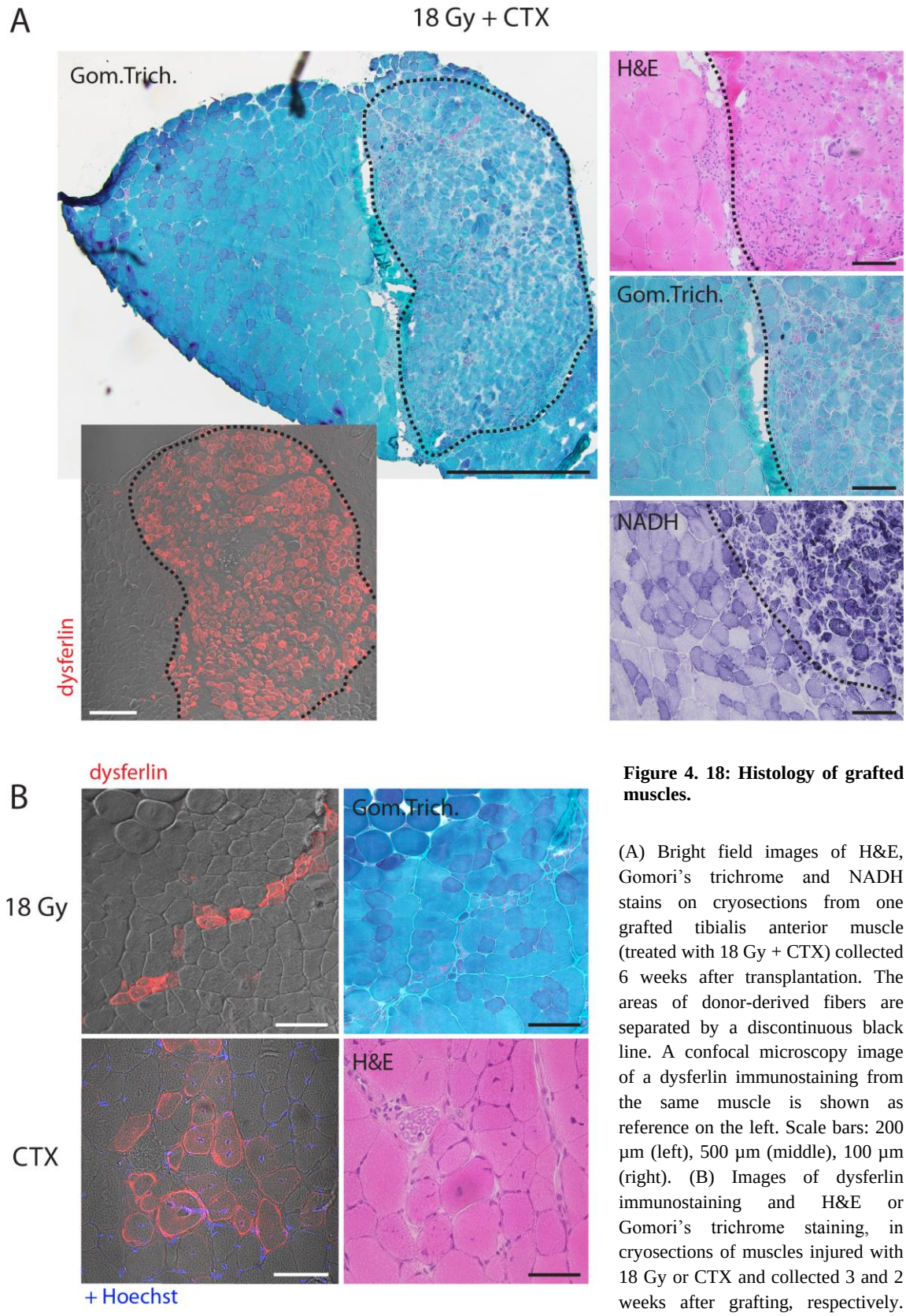

Figure 4. 18: Histology of grafted muscles.

(A) Bright field images of H&E, Gomori's trichrome and NADH stains on cryosections from one grafted tibialis anterior muscle (treated with 18 Gy + CTX) collected 6 weeks after transplantation. The areas of donor-derived fibers are separated by a discontinuous black line. A confocal microscopy image of a dysferlin immunostaining from the same muscle is shown as reference on the left. Scale bars: 200 µm (left), 500 µm (middle), 100 µm (right). (B) Images of dysferlin immunostaining and H&E or Gomori's trichrome staining, in cryosections of muscles injured with 18 Gy or CTX and collected 3 and 2 weeks after grafting, respectively. The images on the left and right are from the same areas containing donor-derived fibers. A more detailed histological analysis of those areas is shown in figure 4.18. Scale bars: 100 µm (top), 50 µm (bottom).

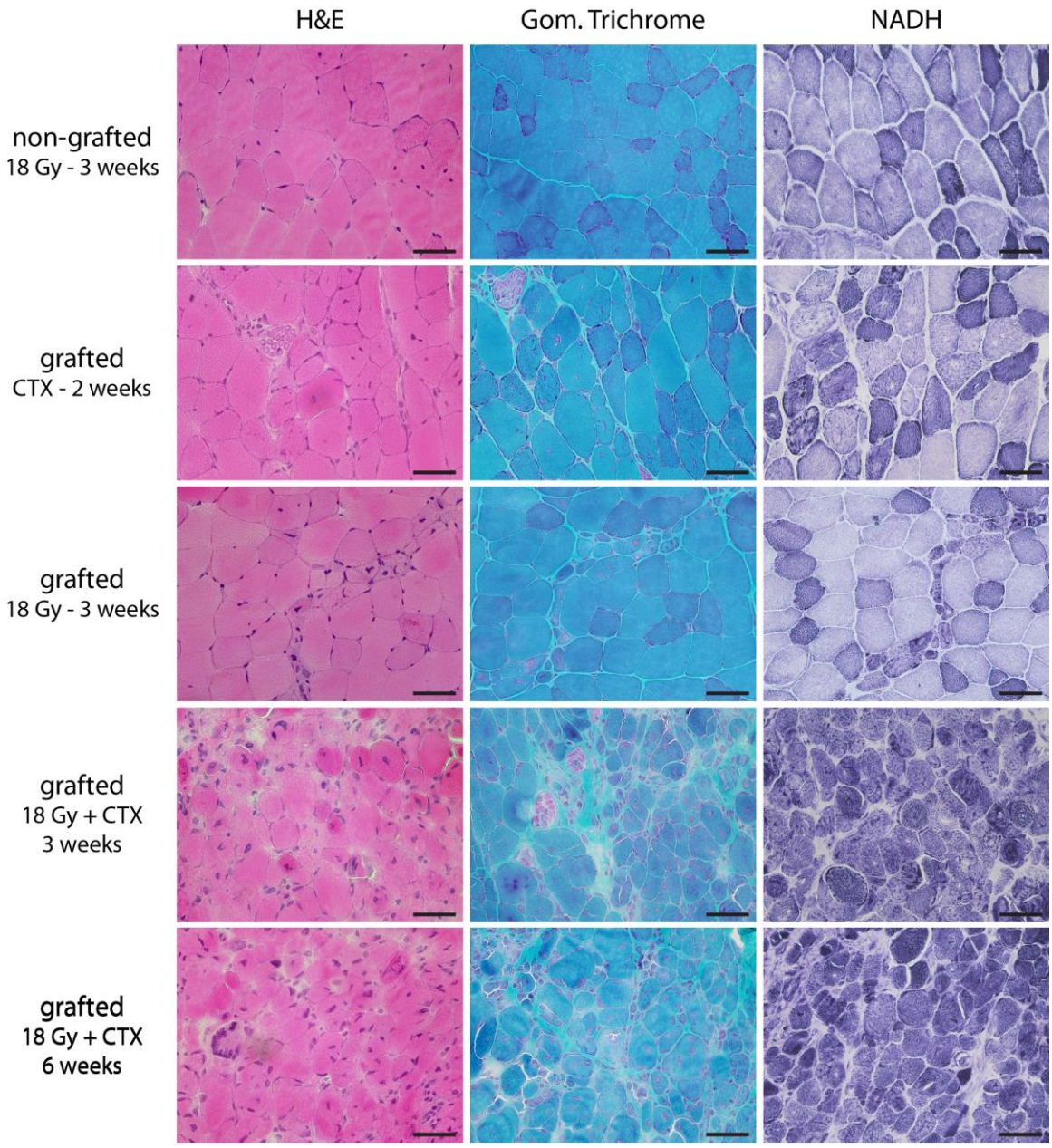

Figure 4. 19: Histological features of donor-derived myofibers.

Bright field images of H&E, Gomori's trichrome and NADH stains performed on cryosections from tibialis anterior muscles of Scid/blAJ mice. The muscles were grafted under different injury regimes and collected at the indicated time points after transplantation of corrected H2K A/J myoblasts. The images show areas containing dysferlin positive myofibers of donor origin. Sections of a non-grafted tibialis anterior muscle from an age-matched Scid/blAJ mouse irradiated with 18 Gy and collected 3 weeks later are shown above as control. Scale bars: 50 µm.

In grafted muscles that were pre-irradiated and injured with cardiotoxin, the large areas enriched in donor-derived myofibers were clearly distinguishable from the areas with no dysferlin expressing fibers regarding architecture of myofibers and connective tissue and fiber type distribution. Both regions seemed to be separated by an area of connective tissue and mononuclear cell infiltrates (Figure 4. 18-A). When closely examining areas of the grafted muscles that contained mainly donor-derived fibers, we found that the overall architecture was

irregular in muscles collected either 3 or 6 weeks after grafting. Most of the fibers were centrally nucleated (best noticeable in the H&E stain), had very variable fiber sizes and were strongly stained with NADH, without any clear distinction of fiber types. The connective tissue was increased as evidenced by the Gomori's trichrome stain. The acid phosphatase stain shows that these areas contained positively stained foci, indicative of macrophage infiltration or lipofuscin. They were not present in the areas lacking donor-derived fibers from the same muscles. The stained foci appeared to be not within muscle fibers but rather in the interstitium (Figure 4. 20). Positively stained acid phosphatase granules could also indicate myofiber necrosis. However, necrotic myofibers generally display a pale Gomori's trichrome and NADH stain, which does not appear to be the case in those areas (Figure 4. 19).

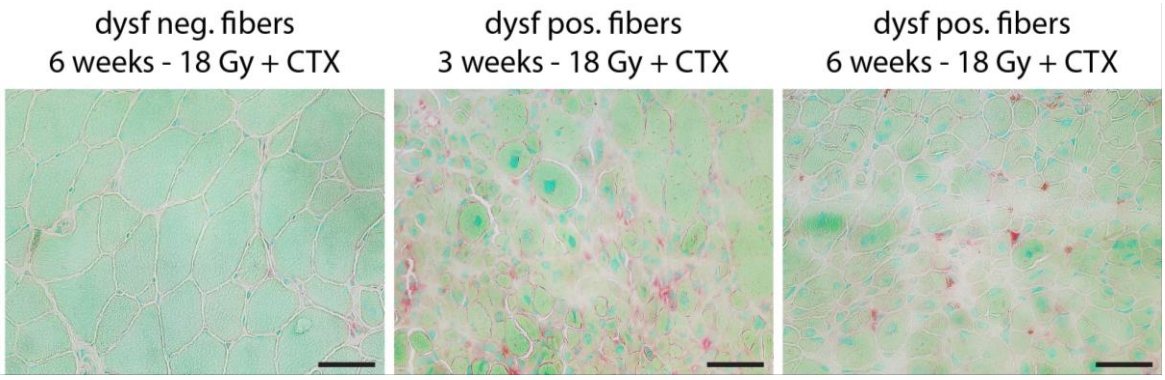

Figure 4. 20: Acid phosphatase foci in areas formed by donor-derived myofibers.

(A) Bright field microscopy images of an acid phosphatase stain in cryosections prepared from grafted muscles subjected to 18 Gy radiation and CTX injection and collected 3 or 6 weeks after transplantation of corrected H2K A/J myoblasts. The middle and right images show areas formed mostly by donor-derived myofibers. The left image shows a representative area without donor-derived fibers from the same muscle as the one shown on the right image. Scale bars: 50 μm.

4.5.4 Donor-derived Pax7+ cells in the grafted muscles

The intrinsic turnover of myonuclei during both homeostasis and regeneration of skeletal muscle is further increased in muscle disorders that induce a degenerative environment (Morgan & Zammit, 2010). Since myonuclei are postmitotic, a long-term therapeutic effect of cell transplantation can only be achieved by repopulation of the satellite cell compartment with the cells of donor origin, which would ensure a long-lasting contribution of the latter to muscle regeneration in pathological circumstances.

I analyzed the satellite cell compartment of the muscles that received a graft following local irradiation, which would have presumable ablated the endogenous satellite cells. As mentioned in page 15, satellite cells are unequivocally identified in skeletal muscle by their expression of the transcription factor Pax7 (Seale et al., 2000) and their localization beneath the basal lamina of myofibers (Mauro, 1961). However, they can also migrate between fibers and muscles during development (Hughes & Blau, 1990) and regeneration (Watt et al., 1987). I performed immunostaining of Pax7 and the basal lamina component laminin in cryosections from grafted muscles. Since it was not possible to obtain a high quality double immunostaining of Pax7 and dysferlin or Pax7 and GFP, first I stained various cryosections along grafted muscles with an antibody against dysferlin. Once I confirmed the continuous presence of large areas with dysferlin positive myofibers along grafted muscles, I stained serial cryosections before and after with

antibodies against Pax7 and laminin. I utilized the images of dysferlin immunostaining as a reference to find areas enriched in donor-derived myofibers (Figure 4. 21). I found numerous Pax7 expressing cells in some areas enriched in dysferlin positive fibers. The myofiber architecture of those areas was not fully organized and the same was true for the basal lamina, as indicated by the laminin immunostaining (Figure 4. 22). However, some Pax7 positive cells appeared to be located beneath the basal lamina of forming myofibers, and most were interstitial (Figure 4. 22-C).

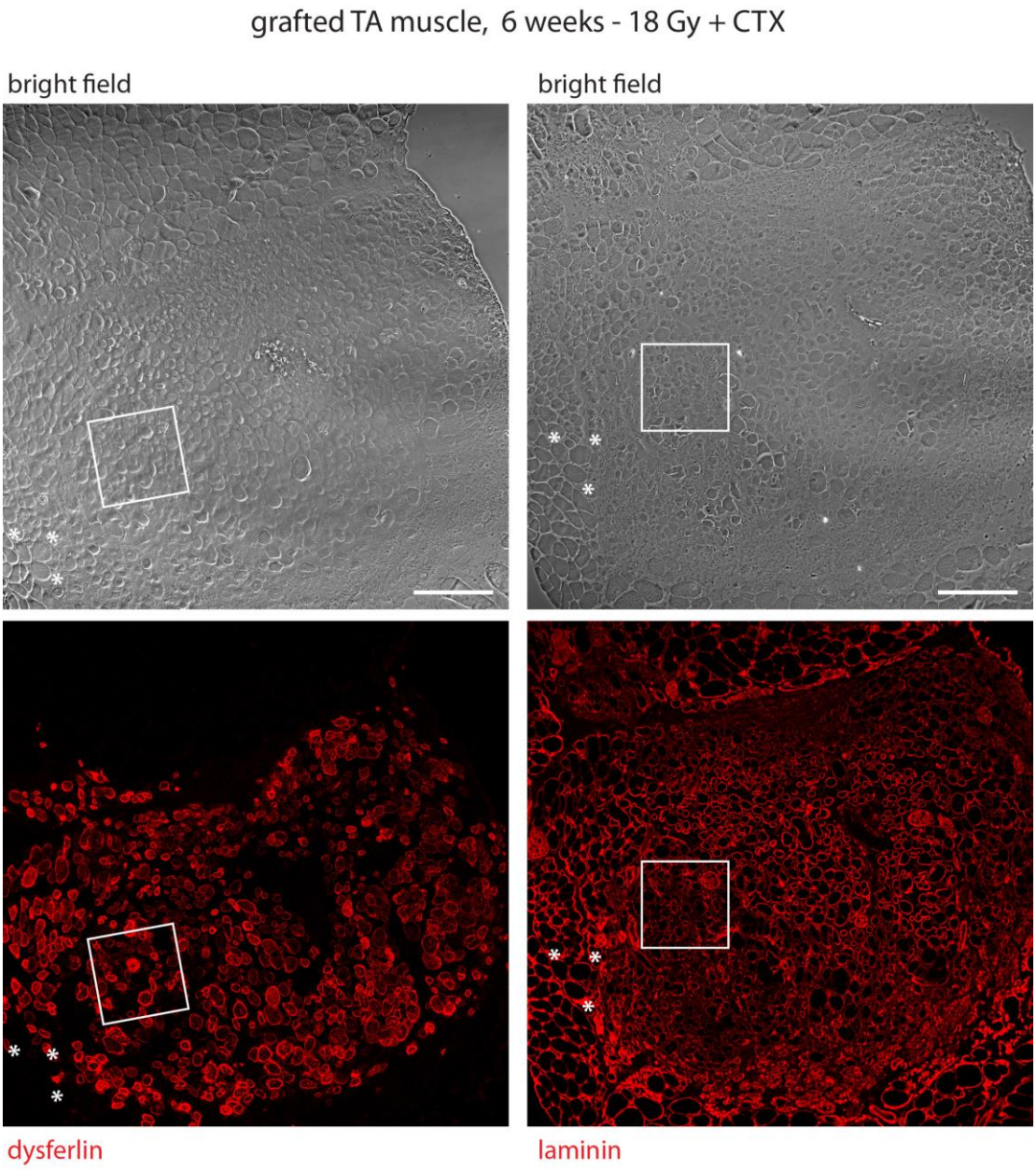

Figure 4. 21: Overview of laminin immunostaining in areas of donor derived myofibers in grafted muscles.

Confocal microscopy images of the same area in serial cryosections from one tibialis anterior muscle collected 6 weeks after transplantation of corrected H2K A/J myoblasts (injury regime: 18 Gy + cardiotoxin). The cryosections were immunostained with antibodies against dysferlin (left, red) and laminin (right, red). The square and asterisks mark the same areas of the muscle in the two images. Scale bars: 200 µm.

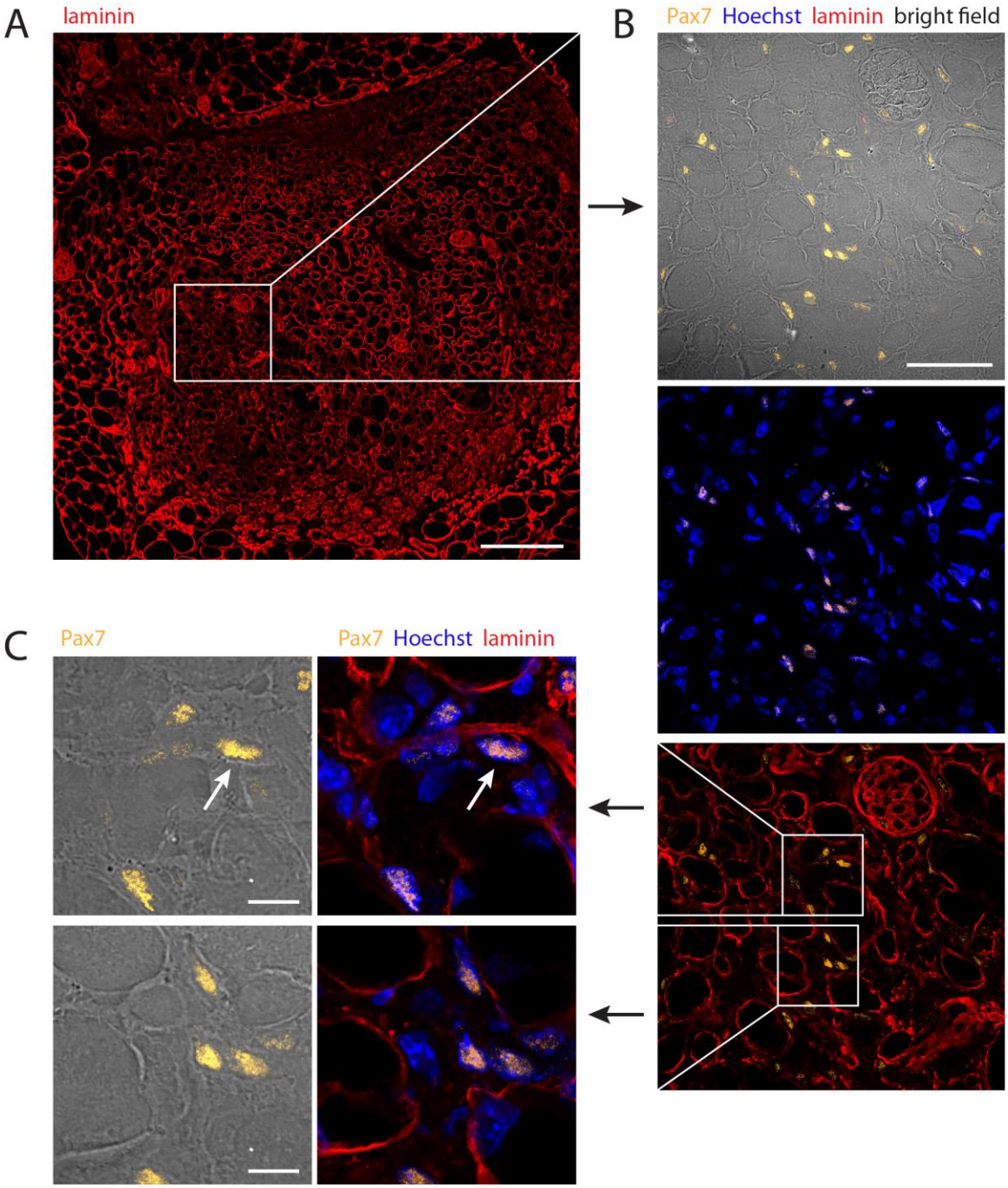

Figure 4. 22: Pax7+ cells in the vicinity of donor-derived myofibers in grafted muscles.

Confocal microscopy images of one cryosection from one grafted tibialis anterior muscle (same as in Figure 4. 21) immunostained with antibodies against Pax7 (yellow) and laminin (red). Nuclei were counterstained with Hoechst (blue). (A) Overview of laminin (red) immunostaining. Scale bar: 200 µm. (B) Higher magnification of an area from A containing numerous Pax7+ (yellow) cells. Scale bar: 50 µm. (C) Higher magnification of two areas with abundant Pax7+ (yellow) cells from B. One Pax7 expressing cell (arrow) appeared to be located underneath a basal lamina (red) structure and the rest are interstitial. Scale bar: 10 µm.

The GFP signal was detectable, although faint, in dysferlin expressing myofibers. Additionally, we found that lipofuscin, which was enriched in donor-derived areas of grafted muscles, accumulated also around nuclei, producing a strong green autofluorescence. This made

the identification of donor-derived satellite cells based on their GFP expression (unstained) unviable. We concluded that, in order to attain definitive proof of the presence of donor-derived satellite cells, a double GFP/Pax7 or dysferlin/Pax7 staining would be necessary.

4.6 Human satellite cells for muscle regeneration and gene therapy

In the previous sections I have described a therapeutic strategy for the treatment of dysferlinopathy based on *ex vivo* gene transfer into muscle. The results of this proof-of-concept preclinical study have provided evidence of dysferlin protein reconstitution in the skeletal muscle of a disease model *in vivo* using mouse myoblasts as a source of grafting material. In order to make our approach more relevant for therapy, we ultimately aim to target and phenotypically correct human muscle stem cells.

In our recently reported method for isolation of human muscle fiber fragments (HMFFs), we do not use any enzymatic digestion, thus preserving the basal lamina. The satellite cells contained in their niche within these HMFFs extensively proliferate in culture, maintaining their expression of Pax7 for prolonged periods of time *ex vivo* (Marg et al., 2014).

4.6.1 Regenerative potential of human satellite cells in HMFFs

In order to assess the regenerative potential of these *ex vivo* expanded human satellite cells, we performed intramuscular transplantation of HMFFs in NOG mice. We chose this mouse strain because of its total absence of adaptive immunity and compromised innate immunity, which make it a suitable model for xenograft studies. Unlike SCID mice, they do not show leakiness of T and B lymphocytes with increasing age and are therefore very unlikely to develop immune rejection against grafts (Ito et al., 2002). We transplanted HMFFs derived from four biopsy donors and cultured for 5-7 days into tibialis anterior muscles of 6-8 week old female NOG mice (n = 23). The recipient muscles were either not subjected to any injury regime or pre-irradiated with 18 Gy using the focal irradiation protocol described in Figure 4. 8. We used a human-specific antibody against the nuclear envelope protein lamin A/C in order to identify human nuclei in the grafted muscles. In muscles grafted without irradiation and collected either 3 or 7-8 weeks after transplantation, we found a small number of human nuclei (Table 4. 3). Almost all of them were interstitial and were not part of myofibers (Figure 4. 23). However, in muscles that were irradiated with 18 Gy before transplantation of HMFFs, we found a much larger number of human nuclei either 3 or 7-8 weeks after grafting (Table 4. 3).

Donor[A]	Irradiation dose	Successful transplantations[B]	Human cells after 3 weeks[C]	Human cells after 7-8 weeks[C]	Donor-derived myofibers
44 f, 47 f	No	9/10	5-150	5-50	No
53 m	9 Gy	1/3	5-50	n.t.	No
53 m, 64 f	18 Gy	8/10	5-300	5-300	Yes

Table 4. 3: Transplantation of HMFFs in NOG mice.

[A]Age in years and gender; [B]transplants with human cells per total number of transplanted tibialis anterior muscles; [C]number of human nuclei per cryosection. f, female; m, male; n.t., not tested. Table modified from (Marg et al., 2014).

Some of the human nuclei were interstitial, but many were participating in regeneration or integrated in myofiber structures at later time points (Figure 4. 23). We also performed transplantation of HMFFs in tibialis anterior muscles of NOG mice irradiated with a lower dose of 9 Gy. However, the engraftment was much less efficient than with 18 Gy, as indicated by the lower number of human nuclei found 3 weeks after transplantation. We also failed to detect human nuclei forming part of myofiber structures or participating in regeneration. This suggests that 9 Gy were not sufficient for ablation of the host muscle's satellite cells (Table 4. 3).

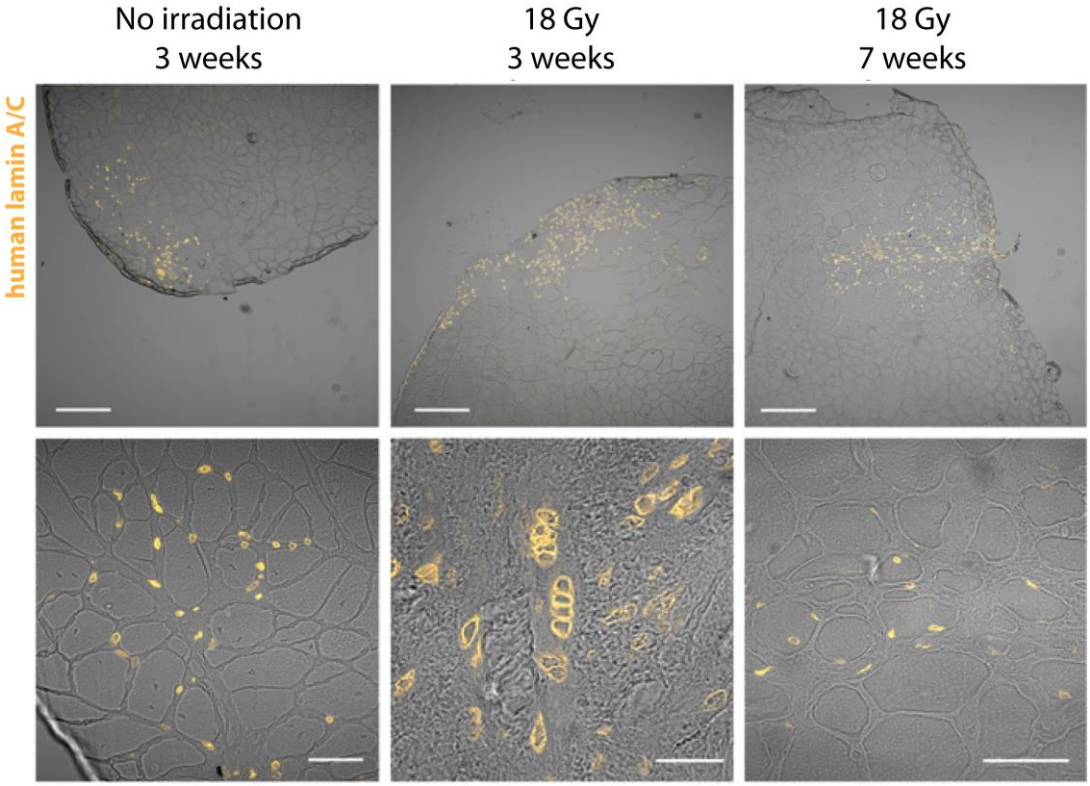

Figure 4. 23: Engraftment of human satellite cells in muscles from NOG mice.

Confocal microscopy images of human lamin A/C immunostaining in cryosections from grafted tibialis anterior muscles of NOG mice. The muscles were collected 3 or 7 weeks after transplantation. Human cells were located in the muscle interstitium 3 weeks after transplantation in non-irradiated muscles (left images). In muscles pre-irradiated with 18 Gy, many human nuclei were part of myofiber structures 7 weeks after transplantation (right images) and some were forming myotubes 3 weeks after transplantation (middle images). This figure is modified from (Marg et al., 2014).

4.6.2 Transfection of human satellite cells in HMFFs

Next, we asked whether human satellite cells could be genetically manipulated *ex vivo* in HMFFs. In muscle disorders where gene transfer would be of therapeutic benefit, *ex vivo* engineering of human satellite cells while maintaining their regenerative potential would be a great advancement towards harnessing autologous transplantation as a therapy.

We showed that numerous fluorescent cells, likely satellite cells, were present within HMFFs transfected with a transposon-based Venus reporter vector and SB100X transposase. Moreover, the fluorescent cells persisted for several weeks and gave rise to myotubes once they migrated outside of the HMFFs and formed colonies, indicating that they preserved their

myogenic capacity (Marg et al., 2014). Here, I show the presence of abundant GFP+ cells in HMFFs 7 days after transfection with pT2-CAG-GFP and SB100X transposase (Figure 4. 24).

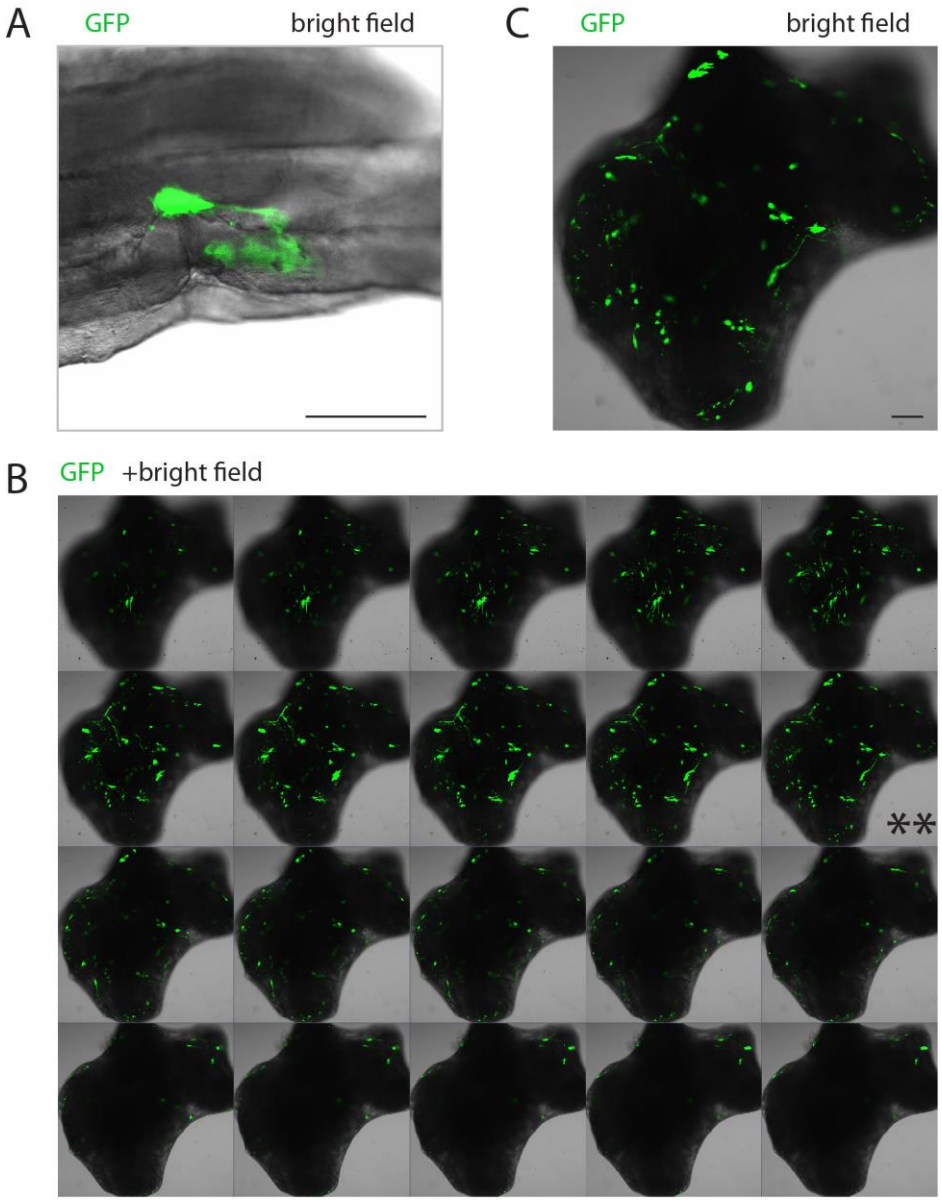

Figure 4. 24: Transfection of human satellite cells in HMFFs.

Confocal microscopy images of GFP+ (green) cells in HMFFS transfected with pT2-CAG-GFP and an expression vector for SB100X transposase. (A) High magnification of GFP+ cells, presumable satellite cells, inside of a fiber bundle 2 days after transfection. (B) Z-stack showing numerous GFP+ cells within a fiber bundle 7 days after transfection. (C) Enlarged image from B**. The HMFFs often contract forming globular structures after several days in culture.

The possibility to introduce DNA vectors in human satellite cells within HMFFs offers a very encouraging platform towards genetic manipulation of cells highly relevant for therapy. In the future, we hope to be able to introduce larger therapeutic cassettes such as the CDS of genes that are mutated in some muscular dystrophies, e.g. dysferlin, into human satellite cells *ex vivo*, and transplant them into the skeletal muscle of disease models.

5 Discussion

Dysferlinopathy is a devastating disease for which no therapy is available. It is caused by mutations in a single gene, *DYSF* (Bashir et al., 1998; J. Liu et al., 1998). Therefore restoring dysferlin expression through gene therapy holds great promise as a treatment. However, the large size (~6.2 kb) of the dysferlin coding sequence hampers the use of viral vectors for gene transfer approaches to treat dysferlinopathy. Transfer of a truncated but partially functional minidysferlin into dysferlin-null mice using AAV vectors restored the membrane repair deficit in myofibers (Krahn et al., 2010) but did not improve the muscle pathology (Lostal et al., 2012). Thus, gene therapy approaches need to be based on restoration of full-length dysferlin. Our aim was to develop a cell-based gene therapy approach for full-length dysferlin reconstitution in the skeletal muscle of dysferlin-null mice. We have focused our investigation on *ex vivo* engineering of dysferlin-null mouse myoblasts using SB as a gene transfer tool.

Dual AAV vector strategies have been used with success to restore dysferlin protein in the skeletal and cardiac muscles of dysferlin-null mice (Grose et al., 2012; Lostal et al., 2010; Sondergaard et al., 2015). The last reports have additionally provided very encouraging results in non-human primates, suggesting that this strategy could be soon translated into a clinical application (Sondergaard et al., 2015). However, AAV vectors target mature muscle fibers but not satellite cells, and are non-integrating. On the one hand, this represents an advantage because they generally pose no risk of insertional mutagenesis, even though random vector integrations can occur at low frequency (Mingozzi & High, 2011). However, muscle tissue homeostasis includes recycling of myonuclei, which are provided by activation and proliferation of satellite cells. Mouse skeletal muscle has been shown to undergo less myonuclei turnover between 12 and 20 months of age, although the extent of this decrease depends on the muscle. Also, satellite cells do contribute to generate new myonuclei even in sedentary muscles of aged mice albeit with varying frequencies (Keefe et al., 2015). The extent of myonuclei turnover and its variation with age, however, have not been studied for human skeletal muscle. Besides, disease conditions that promote degeneration, like dysferlinopathy or other muscular dystrophies, are likely to induce a higher degree of myonuclei turnover (Morgan & Zammit, 2010). Accordingly, a greater number of centrally nucleated fibers expressing markers of regeneration can be observed in muscle biopsies from dysferlinopathy patients (Chiu et al., 2009). This means that non-self-replicating episomal vectors, like AAV genomes, will be progressively eliminated as myonuclei are replaced. Therefore, a long-term therapeutic effect would require repeated vector administrations. Second exposures to the vector would likely result in immune responses against the viral capsid and the need for immunosuppression.

A drawback of gene transfer or *trans*-splicing approaches is that typically only one coding sequence is supplied. For a gene like *DYSF*, coding for multiple transcript variants and protein isoforms, restoring the expression of only one isoform may not be sufficient for fully rescuing function. For example, the cleavage of dysferlin to generate mini-dysferlin$_{C72}$, which has an important role in membrane repair, is done in the domain encoded by the alternatively spliced exon 40a (Redpath et al., 2014). Also, the C2A and C2Av1 domains likely have a different function based on their differential Ca^{2+} and phospholipid binding affinities (Fuson et al., 2014). In *ex vivo* and *in vivo* gene addition as well as *trans*-splicing approaches, it could be considered to deliver vectors or transplant engineered cells carrying various cDNA variants. In this way, all or most protein isoforms could be expressed in the target tissue.

Exon skipping has worked well for restoring dystrophin expression in animal models and has resulted in a moderate protein rescue in patients (van Deutekom et al., 2007). For dysferlinopathy, exon skipping has been successfully used to restore proper dysferlin mRNA and protein through targeting of exons 32 and 44 (Dominov et al., 2014; Wein et al., 2010). However, unlike dystrophin mutations, responsible for DMD and BMD, disease-causing mutations in *DYSF* are scattered all along the gene and there is no mutational hot-spot (Cacciottolo et al., 2011; Krahn et al., 2009). This is an important consideration when designing strategies to restore dysferlin function through gene therapy. Also, the knowledge about the dispensability of domains in dysferlin protein in relation to conservation of protein function is not yet clear. An additional limitation of exon skipping approaches is the consideration of each antisense molecule as an individual medicinal product by the FDA. Therefore, each one of them needs to undergo a separate clinical development to be used in patients. Even if successful, exon skipping does not operate at 100% efficiency.

Unlike CD133+ cells or mesoangioblasts, which have demonstrated a robust engraftment capacity in skeletal muscle tissue when delivered both locally and systemically (Diaz-Manera et al., 2010; Galvez et al., 2006; Guttinger et al., 2006; Negroni et al., 2009; Sampaolesi et al., 2006; Torrente et al., 2004), satellite cells and myoblasts can only be transplanted directly into the muscle (Briggs & Morgan, 2013). Also, they are available in low numbers and they lose part of their regenerative potential when cultured *ex vivo* prior to re-implantation (Briggs & Morgan, 2013). These factors clearly limit their therapeutic use in regenerative medicine. However, they are the true myogenic cell population and the best characterized from all the muscle stem cell types (Tedesco et al., 2010; Yin et al., 2013). Alike satellite cells, CD133+ cells also lose regenerative potential after *ex vivo* expansion (Meng et al., 2014). A very important factor regarding the choice of cell type in regenerative therapies for skeletal muscle is that satellite cells are indispensable for adult muscle regeneration. Their ablation in adult muscle abolishes the regenerative activity of other cell types with known regenerative potential (Lepper et al., 2011; Sambasivan et al., 2011). There have been remarkable advances in myogenic cell derivation from human and mouse iPS cells, seemingly overcoming some of the limitations of satellite cells and myoblasts for regenerative medicine. For example, these induced myogenic cells are derived from highly proliferative pluripotent cells which can be genetically engineered and are an unlimited source of starting material. Also, once derived into a myogenic lineage, they can still be expanded *in vitro* and they can engraft in skeletal muscle following systemic transplantation. However, intramuscular transplantation is still the most effective (Filareto et al., 2013). The optimization of protocols for myogenic cell derivation appears to have succeeded in the generation of committed progenitors that do not form tumors upon engraftment (Darabi et al., 2012; Darabi & Perlingeiro, 2014). However, there are still many safety concerns in the use of iPS-derived cells for regenerative medicine.

Dysferlinopathy affects only certain groups of muscles that vary depending on the clinical manifestation (see page 11). Some of those muscles are accessible for intramuscular cell injections. Importantly, it has been shown in mice that the environment of mature adult dystrophic muscle is receptive for donor satellite cell engraftment and long-term contribution to regeneration (Boldrin et al., 2009). Also, mouse satellite cells that reside in dystrophic muscles of aged *mdx* mice, retain their regenerative capacity. They can engraft with similar efficiency to satellite cells isolated from healthy muscles once they are transplanted into a non-dystrophic muscle environment (Boldrin, Zammit, & Morgan, 2015). It remains to be determined whether this is also the case for satellite cells from dysferlin deficient muscle and whether dysferlinopathic human muscle in late stages of disease progression could still support robust donor-cell engraftment.

Another open question is whether the expression of a therapeutic dysferlin transgene in the context of a dysferlin deficient muscle, even in autologous settings, could trigger an immune response against the non-self-epitopes of the restored protein. Humoral and cellular immunity against dystrophin have been shown for dystrophin gene therapy (Gilchrist, Ontell, Kochanek, & Clemens, 2002; Mendell et al., 2010).

Regarding the vector system, we have chosen SB because of its large cargo size and remarkable gene transfer efficacy in numerous cell types. SB also has a close-to-random genomic integration profile. This makes it probably the safest integrating vector currently available regarding risk of genotoxicity (see page 29). Also, it benefits from the simple and inexpensive manufacture of plasmid-based systems. This is a clear advantage for large-scale production of clinical-grade vectors. These biosafety and vector production features make SB very suitable for gene therapy. Obviously, the gold-standard for gene therapy of monogenic disorders is *in situ* correction of mutations through gene editing. However, the currently available gene editing tools, although powerful, are not yet sufficiently characterized for clinical applications in gene therapy. In contrast, SB is already a relevant vector system utilized in ongoing clinical trials.

5.1 Dysferlin transfer into dysferlin-null myoblasts

5.1.1 Vector design and full-length dysferlin transfer efficacy

I constructed SB-based vectors for full-length dysferlin transfer under the control of the synthetic Spc5-12 promoter. We chose this promoter sequence to drive expression of dysferlin due to its high level of activity in H2K A/J myoblasts and myotubes as well as its short sequence (<400 kb). Transgene expression driven by this synthetic promoter has been shown to occur both in cardiac and skeletal muscle, with no apparent bias towards fast or slow fiber types (B. Wang et al., 2008). Spc5-12 is made of an assembly of transcription factor binding sites that confer tissue specificity to striated muscle genes (Li et al., 1999). Therefore, it is thought to be muscle-specific, although this has not been extensively tested. Even if desirable, for our experimental design it is not strictly necessary to have a promoter sequence that drives expression exclusively in muscle. The reason for this is that engineered cells are injected directly into the skeletal musculature and are unlikely to engraft elsewhere, provided that a pure myoblast population is transplanted. However, donor myoblasts should ideally engraft as satellite cells to provide a long-term therapeutic effect. In this scenario, expression of the transgene should not disturb donor-derived satellite cell function.

The results of this study show that Spc5-12-driven transgene expression is higher in differentiated myotubes than in proliferating myoblasts *in vitro*. In grafted muscles, dysferlin was highly expressed in donor-derived myofibers. We have not yet been able to unequivocally determine whether the Pax7+ cells present in the vicinity of donor-derived myofibers are indeed of donor-origin. If so, it would be important to analyse dysferlin expression in engrafted donor derived satellite cells. This could be achieved either by high quality double immunostaining of dysferlin and satellite cell markers (e.g. Pax7, VCAM1, syndecan4) (Tedesco et al., 2010; Yin et al., 2013) or by isolating them from grafted muscles and studying them *ex vivo*.

Muses et al. showed that myogenic H2K 2B4 cells derived from immorto-wild-type mice were efficiently transfected (30%) with Lipofectamine, although the efficiency was substantially higher (50-70%) using nucleofection (Muses et al., 2011a). In experiments with H2K A/J myoblasts, I obtained very poor transfection rates using X-tremeGENE (Roche) or jetPRIME (Polyplus), which worked very efficiently and showed very low toxicity for transfection of other cell types (data not shown). That prompted me to establish an electroporation protocol using GFP

reporter vectors, which resulted in efficient transfection and SB-mediated transposition (Figure 4. 1 and Figure 4. 4). However, in comparison with the SB-based constructs containing only a GFP reporter, transfection of the full-length dysferlin transfer vectors was inefficient (Figure 4. 4 and Figure 4. 5). Thus, sorting of engineered cells harbouring the full-length dysferlin transgene required extensive expansion of the transfected cells. This represents a considerable limitation when engineering primary myoblasts. The inefficient transfection may be in part due to the large size of the transposon plasmids.

Additionally, the Spc5-12 regulatory sequence showed a robust activity when driving expression of a GFP reporter in H2K A/J myoblasts. We also observed an enhanced activity of two tandem Spc5-12 copies (Figure 4. 5). This is not entirely surprising due to its synthetic nature. However, expression of dysferlin in the selected cells was robust and higher than in H2K wild-type myoblasts and myotubes in all the sorted populations analysed (Figure 4. 6). Thus, poor expression of the GFP reporter is likely caused by an inefficient translation of GFP mediated by the IRES. This might also hinder the detection of all positive transfection events.

For future experiments aiming to transfer large transgenes with SB transposon into cells with limited proliferative capacity, a different vector design might be considered. For example, it is possible to utilize two promoters to drive expression of the therapeutic transgene, in this case dysferlin, and the reporter gene. This strategy has the disadvantage of increasing the size of the transposon cassette by adding a new promoter and poly(A) signal. Also, expression of the reporter would not necessarily imply expression of the therapeutic gene. Some short viral promoters, like SV40 (~200 bp), may be suitable for maintaining a similar sequence length of the cassette but viral promoters frequently trigger transgene silencing in eukaryotic genomes (Papadakis, Nicklin, Baker, & White, 2004). Another option would be to use self-cleaving peptides (Szymczak et al., 2004) so that the two transgenes are translated together as one protein product. The resulting protein is cleaved to generate two individual products. Some drawbacks of this approach are that cleavage does not occur at 100% efficiency and that the coding sequence needs to be slightly modified, so a thorough analysis of protein functionality is required.

Nevertheless, even if very useful to monitor and select engineered cells in proof-of-concept studies, a therapeutic transgene cassette for clinical gene therapy should not contain any fluorescent reporter. An indirect strategy to enrich for engineered cells is to tag the transposase or incorporate a fluorescent reporter in the transposase expression vector. This strategy might be beneficial for avoiding a reporter gene in the transposon plasmid. In this regard, an important observation is that the rate of stably transfected cells in the presence of SB100X was high when normalized to the initial transfection efficiency. However, much less transposase plasmid was transfected in comparison with transposon plasmid considering molar ratio or total mass. This suggests that the limiting factor is not transfection of the small SB100X expression vector or cellular expression of the transposase but rather transfection of the larger vectors or IRES-mediated translation of GFP. Therefore, adding a fluorescent reporter as a tag to the transposase or as an independent ORF in the transposase expression vector may be suitable when transferring small transposon cassettes. However, it might not be useful to indirectly enrich for cells harbouring insertions of large transposon cassettes. Also, careful examination of transposase activity when modifying its coding sequence with a tag should be performed to ensure that it remains fully functional.

An alternative that might be useful in this scenario is to add a reporter gene in the backbone of the transposon-containing plasmid. In this way, selection of the cells transfected with the transposon could be performed between 2 and 5 days after transfection, before the fluorescent signal from non-integrated cassettes starts to decline. Expression of the reporter gene from an independent ORF would likely provide a stronger fluorescent signal, more suitable for selection.

Although indirect, samples enriched through this method would be likelier to contain cells with stable transposon integrations. Also, the promoter driving expression of the reporter gene, even if susceptible to silencing, would not influence the transgene cassette once this was integrated. Moreover, cells stably expressing the reporter due to random genomic insertions of the plasmid backbone could later be eliminated by FACS sorting.

Since cells transfected with the dysferlin transfer vectors contained a fairly low percentage of GFP expressing cells before sorting (Figure 4. 5), it is possible that the enriched populations are not truly heterogeneous in terms of transposon integrations but rather contain only a few clones. To answer this, a transposon insertion site analysis needs to be performed on single expanded clones from the sorted populations.

The most effective method to provide comprehensive information about population clonality and insertion sites would be splinkerette-PCR (Devon, Porteous, & Brookes, 1995; Uren et al., 2009). It consists on digesting the genomic DNA with restriction enzymes that do not cut within the terminal region of the transposon ITRs. A double stranded DNA linker fragment with known sequence is cut with the same restriction enzyme to provide compatible ends and ligated to the digested genomic DNA. Ligation results in the formation of hybrid DNA fragments containing genomic + linker DNA. Transposon ends and their neighbouring genomic sequences can then be amplified with a nested PCR, using primers specific to the linker and the transposon ITRs. This PCR will produce amplicons of different sizes depending on the genomic sequences flanking the transposon insertion. Each band can then be isolated and sequenced to determine the transposon insertion site(s). This method requires monoclonal populations, namely homogeneous regarding transposon insertions. It is sensitive but may not detect all integrations, as it relies on the efficiency of the PCR to amplify the corresponding sequence. Ultimately, the most robust method to determine transposon copy number is southern blot.

Information on transposon copy number and insertion sites would also be important to determine how many integrated copies of the full-length dysferlin transfer cassettes driven by Spc5-12 are necessary for robust transgene expression.

Although provided in small amounts, the transposase expression vector can also randomly integrate in the genome of the target cells. Despite the fact that SB100X does not bind class II transposon sequences in the human genome (Hackett et al., 2013), this would be highly undesirable for obvious reasons. First, it could excise or remobilize the integrated therapeutic SB-transposon cassettes. Second, it could elicit immunogenicity and third, it could cause cellular toxicity (Galla et al., 2011). To eliminate this risk in a clinical setting, the source of transposase should be *in vitro* transcribed mRNA instead of a DNA expression vector.

5.2 Engraftment of corrected H2K A/J myoblasts in Scid/blAJ muscles and dysferlin reconstitution

Transplantation of H2K A/J myoblasts carrying the full-length *hDYSF_v1* transgene into the tibialis anterior muscles of Scid/blAJ mice resulted in successful engraftment at all the examined time points (2, 3 and 6 weeks). We determined engraftment efficiency based on the presence of donor-derived myofibers. Those could be detected based on their expression of dysferlin. In fact, this study shows so far the most robust reconstitution of dysferlin protein in myofibers of dysferlin-null mice using transplantation of either wild type or engineered cells. The injury model applied to the recipient muscles played a major role in the extent of donor cell engraftment.

The most abundant literature reports on myoblast transplantation into skeletal muscle have been performed on the dystrophin-null *mdx* mouse strain or immunocompromised mice with the *mdx* mutation. The presence and progressive increase of revertant fibers with age is characteristic of dystrophinopathy both in patients and in the *mdx* mouse. Revertant fibers in DMD/BMD patients and mice are myofibers that spontaneously express dystrophin protein and are labelled with anti-dystrophin antibodies (Hoffman, Morgan, Watkins, & Partridge, 1990; Nicholson, 1993). They are thought to be product of alternative splicing or secondary mutations that restore protein expression. However, the mechanism through which they appear in clusters and progressively increase in number is not yet fully understood. The presence of revertant fibers has been a confound variable in the interpretation of grafting results whose readout was based on dystrophin reconstitution in the *mdx* model. Xenograft studies of human cell grafting into mouse skeletal muscle have relied on immunolabeling with anti-human specific antibodies to detect donor-derived myofibers (Marg et al., 2014; Meng, Adkin, Xu, Muntoni, & Morgan, 2011; Meng et al., 2014; Negroni et al., 2009). It has recently been shown that the widely used anti-human spectrin antibody, thought to be specific for human spectrin expressed at the sarcolemma of donor-derived myofibers, also recognizes regenerating mouse fibers. This is probably due to the presence of spectrin motifs in utrophin, a protein homolog to dystrophin that is expressed only at the NMJ of mature myofibers but present along the complete sarcolemma in developing or regenerating fibers (Rozkalne et al., 2014). These examples illustrate the need for cautious conclusion-drawing in the interpretation of grafting results.

We based our detection method on the presence of dysferlin expressing myofibers in the grafted muscles. In dysferlin-null mouse models the existence of revertant fibers has not been reported, nor has it been demonstrated in patients. Mice carrying a homozygous *dysf*^{prmd} allele do not express any dysferlin protein (Farini et al., 2012; Ho et al., 2004). In accordance to that, we have not seen any dysferlin positive fibers in non-grafted muscles of Scid/blAJ mice that were either uninjured, only irradiated or only injected with cardiotoxin. Therefore, we are confident that our readout for engraftment is reliable.

Although H2K myoblasts are only conditionally immortalized and are thus not expected to form tumors *in vivo*, spontaneous transformation or some cells during *in vitro* culture could occur. Immortalized C2C12 myoblasts have been shown to rapidly form tumors when transplanted into tibialis anterior muscles of *mdx nu/nu* and non-dystrophic *beige/nu/Xid* mice (Morgan et al., 2002). In those studies, tumor formation was especially evident in muscles that had been irradiated with 18 Gy three days before cell transplantation. In our immunosuppressed dysferlin knock-out model, we did not observe any tumors in the grafted muscles or the surrounding tissues at any of the examined time points and with any of the injury models. This strongly suggests that the transplanted cells had not undergone spontaneous transformation *in vitro*.

5.2.1 Effect of the injury models on donor cell engraftment

We found that 18Gy irradiation one day before grafting plus injection of cardiotoxin simultaneous to cell transplantation was the most efficient injury model in promoting donor cell engraftment and contribution to myofibers.

It is well known that inactivation of the endogenous satellite cells of the host muscles by radiation or cryoinjury enhances the engraftment of the donor cells (Boldrin et al., 2012; Gross, Bou-Gharios, & Morgan, 1999; Gross & Morgan, 1999). We chose a radiation dose of 18 Gy because it has been described in several studies as optimal to promote donor cell engraftment in mouse skeletal muscle (Boldrin et al., 2012). Also, inducing regeneration in response to acute

damage inflicted by injection of myotoxins has been used to boost engraftment of transplanted cells (Briggs & Morgan, 2013). However, studies on transplantation of freshly isolated mouse satellite cells into the muscles of *mdx* nude mice showed no significant increase in engraftment when the recipient muscles were injected with notexin in addition to 18 Gy radiation (Boldrin et al., 2012).

Some muscle pathologies affect satellite cell function either directly due to mutations in genes important for their maintenance or indirectly by generating a hostile environment. For example, in some muscular dystrophies where the disease causing mutation does not affect satellite cells, their function can still be compromised by over-use (Morgan & Zammit, 2010). It is possible that the efficiency of different injury models in promoting donor myoblast engraftment in different mouse strains depends on the rate of myonuclei turnover of the host muscles. Besides, different cytokine release, muscle environment or immune response in different strains and genetic backgrounds could also play a role. If the host muscle is continuously subject to regeneration, donor myoblasts may be recruited more efficiently to myofibers without the need to experimentally induce regeneration.

A recent study reported that engraftment of human pericytes or CD133+ cells in muscles of *Rag2^{-}/γchain^{-}/C5^{-}* or dystrophic *mdx* nude mice showed no significantly differences between muscles that had been cryodamaged or irradiated + cryodamaged prior to cell transplantation. However, both injury models promoted donor cell engraftment and contribution to myofibers more robustly than 18 Gy radiation alone. Importantly, this study used stringent criteria for identification of human derived fibers, consisting on double human lamin A/C and human spectrin labelling (Meng, Bencze, Asfahani, Muntoni, & Morgan, 2015). In a double dystrophin/utrophin knock-out mouse model, miPS cell-derived myogenic progenitors robustly engrafted in uninjured skeletal muscle following either intramuscular or systemic transplantation (Filareto et al., 2013). Several other studies of H2K myoblast transplantation in various mouse models have successfully used irradiation alone as injury model (Beauchamp, Morgan, Pagel, & Partridge, 1999; Morgan et al., 1994; Muses et al., 2011a)**.** The source of this striking variation in the effect of different injury models on donor cell engraftment may be in part technical. However, the fact that this variation has been reported in various studies performed by the same team and with very similar experimental conditions strongly indicates that different injury models are best suited for different mouse strains and donor cell types.

Dysferlinopathic muscle also undergoes degeneration and progressive atrophy, but the muscle pathology in dysferlin deficient mouse models is mild compared to the human situation (Bittner, Anderson, et al., 1999; Ho et al., 2004). Also, the onset of dystrophic symptoms in A/J or Scid/blAJ mice is at around 5 months of age (Farini et al., 2012; Ho et al., 2004). This could explain why we detected only a few dysferlin expressing fibers clustered in areas seemingly undergoing regeneration in grafted muscles that were only irradiated (Figure 4. 11). Other studies in Scid/blAJ mice have reported extensive engraftment of mouse mesoangioblasts following intramuscular transplantation into muscles injured only with cardiotoxin (Diaz-Manera et al., 2010). Meregalli et al. showed a very limited extent of donor cell engraftment after transplantation of control and engineered human blood-derived CD133+ cells into notexin treated muscles of Scid/blAJ mice that had not been irradiated (Meregalli et al., 2013).

It is an open question whether human muscle would support sufficient engraftment of donor cells, either in autologous or in allogeneic grafts, if endogenous satellite cell function was not compromised. The injury models applied here are experimental and serve the purpose to study the effect of the muscle environment in the engraftment of donor cells, but they could not be applied to patients. However, if needed, it might be possible to apply other types of treatments to render patients' muscles receptive recipients of cell grafts while avoiding irreversible tissue

damage. For example, exercise could induce a regenerative response in dystrophic muscles. In an intramuscular transplantation approach, a milder dose of focal radiation could be considered in order to promote engraftment of donor cells proximal to the site of injection. However, although radiation has long been used for bone marrow transplantation, long-term effects of radiation in human skeletal muscle are not well-studied. Even if myofibers were not harmed, radiation could affect surrounding structures and resident cells important for long-term maintenance of tissue architecture and homeostasis like blood vessels, connective tissue, fibroadipogenic progenitors and nerve terminals among others.

Importantly, we found that the injury model also had a major impact on the histology of the grafted muscles. In muscles irradiated and injured with cardiotoxin, donor-derived fibers built a whole new area of muscle tissue with clearly distinctive histological features (Figure 4. 18). Interestingly, those areas appeared to be still undergoing regeneration even 6 weeks after grafting/cardiotoxin injury. Also, the tissue architecture was irregular and not fully restored. This could be due to the fact that H2K myoblasts were expanded for numerous passages *ex vivo* and may have lost part of their regenerative capacity. Also, grafted muscles that were irradiated and injured with cardiotoxin had areas where tissue architecture appeared completely normal, likely because cardiotoxin did not reach the full muscle. That might also explain why those areas were devoid of donor-derived fibers. It is possible that tissue architecture at later time points after transplantation would be better restored. The imperfect histology of the newly-built muscle may be overcome by grafting primary satellite cells that have not been cultured for long before re-implantation.

5.2.2 Distribution of donor-derived myofibers in grafted muscles

We observed large areas of donor-derived myofibers in grafted muscles that were irradiated with 18 Gy and treated with cardiotoxin (Figure 4. 12). We could find dysferlin expressing fibers covering up to approximately 1000 x 800 μm in a transversal plane and up to about 5 mm in a longitudinal plane. The overall length on a mouse tibialis anterior muscle is about 7-8 mm.

Transplantation studies in dystrophin knock-out mice have shown that dystrophin protein expressed in donor-derived myofibers spreads only a short distance from the dystrophin expressing nuclei in fibers with a mosaic of host and donor myonuclei (Blaveri et al., 1999; Partridge & Morgan, 2014). This was shown by isolating myofibers from *mdx nu/nu* mouse muscles ~3-7 weeks after transplantation of wild-type H2K myoblasts labelled with nLacZ. The spread of nuclear-localizing β-gal from a nucleus that encoded it to non-donor derived nuclei was ~200 μm and dystrophin protein was detected only as far as the nuclear-localizing β-gal in most fibers (Blaveri et al., 1999). According to these reports, the widespread longitudinal distribution of dysferlin expressing fibers we observed in our grafts suggests that donor myoblasts migrated large distances along the length of the muscle and fused to existing or new fibers far from the injection site. However, the extent of spreading of different proteins along the length of a myofiber might vary and it could also depend on their expression level.

Some studies have determined in detail the overall distribution of donor-derived myonuclei along the length of grafted muscles. For example, in the aforementioned study by Blaveri et al., some isolated myofibers contained nLacZ positive nuclei along their entire length after grafting of labelled H2K myoblasts (Blaveri et al., 1999). Also, Negroni et al. reported a maximum longitudinal spreading of human lamin A/C+ nuclei of ~4.8 mm and ~6.2 mm 4 weeks after grafting of human myoblasts, and human CD133+ cells, respectively, into cryoinjured muscles of *Rag2*$^{-/-}$*γC*$^{-/-}$*C5*$^{-/-}$ mice. This spreading was determined by analyzing cryosections from the grafted muscles and was very similar to the spreading of human spectrin+ fibers in the

same muscles (Negroni et al., 2009). In our experiments of HMFF transplantation into irradiated tibialis anterior muscles of NOG mice, we found a maximum spreading of human lamin A/C+ nuclei of 800 × 400 × 400 μm (Marg et al., 2014). Here, transplantation was performed by surgical implantation of human satellite cell-containing HMFFs instead of injection of cell suspensions. Thus, the extent of donor cell migration along grafted muscles greatly varies depending on the experimental conditions and the transplanted cell type.

5.2.3 Dysferlin expression and localization in donor-derived myofibers

We found dysferlin localized both at the membrane and cytoplasm of donor-derived myofibers. Membrane labelling was more prominent in most of the fibers. This is in accordance with other studies describing dysferlin as a sarcolemmal protein (Anderson et al., 1999; Matsuda et al., 2001). However, several more recent studies have described a homogeneous labelling of dysferlin at the T-tubule membranes in regenerating and mature muscle fibers (Kerr et al., 2013; Klinge et al., 2010). Also, one of those studies highlighted the connection between the immunolabeling technique and the detection of T-tubule-associated dysferlin in mouse and human skeletal muscle. Especially, an optimal labeling of cytoplasmic dysferlin in mouse muscles seems to require perfusion fixation with para-formaldehyde and antigen retrieval followed by immunostaining with an antibody against C-terminal dysferlin. This type of fixation appears to better preserve the sarcomere and T-tubule architecture (Roche et al., 2011).

The detection method used in this study was based on immunolabeling with an antibody against N-terminal dysferlin in muscles not fixed prior to cryopreservation. Nevertheless, we have observed various patterns of cytoplasmic dysferlin distribution in myofibers of grafted muscles. In many fibers, dysferlin labelling in the cytoplasm followed an irregular punctate pattern, whereas in others it appeared more homogeneous (Figure 4. 17). The presence of dysferlin in irregular puncta might be due to an inability of our detection method to properly label cytoplasmic dysferlin, or to the presence of protein aggregates because of overexpression. This needs to be addressed by co-staining with other proteins or by labelling with antibodies against C-terminal dysferlin in para-formaldehyde fixed sections.

It is important to point out that in dual AAV-based dysferlin gene transfer studies, the pattern of human dysferlin localization in mouse skeletal muscle differs from that of endogenous mouse dysferlin. The human protein shows a more prominent cytoplasmic labeling (Lostal et al., 2010; Sondergaard et al., 2015). Also, we have transplanted engineered myoblasts expressing the human dysferlin_v1 isoform. This isoform constitutes about 13% of total dysferlin in human skeletal muscle at the mRNA level (Pramono et al., 2009). Since antibodies specific to the C2A or C2Av1 domains of dysferlin are not available, the relative abundancy of the v1 and canonical protein isoforms has not yet been determined. It is also not known whether their localization pattern is identical. The same is true for the other predicted dysferlin isoforms based on the known mRNA splice variants.

5.2.4 Expression level of dysferlin in donor-derived myofibers

Previous studies on cell transplantation have never succeeded to restore dysferlin protein in the skeletal muscle of dysferlin-null mice to more than ~20% of wild-type levels (Diaz-Manera et al., 2010; Flix et al., 2013; Kong et al., 2004; Leriche-Guerin et al., 2002; Meregalli et al., 2013). We found a very robust and sustained expression of dysferlin in myofibers 3 and 6 weeks after transplantation of corrected H2K A/J myoblasts. Donor-derived fibers expressed dysferlin protein at levels substantially higher than those for endogenous dysferlin in wild-type muscles (Figure 4. 15). It has been shown that overexpression of dysferlin in skeletal muscle has detrimental effects.

Transgenic mice with ectopic overexpression of full-length human dysferlin (36 to 176-fold of endogenous mouse dysferlin levels) driven by the human skeletal α-actin promoter show severe kyphosis, hind-limb atrophy and dehydration. They also show upregulation of ER-stress markers and histological features of a non-necrotic, congenital myopathy with reduced myofiber diameter, increased connective tissue and more central nuclei (Glover et al., 2010). Also, over-physiological expression of minidysferlin following AAV delivery into dysferlin-null mice resulted in more central nucleation and worsening of dystrophic features. However, although minidysferlin restores membrane repair, it does not recapitulate the function of full-length dysferlin (Lostal et al., 2012). Nevertheless, an over-physiological expression of dysferlin in grafted muscles could be detrimental. Thus, a therapeutic approach should ideally restore the protein to levels close-to-physiological in muscle fibers.

An important consideration for our approach is that engineered cells are transplanted into a dysferlin deficient muscle environment. Even in a best case scenario of robust engraftment, myofibers of grafted muscles will most likely be formed by a mosaic of donor-derived and host nuclei. Therefore, in order to achieve a close-to-physiological expression in the tissue, donor-derived nuclei may need to produce more protein. Some studies have shown an improvement of membrane repair in dysferlin-null mouse muscles grafted with mouse mesoangioblasts and engineered human CD133+ cells even if dysferlin was restored to only ~10% of wild-type levels (Diaz-Manera et al., 2010; Meregalli et al., 2013). However, it has been shown that the outcome of membrane repair does not correlate with the improvement of locomotor parameters or dystrophic features (Lostal et al., 2012).

In our approach, the level of dysferlin expression by corrected myoblasts may also be controlled by establishing conditions favorable for single copy transposon insertions. However, a correlation of transposon copy number, insertion site and level of transgene expression in our model still needs to be addressed. For this purpose, determining the insertion sites and expression levels of dysferlin in clonal populations of engineered myoblasts would be required.

5.3 Contribution of donor-derived cells to the satellite cell compartment

Repopulation of the satellite cell compartment is required for a long-term therapeutic effect and contribution of donor cells to the regeneration of the recipient muscles. Since H2K myoblasts needed to be cultured extensively before transplantation, we were surprised to observe areas with numerous Pax7 expressing cells in the vicinity of donor-derived myofibers (Figure 4. 22). The fact that the host muscles were irradiated before grafting suggests that this Pax7+ cells were of donor origin. Previous studies on transplantation of *ex vivo* expanded H2K myoblasts into mouse skeletal muscle have shown that they can engraft as satellite cells and endure serial transplantations. Moreover, they contributed to subsequent rounds of acute injury-induced regeneration in the recipient muscles (Morgan et al., 1994; Muses et al., 2011a).

However, although high radiation doses incapacitate satellite cells, it has been shown that some can survive radiation. Those escapers can contribute to muscle regeneration in irradiated host muscles or when isolated and re-implanted into other recipient muscles (Boldrin et al., 2012; Muses et al., 2011a). Therefore, it still needs to be unequivocally determined whether the Pax7+ cells we observed in grafted muscles are of donor origin or endogenous satellite cells that escaped radiation.

As mentioned previously, we have so far not succeeded to obtain a high quality double immunolabeling of GFP/Pax7 or dysferlin/Pax7. *In vitro*, GFP expression in corrected H2K A/J myoblasts was detected by FACS. However, under the microscope it was only visible after differentiation into myotubes (data not shown). *In vivo*, we found that GFP expression in donor-derived fibers was faint and only clearly distinguishable from the background in cryosections of some grafted muscles. Moreover, lipofuscin foci, which also have green autofluorescence, were abundant in regenerating areas of grafted muscles that had been injured with cardiotoxin and accumulated also around nuclei. This hampered the identification of donor-derived satellite cells based only on GFP expression without immunolabeling. Some studies have based the identification of donor-derived satellite cells on expression of GFP (Chang et al., 2009; Filareto et al., 2013). According to our experiments, a double immunostaining using secondary antibodies with an emission wavelength other that within the green spectrum would be preferable.

5.4 Human satellite cells for muscle regeneration and gene therapy

We have developed a novel method for isolation and culture of human satellite cells within their natural niche in HMFFs. In contrast to previous methods based on single cell culture (Montarras et al., 2005), our method allowed extensive expansion of human satellite cells that maintained Pax7 expression for a long time period in culture (Marg et al., 2014). These HMFFs engrafted in mouse muscles and incorporated into myofibers, as indicated by the presence of numerous myonuclei of human origin. Importantly, ablation of the host satellite cells by radiation with 18 Gy was also required for robust engraftment and contribution to muscle regeneration of human cells in the NOG model. However, human cells within HMFFs engrafted robustly without cardiotoxin injury of the recipient muscles (Figure 4. 23). We did not study a potential additional effect of irradiation plus cardiotoxin in this model. It is important to note that, in those experiments, the muscles were injured by the transplantation procedure itself, which consisted on opening an incision to introduce the HMFFs. We also showed that human satellite cells engrafted as Pax7+ cells following transplantation. Moreover, HMFFs isolated from human biopsies that were stored for several weeks at 4°C not only were enriched 100% in myogenic cells but also contained viable satellite cells with enhanced regenerative potential upon transplantation (Marg et al., 2014).

One limitation, however, is the limited migration of donor cells from the site of transplantation. We found a maximum spreading of human lamin A/C+ nuclei of 800 × 400 × 400 μm in the grafted muscles (Marg et al., 2014). A recent study showed that it is possible to enhance satellite cell motility upon transplantation through stimulation of Wnt7a/Fzd7 signaling during *ex vivo* culture prior to reimplantation (Bentzinger et al., 2014). Thus, it might be possible to enlarge the area of dissemination of a graft in our model by modulating certain biological parameters.

We showed that human satellite cells could be transfected in the fiber fragment culture system, and that numerous GFP+ cells were present throughout the fiber bundle 7 days after transfection (Figure 4. 24). A drawback of engineering satellite cells within HMFFs is that it is not possible to precisely determine the frequency of engineered cells. Also, unless optimized culture conditions allow to outgrow human satellite cells from HMFFs while fully maintaining their regenerative capacity, it is not possible to enrich for engineered cells through sorting. Thus, gene transfer efficiency needs to be addressed in detail and further improved. Importantly, cells transfected with a SB-based reporter vector and SB100X transposase gave rise to myotubes in

culture 35 days after transfection, showing that they were stably engineered and that they preserved their myogenic capacity (Marg et al., 2014). Future experiments will need to address the feasibility of delivering therapeutic cassettes for gene therapy of muscular dystrophies.

Our results show that HMFFs overcome various limitations of traditional myoblast culture regarding *ex vivo* expansion and successful engraftment of human satellite cells following intramuscular transplantation. This culture system is a remarkable advance towards the use of human satellite cells for autologous and allogeneic grafts. Those could be tremendously beneficial for individuals with muscular dystrophies, trauma-induced muscle injuries or muscle dysfunction due to advanced age.

5.5 Relevance of the study

We have used a clinically relevant vector system for dysferlin gene transfer into dysferlin-null mouse myoblasts. We have succeeded in restoring full-length dysferlin *in vitro* an *in vivo* following transplantation of the corrected myoblasts into the muscle of dysferlin-null mice. We have also dissected the influence of the host muscle environment and injury model in the success of myoblast transplantation in dysferlin-null skeletal muscle. Last, we have developed a novel isolation and culture method for human satellite cells that addresses many of the limitations of previously existing methods.

Altogether, this study provides the first proof of robust dysferlin reconstitution in skeletal muscle through a cell-based gene therapy approach. It also provides the first proof of dysferlin reconstitution *in vivo* using a non-viral vector for gene transfer. Moreover, the development of a novel culture system for human satellite cells that enables expansion, genetic modification and robust engraftment has put at our disposal a very promising tool for genetic correction and grafting of patient-derived cells.

6 Future prospects

In this study, I have shown that expression of full-length dysferlin was restored in dysferlin-null H2K A/J myoblasts enriched in reporter expression by FACS sorting. I have performed a characterization of corrected myoblasts and myotubes expressing *hDYSF_v1*. I have transplanted them into the skeletal muscle of Scid/blAJ mice and shown that they robustly engrafted and reconstituted dysferlin protein *in vivo*. Next, I want to characterize the corrected H2K A/J myoblast populations expressing *hDYSF_c*. These cells are a very valuable tool to study the localization and function of canonical and v1 dysferlin. Transplantation of those cells into Scid/blAJ mice could also provide very relevant information on *in vivo* localization and function of both protein isoforms.

I have shown that corrected H2K A/J myoblasts were able not only to reconstitute dysferlin *in vivo* but also to give rise to full areas of donor-derived muscle following intramuscular transplantation in Scid/blAJ mice. These results have proven that *ex vivo* genetic correction of dysferlin-null myoblasts with SB is a feasible and promising strategy for gene therapy of dysferlinopathy. The next step would be to translate these results into primary satellite cells in order to test whether this approach is efficient and safe enough for a future clinical application. We plan to use our validated SB-based vectors for *ex vivo* engineering of freshly isolated dysferlin-null mouse satellite cells and patient-derived satellite cells in our novel HMFF culture model. For this purpose, we will work on optimization of gene transfer into those primary cell types. If this step is successful, we would like to perform transplantation of engineered primary cells into the skeletal muscle of Scid/blAJ mice in order to analyze dysferlin reconstitution and muscle histology at later time points. This will serve to find out whether the dystrophic features of dysferlinopathic muscle can be slowed down or fully rescued by transplantation of engineered satellite cells.

A question that needs to be answered is whether SB-mediated transfer of transgenic dysferlin restores membrane repair in myofibers. To answer this, a laser wounding assay in isolated myofibers of grafted muscles should be performed. Ultimately, dysferlin reconstitution in skeletal muscle should lead to an amelioration of clinical symptoms and an improvement of muscle force parameters. This can be tested by *in situ* muscle force and fatigue resistance measurements in grafted tibialis anterior muscles. However, in order to obtain relevant results in this type of assay, transplantation of corrected myoblasts should be performed in conditions where tissue architecture is fully restored. This is still a challenge for all cell therapy approaches for skeletal muscle.

Altogether, we hope that those results will make a substantial contribution to the field of dysferlinopathy and ultimately translate into the advancement of genetic therapies to treat this disease.

7 Publications

Marg, A., **H. Escobar**, S. Gloy, M. Kufeld, J. Zacher, A. Spuler, C. Birchmeier, Z. Izsvák and S. Spuler (2014). "Human satellite cells have regenerative capacity and are genetically manipulable." *J Clin Invest* 124(10): 4257-4265.

Escobar H., V. Schöwel, S. Spuler, A. Marg* and Z. Izsvák*. "Full-length Dysferlin Transfer by the Hyperactive *Sleeping Beauty* Transposase Restores Dysferlin-deficient Muscle." *Molecular Therapy Nucleic Acids* (2016) **5**, e277; http://dx.doi.org/10.1038/mtna.2015.52 (*contributed equally).

Schöwel V., T. Opialla, **H. Escobar**, S. Keller, F.E. Rojas-Rusak, M. Pietzke, C. Herrmann, M. Boschmann, G. Mastrobuoni, A.L. Birkenfeld, H. Al-Hasani, M. Treier, Z. Izsvák, S. Kempa and S. Spuler. "Dysferlin guards glycolysis in skeletal muscle." Submitted manuscript.

8 Appendix

8.1. Plasmid maps

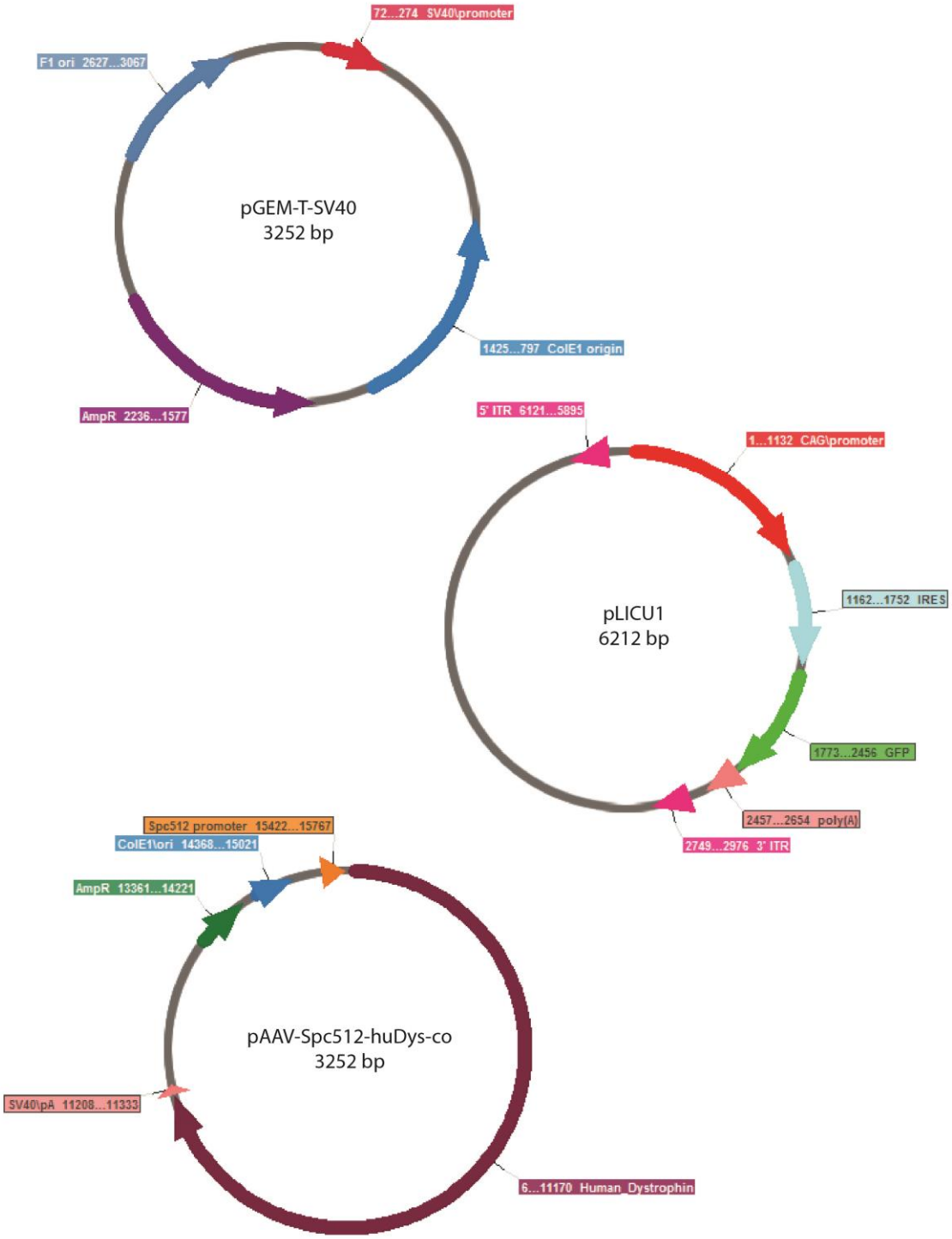

9 Bibliography

Abdullah, N., Padmanarayana, M., Marty, N. J., & Johnson, C. P. (2014). Quantitation of the calcium and membrane binding properties of the C2 domains of dysferlin. *Biophys J, 106*(2), 382-389. doi: 10.1016/j.bpj.2013.11.4492

Aiuti, A., Biasco, L., Scaramuzza, S., Ferrua, F., Cicalese, M. P., Baricordi, C., . . . Naldini, L. (2013). Lentiviral hematopoietic stem cell gene therapy in patients with Wiskott-Aldrich syndrome. *Science, 341*(6148), 1233151. doi: 10.1126/science.1233151

Ampong, B. N., Imamura, M., Matsumiya, T., Yoshida, M., & Takeda, S. (2005). Intracellular localization of dysferlin and its association with the dihydropyridine receptor. *Acta Myol, 24*(2), 134-144.

Anderson, L. V., Davison, K., Moss, J. A., Young, C., Cullen, M. J., Walsh, J., . . . Bushby, K. M. (1999). Dysferlin is a plasma membrane protein and is expressed early in human development. *Hum Mol Genet, 8*(5), 855-861.

Aoki, M., Liu, J., Richard, I., Bashir, R., Britton, S., Keers, S. M., . . . Brown, R. H., Jr. (2001). Genomic organization of the dysferlin gene and novel mutations in Miyoshi myopathy. *Neurology, 57*(2), 271-278.

Aronovich, E. L., Bell, J. B., Belur, L. R., Gunther, R., Koniar, B., Erickson, D. C., . . . Hackett, P. B. (2007). Prolonged expression of a lysosomal enzyme in mouse liver after Sleeping Beauty transposon-mediated gene delivery: implications for non-viral gene therapy of mucopolysaccharidoses. *J Gene Med, 9*(5), 403-415. doi: 10.1002/jgm.1028

Aronovich, E. L., Bell, J. B., Khan, S. A., Belur, L. R., Gunther, R., Koniar, B., . . . Hackett, P. B. (2009). Systemic correction of storage disease in MPS I NOD/SCID mice using the sleeping beauty transposon system. *Mol Ther, 17*(7), 1136-1144. doi: 10.1038/mt.2009.87

Asakura, A., Seale, P., Girgis-Gabardo, A., & Rudnicki, M. A. (2002). Myogenic specification of side population cells in skeletal muscle. *J Cell Biol, 159*(1), 123-134. doi: 10.1083/jcb.200202092

Azakir, B. A., Di Fulvio, S., Kinter, J., & Sinnreich, M. (2012). Proteasomal inhibition restores biological function of mis-sense mutated dysferlin in patient-derived muscle cells. *J Biol Chem, 287*(13), 10344-10354. doi: 10.1074/jbc.M111.329078

Azakir, B. A., Erne, B., Di Fulvio, S., Stirnimann, G., & Sinnreich, M. (2014). Proteasome inhibitors increase missense mutated dysferlin in patients with muscular dystrophy. *Sci Transl Med, 6*(250), 250ra112. doi: 10.1126/scitranslmed.3009612

Babatz, T. D., & Burns, K. H. (2013). Functional impact of the human mobilome. *Curr Opin Genet Dev, 23*(3), 264-270. doi: 10.1016/j.gde.2013.02.007

Bansal, D., Miyake, K., Vogel, S. S., Groh, S., Chen, C. C., Williamson, R., . . . Campbell, K. P. (2003). Defective membrane repair in dysferlin-deficient muscular dystrophy. *Nature, 423*(6936), 168-172. doi: 10.1038/nature01573

Bashir, R., Britton, S., Strachan, T., Keers, S., Vafiadaki, E., Lako, M., . . . Bushby, K. (1998). A gene related to Caenorhabditis elegans spermatogenesis factor fer-1 is mutated in limb-girdle muscular dystrophy type 2B. *Nat Genet, 20*(1), 37-42. doi: 10.1038/1689

Bashir, R., Keers, S., Strachan, T., Passos-Bueno, R., Zatz, M., Weissenbach, J., . . . Bushby, K. (1996). Genetic and physical mapping at the limb-girdle muscular dystrophy locus (LGMD2B) on chromosome 2p. *Genomics, 33*(1), 46-52. doi: 10.1006/geno.1996.0157

Baus, J., Liu, L., Heggestad, A. D., Sanz, S., & Fletcher, B. S. (2005). Hyperactive transposase mutants of the Sleeping Beauty transposon. *Mol Ther, 12*(6), 1148-1156. doi: 10.1016/j.ymthe.2005.06.484

Beauchamp, J. R., Morgan, J. E., Pagel, C. N., & Partridge, T. A. (1999). Dynamics of myoblast transplantation reveal a discrete minority of precursors with stem cell-like properties as the myogenic source. *J Cell Biol, 144*(6), 1113-1122.

Belanto, J. J., Diaz-Perez, S. V., Magyar, C. E., Maxwell, M. M., Yilmaz, Y., Topp, K., . . . Jamieson, C. A. (2010). Dexamethasone induces dysferlin in myoblasts and enhances their myogenic differentiation. *Neuromuscul Disord, 20*(2), 111-121. doi: 10.1016/j.nmd.2009.12.003

Benchaouir, R., Meregalli, M., Farini, A., D'Antona, G., Belicchi, M., Goyenvalle, A., . . . Torrente, Y. (2007). Restoration of human dystrophin following transplantation of exon-skipping-engineered DMD patient stem cells into dystrophic mice. *Cell Stem Cell, 1*(6), 646-657. doi: 10.1016/j.stem.2007.09.016

Bentzinger, C. F., von Maltzahn, J., Dumont, N. A., Stark, D. A., Wang, Y. X., Nhan, K., . . . Rudnicki, M. A. (2014). Wnt7a stimulates myogenic stem cell motility and engraftment resulting in improved muscle strength. *J Cell Biol, 205*(1), 97-111. doi: 10.1083/jcb.201310035

Bentzinger, C. F., Wang, Y. X., & Rudnicki, M. A. (2012). Building muscle: molecular regulation of myogenesis. *Cold Spring Harb Perspect Biol, 4*(2). doi: 10.1101/cshperspect.a008342

Besson, V., Smeriglio, P., Wegener, A., Relaix, F., Nait Oumesmar, B., Sassoon, D. A., & Marazzi, G. (2011). PW1 gene/paternally expressed gene 3 (PW1/Peg3) identifies multiple adult stem and progenitor cell populations. *Proc Natl Acad Sci U S A, 108*(28), 11470-11475. doi: 10.1073/pnas.1103873108

Bhagavati, S., & Xu, W. (2005). Generation of skeletal muscle from transplanted embryonic stem cells in dystrophic mice. *Biochem Biophys Res Commun, 333*(2), 644-649. doi: 10.1016/j.bbrc.2005.05.135

Biffi, A., Montini, E., Lorioli, L., Cesani, M., Fumagalli, F., Plati, T., . . . Naldini, L. (2013). Lentiviral hematopoietic stem cell gene therapy benefits metachromatic leukodystrophy. *Science, 341*(6148), 1233158. doi: 10.1126/science.1233158

Bittner, R. E., Anderson, L. V., Burkhardt, E., Bashir, R., Vafiadaki, E., Ivanova, S., . . . Reis, A. (1999). Dysferlin deletion in SJL mice (SJL-Dysf) defines a natural model for limb girdle muscular dystrophy 2B. *Nat Genet, 23*(2), 141-142. doi: 10.1038/13770

Bittner, R. E., Schofer, C., Weipoltshammer, K., Ivanova, S., Streubel, B., Hauser, E., . . . Wachtler, F. (1999). Recruitment of bone-marrow-derived cells by skeletal and cardiac muscle in adult dystrophic mdx mice. *Anat Embryol (Berl), 199*(5), 391-396.

Blaveri, K., Heslop, L., Yu, D. S., Rosenblatt, J. D., Gross, J. G., Partridge, T. A., & Morgan, J. E. (1999). Patterns of repair of dystrophic mouse muscle: studies on isolated fibers. *Dev Dyn, 216*(3), 244-256. doi: 10.1002/(SICI)1097-0177(199911)216:3<244::AID-DVDY3>3.0.CO;2-9

Boldrin, L., Neal, A., Zammit, P. S., Muntoni, F., & Morgan, J. E. (2012). Donor satellite cell engraftment is significantly augmented when the host niche is preserved and endogenous satellite cells are incapacitated. *Stem Cells, 30*(9), 1971-1984. doi: 10.1002/stem.1158

Boldrin, L., Zammit, P. S., & Morgan, J. E. (2015). Satellite cells from dystrophic muscle retain regenerative capacity. *Stem Cell Res, 14*(1), 20-29. doi: 10.1016/j.scr.2014.10.007

Boldrin, L., Zammit, P. S., Muntoni, F., & Morgan, J. E. (2009). Mature adult dystrophic mouse muscle environment does not impede efficient engrafted satellite cell regeneration and self-renewal. *Stem Cells, 27*(10), 2478-2487. doi: 10.1002/stem.162

Bonfanti, C., Rossi, G., Tedesco, F. S., Giannotta, M., Benedetti, S., Tonlorenzi, R., . . . Messina, G. (2015). PW1/Peg3 expression regulates key properties that determine mesoangioblast stem cell competence. *Nat Commun, 6*, 6364. doi: 10.1038/ncomms7364

Brack, A. S., & Rando, T. A. (2012). Tissue-specific stem cells: lessons from the skeletal muscle satellite cell. *Cell Stem Cell, 10*(5), 504-514. doi: 10.1016/j.stem.2012.04.001

Braun, C. J., Boztug, K., Paruzynski, A., Witzel, M., Schwarzer, A., Rothe, M., . . . Klein, C. (2014). Gene therapy for Wiskott-Aldrich syndrome--long-term efficacy and genotoxicity. *Sci Transl Med, 6*(227), 227ra233. doi: 10.1126/scitranslmed.3007280

Briggs, D., & Morgan, J. E. (2013). Recent progress in satellite cell/myoblast engraftment -- relevance for therapy. *FEBS J, 280*(17), 4281-4293. doi: 10.1111/febs.12273

Brohl, D., Vasyutina, E., Czajkowski, M. T., Griger, J., Rassek, C., Rahn, H. P., . . . Birchmeier, C. (2012). Colonization of the satellite cell niche by skeletal muscle progenitor cells depends on Notch signals. *Dev Cell, 23*(3), 469-481. doi: 10.1016/j.devcel.2012.07.014

Burstone, M. S. (1958). The relationship between fixation and techniques for the histochemical localization of hydrolytic enzymes. *J Histochem Cytochem, 6*(5), 322-339.

Bushby, K. M. (1995). Diagnostic criteria for the limb-girdle muscular dystrophies: report of the ENMC Consortium on Limb-Girdle Dystrophies. *Neuromuscul Disord, 5*(1), 71-74.

Cacciottolo, M., Numitone, G., Aurino, S., Caserta, I. R., Fanin, M., Politano, L., . . . Nigro, V. (2011). Muscular dystrophy with marked Dysferlin deficiency is consistently caused by primary dysferlin gene mutations. *Eur J Hum Genet, 19*(9), 974-980. doi: 10.1038/ejhg.2011.70

Cai, C., Weisleder, N., Ko, J. K., Komazaki, S., Sunada, Y., Nishi, M., . . . Ma, J. (2009). Membrane repair defects in muscular dystrophy are linked to altered interaction between MG53, caveolin-3, and dysferlin. *J Biol Chem, 284*(23), 15894-15902. doi: 10.1074/jbc.M109.009589

Carreira, P. E., Richardson, S. R., & Faulkner, G. J. (2014). L1 retrotransposons, cancer stem cells and oncogenesis. *FEBS J, 281*(1), 63-73. doi: 10.1111/febs.12601

Cattoglio, C., Maruggi, G., Bartholomae, C., Malani, N., Pellin, D., Cocchiarella, F., . . . Recchia, A. (2010). High-definition mapping of retroviral integration sites defines the fate of allogeneic T cells after donor lymphocyte infusion. *PLoS One, 5*(12), e15688. doi: 10.1371/journal.pone.0015688

Cerletti, M., Jurga, S., Witczak, C. A., Hirshman, M. F., Shadrach, J. L., Goodyear, L. J., & Wagers, A. J. (2008). Highly efficient, functional engraftment of skeletal muscle stem cells in dystrophic muscles. *Cell, 134*(1), 37-47. doi: 10.1016/j.cell.2008.05.049

Ceyhan-Birsoy, O., Talim, B., Swanson, L. C., Karakaya, M., Graff, M. A., Beggs, A. H., & Topaloglu, H. (2015). Whole Exome Sequencing Reveals , , and Mutations in Congenital Muscular Dystrophy Without Brain or Eye Involvement. *J Neuromuscul Dis, 2*(1), 87-92. doi: 10.3233/JND-140038

Chang, H., Yoshimoto, M., Umeda, K., Iwasa, T., Mizuno, Y., Fukada, S., . . . Nakahata, T. (2009). Generation of transplantable, functional satellite-like cells from mouse embryonic stem cells. *FASEB J, 23*(6), 1907-1919. doi: 10.1096/fj.08-123661

Chen, Z. J., Kren, B. T., Wong, P. Y., Low, W. C., & Steer, C. J. (2005). Sleeping Beauty-mediated down-regulation of huntingtin expression by RNA interference. *Biochem Biophys Res Commun, 329*(2), 646-652. doi: 10.1016/j.bbrc.2005.02.024

Chiu, Y. H., Hornsey, M. A., Klinge, L., Jorgensen, L. H., Laval, S. H., Charlton, R., . . . Bushby, K. (2009). Attenuated muscle regeneration is a key factor in dysferlin-deficient muscular dystrophy. *Hum Mol Genet, 18*(11), 1976-1989. doi: 10.1093/hmg/ddp121

Cohen, T. V., Cohen, J. E., & Partridge, T. A. (2012). Myogenesis in dysferlin-deficient myoblasts is inhibited by an intrinsic inflammatory response. *Neuromuscul Disord, 22*(7), 648-658. doi: 10.1016/j.nmd.2012.03.002

Collins, C. A., Olsen, I., Zammit, P. S., Heslop, L., Petrie, A., Partridge, T. A., & Morgan, J. E. (2005). Stem cell function, self-renewal, and behavioral heterogeneity of cells from the adult muscle satellite cell niche. *Cell, 122*(2), 289-301. doi: 10.1016/j.cell.2005.05.010

Conboy, M. J., Karasov, A. O., & Rando, T. A. (2007). High incidence of non-random template strand segregation and asymmetric fate determination in dividing stem cells and their progeny. *PLoS Biol, 5*(5), e102. doi: 10.1371/journal.pbio.0050102

Covian-Nares, J. F., Koushik, S. V., Puhl, H. L., 3rd, & Vogel, S. S. (2010). Membrane wounding triggers ATP release and dysferlin-mediated intercellular calcium signaling. *J Cell Sci, 123*(Pt 11), 1884-1893. doi: 10.1242/jcs.066084

Dalsgaard, T., Moldt, B., Sharma, N., Wolf, G., Schmitz, A., Pedersen, F. S., & Mikkelsen, J. G. (2009). Shielding of sleeping beauty DNA transposon-delivered transgene cassettes by heterologous insulators in early embryonal cells. *Mol Ther, 17*(1), 121-130. doi: 10.1038/mt.2008.224

Darabi, R., Arpke, R. W., Irion, S., Dimos, J. T., Grskovic, M., Kyba, M., & Perlingeiro, R. C. (2012). Human ES- and iPS-derived myogenic progenitors restore DYSTROPHIN and improve contractility upon transplantation in dystrophic mice. *Cell Stem Cell, 10*(5), 610-619. doi: 10.1016/j.stem.2012.02.015

Darabi, R., Pan, W., Bosnakovski, D., Baik, J., Kyba, M., & Perlingeiro, R. C. (2011). Functional myogenic engraftment from mouse iPS cells. *Stem Cell Rev, 7*(4), 948-957. doi: 10.1007/s12015-011-9258-2

Darabi, R., & Perlingeiro, R. C. (2014). Derivation of Skeletal Myogenic Precursors from Human Pluripotent Stem Cells Using Conditional Expression of PAX7. *Methods Mol Biol*. doi: 10.1007/7651_2014_134

Darabi, R., Santos, F. N., Filareto, A., Pan, W., Koene, R., Rudnicki, M. A., . . . Perlingeiro, R. C. (2011). Assessment of the myogenic stem cell compartment following transplantation of Pax3/Pax7-induced embryonic stem cell-derived progenitors. *Stem Cells, 29*(5), 777-790. doi: 10.1002/stem.625

De Angelis, L., Berghella, L., Coletta, M., Lattanzi, L., Zanchi, M., Cusella-De Angelis, M. G., . . . Cossu, G. (1999). Skeletal myogenic progenitors originating from embryonic dorsal aorta coexpress endothelial and myogenic markers and contribute to postnatal muscle growth and regeneration. *J Cell Biol, 147*(4), 869-878.

De Luna, N., Diaz-Manera, J., Paradas, C., Iturriaga, C., Rojas-Garcia, R., Araque, J., . . . Gallardo, E. (2012). 1alpha,25(OH)(2)-Vitamin D3 increases dysferlin expression in vitro and in a human clinical trial. *Mol Ther, 20*(10), 1988-1997. doi: 10.1038/mt.2012.156

De Luna, N., Gallardo, E., & Illa, I. (2004). In vivo and in vitro dysferlin expression in human muscle satellite cells. *J Neuropathol Exp Neurol, 63*(10), 1104-1113.

de Morree, A., Flix, B., Bagaric, I., Wang, J., van den Boogaard, M., Grand Moursel, L., . . . van der Maarel, S. M. (2013). Dysferlin regulates cell adhesion in human monocytes. *J Biol Chem, 288*(20), 14147-14157. doi: 10.1074/jbc.M112.448589

Defour, A., Van der Meulen, J. H., Bhat, R., Bigot, A., Bashir, R., Nagaraju, K., & Jaiswal, J. K. (2014). Dysferlin regulates cell membrane repair by facilitating injury-triggered acid sphingomyelinase secretion. *Cell Death Dis, 5*, e1306. doi: 10.1038/cddis.2014.272

Deichmann, A., Hacein-Bey-Abina, S., Schmidt, M., Garrigue, A., Brugman, M. H., Hu, J., . . . Cavazzana-Calvo, M. (2007). Vector integration is nonrandom and clustered and influences the fate of lymphopoiesis in SCID-X1 gene therapy. *J Clin Invest, 117*(8), 2225-2232. doi: 10.1172/JCI31659

Dellavalle, A., Maroli, G., Covarello, D., Azzoni, E., Innocenzi, A., Perani, L., . . . Cossu, G. (2011). Pericytes resident in postnatal skeletal muscle differentiate into muscle fibres and generate satellite cells. *Nat Commun, 2*, 499. doi: 10.1038/ncomms1508

Dellavalle, A., Sampaolesi, M., Tonlorenzi, R., Tagliafico, E., Sacchetti, B., Perani, L., . . . Cossu, G. (2007). Pericytes of human skeletal muscle are myogenic precursors distinct from satellite cells. *Nat Cell Biol, 9*(3), 255-267. doi: 10.1038/ncb1542

Demonbreun, A. R., Fahrenbach, J. P., Deveaux, K., Earley, J. U., Pytel, P., & McNally, E. M. (2011). Impaired muscle growth and response to insulin-like growth factor 1 in dysferlin-mediated muscular dystrophy. *Hum Mol Genet, 20*(4), 779-789. doi: 10.1093/hmg/ddq522

Devon, R. S., Porteous, D. J., & Brookes, A. J. (1995). Splinkerettes--improved vectorettes for greater efficiency in PCR walking. *Nucleic Acids Res, 23*(9), 1644-1645.

Di Matteo, M., Matrai, J., Belay, E., Firdissa, T., Vandendriessche, T., & Chuah, M. K. (2012). PiggyBac toolbox. *Methods Mol Biol, 859*, 241-254. doi: 10.1007/978-1-61779-603-6_14

Diaz-Manera, J., Touvier, T., Dellavalle, A., Tonlorenzi, R., Tedesco, F. S., Messina, G., . . . Cossu, G. (2010). Partial dysferlin reconstitution by adult murine mesoangioblasts is sufficient for full functional recovery in a murine model of dysferlinopathy. *Cell Death Dis, 1*, e61. doi: 10.1038/cddis.2010.35

Dillingham, B. C., Benny Klimek, M. E., Gernapudi, R., Rayavarapu, S., Gallardo, E., Van der Meulen, J. H., . . . Nagaraju, K. (2015). Inhibition of inflammation with celastrol fails to improve muscle function in dysferlin-deficient A/J mice. *J Neurol Sci*. doi: 10.1016/j.jns.2015.06.042

Doherty, J. E., Huye, L. E., Yusa, K., Zhou, L., Craig, N. L., & Wilson, M. H. (2012). Hyperactive piggyBac gene transfer in human cells and in vivo. *Hum Gene Ther, 23*(3), 311-320. doi: 10.1089/hum.2011.138

Doherty, M. J., Ashton, B. A., Walsh, S., Beresford, J. N., Grant, M. E., & Canfield, A. E. (1998). Vascular pericytes express osteogenic potential in vitro and in vivo. *J Bone Miner Res, 13*(5), 828-838. doi: 10.1359/jbmr.1998.13.5.828

Dominov, J. A., Uyan, O., Sapp, P. C., McKenna-Yasek, D., Nallamilli, B. R., Hegde, M., & Brown, R. H., Jr. (2014). A novel dysferlin mutant pseudoexon bypassed with antisense oligonucleotides. *Ann Clin Transl Neurol, 1*(9), 703-720. doi: 10.1002/acn3.96

Duan, D., Yue, Y., & Engelhardt, J. F. (2001). Expanding AAV packaging capacity with trans-splicing or overlapping vectors: a quantitative comparison. *Mol Ther, 4*(4), 383-391. doi: 10.1006/mthe.2001.0456

Duchen, L. W., Excell, B. J., Patel, R., & Smith, B. (1974). Changes in motor end-plates resulting from muscle fibre necrosis and regeneration. A light and electron microscopic study of the effects of the depolarizing fraction (cardiotoxin) of Dendroaspis jamesoni venom. *J Neurol Sci, 21*(4), 391-417.

Engel, W. K., & Cunningham, G. G. (1963). Rapid Examination of Muscle Tissue. An Improved Trichrome Method for Fresh-Frozen Biopsy Sections. *Neurology, 13*, 919-923.

Farini, A., Sitzia, C., Navarro, C., D'Antona, G., Belicchi, M., Parolini, D., . . . Torrente, Y. (2012). Absence of T and B lymphocytes modulates dystrophic features in dysferlin deficient animal model. *Exp Cell Res, 318*(10), 1160-1174. doi: 10.1016/j.yexcr.2012.03.010

Farrington-Rock, C., Crofts, N. J., Doherty, M. J., Ashton, B. A., Griffin-Jones, C., & Canfield, A. E. (2004). Chondrogenic and adipogenic potential of microvascular pericytes. *Circulation, 110*(15), 2226-2232. doi: 10.1161/01.CIR.0000144457.55518.E5

Ferrari, G., Cusella-De Angelis, G., Coletta, M., Paolucci, E., Stornaiuolo, A., Cossu, G., & Mavilio, F. (1998). Muscle regeneration by bone marrow-derived myogenic progenitors. *Science, 279*(5356), 1528-1530.

Filareto, A., Darabi, R., & Perlingeiro, R. C. (2012). Engraftment of ES-Derived Myogenic Progenitors in a Severe Mouse Model of Muscular Dystrophy. *J Stem Cell Res Ther, 10*(1). doi: 10.4172/2157-7633.S10-001

Filareto, A., Parker, S., Darabi, R., Borges, L., Iacovino, M., Schaaf, T., . . . Perlingeiro, R. C. (2013). An ex vivo gene therapy approach to treat muscular dystrophy using inducible pluripotent stem cells. *Nat Commun, 4*, 1549. doi: 10.1038/ncomms2550

Flix, B., Suarez-Calvet, X., Diaz-Manera, J., Santos-Nogueira, E., Mancuso, R., Barquinero, J., . . . Gallardo, E. (2013). Bone marrow transplantation in dysferlin-deficient mice results in a mild functional improvement. *Stem Cells Dev, 22*(21), 2885-2894. doi: 10.1089/scd.2013.0049

Foster, H., Sharp, P. S., Athanasopoulos, T., Trollet, C., Graham, I. R., Foster, K., . . . Dickson, G. (2008). Codon and mRNA sequence optimization of microdystrophin transgenes improves expression and physiological outcome in dystrophic mdx mice following AAV2/8 gene transfer. *Mol Ther, 16*(11), 1825-1832. doi: 10.1038/mt.2008.186

Fujita, E., Kouroku, Y., Isoai, A., Kumagai, H., Misutani, A., Matsuda, C., . . . Momoi, T. (2007). Two endoplasmic reticulum-associated degradation (ERAD) systems for the novel variant of the mutant dysferlin: ubiquitin/proteasome ERAD(I) and autophagy/lysosome ERAD(II). *Hum Mol Genet, 16*(6), 618-629. doi: 10.1093/hmg/ddm002

Fuson, K., Rice, A., Mahling, R., Snow, A., Nayak, K., Shanbhogue, P., . . . Sutton, R. B. (2014). Alternate splicing of dysferlin C2A confers Ca(2)(+)-dependent and Ca(2)(+)-independent binding for membrane repair. *Structure, 22*(1), 104-115. doi: 10.1016/j.str.2013.10.001

Galla, M., Schambach, A., Falk, C. S., Maetzig, T., Kuehle, J., Lange, K., . . . Baum, C. (2011). Avoiding cytotoxicity of transposases by dose-controlled mRNA delivery. *Nucleic Acids Res, 39*(16), 7147-7160. doi: 10.1093/nar/gkr384

Gallardo, E., de Luna, N., Diaz-Manera, J., Rojas-Garcia, R., Gonzalez-Quereda, L., Flix, B., . . . Illa, I. (2011). Comparison of dysferlin expression in human skeletal muscle with that in monocytes for the diagnosis of dysferlin myopathy. *PLoS One, 6*(12), e29061. doi: 10.1371/journal.pone.0029061

Galvez, B. G., Sampaolesi, M., Brunelli, S., Covarello, D., Gavina, M., Rossi, B., . . . Cossu, G. (2006). Complete repair of dystrophic skeletal muscle by mesoangioblasts with enhanced migration ability. *J Cell Biol, 174*(2), 231-243. doi: 10.1083/jcb.200512085

Garrison, B. S., Yant, S. R., Mikkelsen, J. G., & Kay, M. A. (2007). Postintegrative gene silencing within the Sleeping Beauty transposition system. *Mol Cell Biol, 27*(24), 8824-8833. doi: 10.1128/MCB.00498-07

Gilchrist, S. C., Ontell, M. P., Kochanek, S., & Clemens, P. R. (2002). Immune response to full-length dystrophin delivered to Dmd muscle by a high-capacity adenoviral vector. *Mol Ther, 6*(3), 359-368.

Glover, L. E., Newton, K., Krishnan, G., Bronson, R., Boyle, A., Krivickas, L. S., & Brown, R. H., Jr. (2010). Dysferlin overexpression in skeletal muscle produces a progressive myopathy. *Ann Neurol, 67*(3), 384-393. doi: 10.1002/ana.21926

Gowers, W. R. (1902). A Lecture on Myopathy and a Distal Form: Delivered at the National Hospital for the Paralysed and Epileptic. *Br Med J, 2*(2167), 89-92.

Grabundzija, I., Irgang, M., Mates, L., Belay, E., Matrai, J., Gogol-Doring, A., . . . Ivics, Z. (2010). Comparative analysis of transposable element vector systems in human cells. *Mol Ther, 18*(6), 1200-1209. doi: 10.1038/mt.2010.47

Grabundzija, I., Izsvak, Z., & Ivics, Z. (2011). Insertional engineering of chromosomes with Sleeping Beauty transposition: an overview. *Methods Mol Biol, 738*, 69-85. doi: 10.1007/978-1-61779-099-7_5

Grose, W. E., Clark, K. R., Griffin, D., Malik, V., Shontz, K. M., Montgomery, C. L., . . . Rodino-Klapac, L. R. (2012). Homologous recombination mediates functional recovery of dysferlin deficiency following AAV5 gene transfer. *PLoS One, 7*(6), e39233. doi: 10.1371/journal.pone.0039233

Gross, J. G., Bou-Gharios, G., & Morgan, J. E. (1999). Potentiation of myoblast transplantation by host muscle irradiation is dependent on the rate of radiation delivery. *Cell Tissue Res, 298*(2), 371-375.

Gross, J. G., & Morgan, J. E. (1999). Muscle precursor cells injected into irradiated mdx mouse muscle persist after serial injury. *Muscle Nerve, 22*(2), 174-185.

Gussoni, E., Soneoka, Y., Strickland, C. D., Buzney, E. A., Khan, M. K., Flint, A. F., . . . Mulligan, R. C. (1999). Dystrophin expression in the mdx mouse restored by stem cell transplantation. *Nature, 401*(6751), 390-394. doi: 10.1038/43919

Guttinger, M., Tafi, E., Battaglia, M., Coletta, M., & Cossu, G. (2006). Allogeneic mesoangioblasts give rise to alpha-sarcoglycan expressing fibers when transplanted into dystrophic mice. *Exp Cell Res, 312*(19), 3872-3879. doi: 10.1016/j.yexcr.2006.08.012

Hacein-Bey-Abina, S., Garrigue, A., Wang, G. P., Soulier, J., Lim, A., Morillon, E., . . . Cavazzana-Calvo, M. (2008). Insertional oncogenesis in 4 patients after retrovirus-mediated gene therapy of SCID-X1. *J Clin Invest, 118*(9), 3132-3142. doi: 10.1172/JCI35700

Hacein-Bey-Abina, S., Pai, S. Y., Gaspar, H. B., Armant, M., Berry, C. C., Blanche, S., . . . Thrasher, A. J. (2014). A modified gamma-retrovirus vector for X-linked severe combined immunodeficiency. *N Engl J Med, 371*(15), 1407-1417. doi: 10.1056/NEJMoa1404588

Hacein-Bey-Abina, S., Von Kalle, C., Schmidt, M., McCormack, M. P., Wulffraat, N., Leboulch, P., . . . Cavazzana-Calvo, M. (2003). LMO2-associated clonal T cell proliferation in two patients after gene therapy for SCID-X1. *Science, 302*(5644), 415-419. doi: 10.1126/science.1088547

Hackett, P. B., Largaespada, D. A., Switzer, K. C., & Cooper, L. J. (2013). Evaluating risks of insertional mutagenesis by DNA transposons in gene therapy. *Transl Res, 161*(4), 265-283. doi: 10.1016/j.trsl.2012.12.005

Han, R. (2011). Muscle membrane repair and inflammatory attack in dysferlinopathy. *Skelet Muscle, 1*(1), 10. doi: 10.1186/2044-5040-1-10

Han, R., Bansal, D., Miyake, K., Muniz, V. P., Weiss, R. M., McNeil, P. L., & Campbell, K. P. (2007). Dysferlin-mediated membrane repair protects the heart from stress-induced left ventricular injury. *J Clin Invest, 117*(7), 1805-1813. doi: 10.1172/JCI30848

Han, R., Frett, E. M., Levy, J. R., Rader, E. P., Lueck, J. D., Bansal, D., . . . Campbell, K. P. (2010). Genetic ablation of complement C3 attenuates muscle pathology in dysferlin-deficient mice. *J Clin Invest, 120*(12), 4366-4374. doi: 10.1172/JCI42390

Hausl, M. A., Zhang, W., Muther, N., Rauschhuber, C., Franck, H. G., Merricks, E. P., . . . Ehrhardt, A. (2010). Hyperactive sleeping beauty transposase enables persistent phenotypic correction in mice and a canine model for hemophilia B. *Mol Ther, 18*(11), 1896-1906. doi: 10.1038/mt.2010.169

Ho, M., Gallardo, E., McKenna-Yasek, D., De Luna, N., Illa, I., & Brown Jr, R. H. (2002). A novel, blood-based diagnostic assay for limb girdle muscular dystrophy 2B and Miyoshi myopathy. *Ann Neurol, 51*(1), 129-133.

Ho, M., Post, C. M., Donahue, L. R., Lidov, H. G., Bronson, R. T., Goolsby, H., . . . Brown, R. H., Jr. (2004). Disruption of muscle membrane and phenotype divergence in two novel mouse models of dysferlin deficiency. *Hum Mol Genet, 13*(18), 1999-2010. doi: 10.1093/hmg/ddh212

Hoffman, E. P., Morgan, J. E., Watkins, S. C., & Partridge, T. A. (1990). Somatic reversion/suppression of the mouse mdx phenotype in vivo. *J Neurol Sci, 99*(1), 9-25.

Howe, S. J., Mansour, M. R., Schwarzwaelder, K., Bartholomae, C., Hubank, M., Kempski, H., . . . Thrasher, A. J. (2008). Insertional mutagenesis combined with acquired somatic mutations causes leukemogenesis following gene therapy of SCID-X1 patients. *J Clin Invest, 118*(9), 3143-3150. doi: 10.1172/JCI35798

Huang, X., Guo, H., Kang, J., Choi, S., Zhou, T. C., Tammana, S., . . . Zhou, X. (2008). Sleeping Beauty transposon-mediated engineering of human primary T cells for therapy of CD19+ lymphoid malignancies. *Mol Ther, 16*(3), 580-589. doi: 10.1038/sj.mt.6300404

Huang, X., Guo, H., Tammana, S., Jung, Y. C., Mellgren, E., Bassi, P., . . . Zhou, X. (2010). Gene transfer efficiency and genome-wide integration profiling of Sleeping Beauty, Tol2, and piggyBac transposons in human primary T cells. *Mol Ther, 18*(10), 1803-1813. doi: 10.1038/mt.2010.141

Huang, Y., Laval, S. H., van Remoortere, A., Baudier, J., Benaud, C., Anderson, L. V., . . . van der Maarel, S. M. (2007). AHNAK, a novel component of the dysferlin protein complex, redistributes to the cytoplasm with dysferlin during skeletal muscle regeneration. *FASEB J, 21*(3), 732-742. doi: 10.1096/fj.06-6628com

Hughes, S. M., & Blau, H. M. (1990). Migration of myoblasts across basal lamina during skeletal muscle development. *Nature, 345*(6273), 350-353. doi: 10.1038/345350a0

Hyland, K. A., Olson, E. R., Clark, K. J., Aronovich, E. L., Hackett, P. B., Blazar, B. R., . . . Scott McIvor, R. (2011). Sleeping Beauty-mediated correction of Fanconi anemia type C. *J Gene Med, 13*(9), 462-469. doi: 10.1002/jgm.1589

Illa, I., Serrano-Munuera, C., Gallardo, E., Lasa, A., Rojas-Garcia, R., Palmer, J., . . . Brown, R. H. (2001). Distal anterior compartment myopathy: a dysferlin mutation causing a new muscular dystrophy phenotype. *Ann Neurol, 49*(1), 130-134.

Illarioshkin, S. N., Ivanova-Smolenskaya, I. A., Greenberg, C. R., Nylen, E., Sukhorukov, V. S., Poleshchuk, V. V., . . . Wrogemann, K. (2000). Identical dysferlin mutation in limb-girdle muscular dystrophy type 2B and distal myopathy. *Neurology, 55*(12), 1931-1933.

Illarioshkin, S. N., Ivanova-Smolenskaya, I. A., Tanaka, H., Vereshchagin, N. V., Markova, E. D., Poleshchuk, V. V., . . . Tsuji, S. (1996). Clinical and molecular analysis of a large family with three distinct phenotypes of progressive muscular dystrophy. *Brain, 119 (Pt 6)*, 1895-1909.

Ito, M., Hiramatsu, H., Kobayashi, K., Suzue, K., Kawahata, M., Hioki, K., . . . Nakahata, T. (2002). NOD/SCID/gamma(c)(null) mouse: an excellent recipient mouse model for engraftment of human cells. *Blood, 100*(9), 3175-3182. doi: 10.1182/blood-2001-12-0207

Ivics, Z., Hackett, P. B., Plasterk, R. H., & Izsvak, Z. (1997). Molecular reconstruction of Sleeping Beauty, a Tc1-like transposon from fish, and its transposition in human cells. *Cell, 91*(4), 501-510.

Izsvak, Z., Ivics, Z., & Plasterk, R. H. (2000). Sleeping Beauty, a wide host-range transposon vector for genetic transformation in vertebrates. *J Mol Biol, 302*(1), 93-102. doi: 10.1006/jmbi.2000.4047

Jacobsen, R. B., Hronek, B. W., Schmidt, G. A., & Schilling, M. L. (2011). Hypervitaminosis D associated with a vitamin D dispensing error. *Ann Pharmacother, 45*(10), e52. doi: 10.1345/aph.1Q330

Jarmin, S., Kymalainen, H., Popplewell, L., & Dickson, G. (2014). New developments in the use of gene therapy to treat Duchenne muscular dystrophy. *Expert Opin Biol Ther, 14*(2), 209-230. doi: 10.1517/14712598.2014.866087

Jat, P. S., Noble, M. D., Ataliotis, P., Tanaka, Y., Yannoutsos, N., Larsen, L., & Kioussis, D. (1991). Direct derivation of conditionally immortal cell lines from an H-2Kb-tsA58 transgenic mouse. *Proc Natl Acad Sci U S A, 88*(12), 5096-5100.

Johnen, S., Izsvak, Z., Stocker, M., Harmening, N., Salz, A. K., Walter, P., & Thumann, G. (2012). Sleeping Beauty transposon-mediated transfection of retinal and iris pigment epithelial cells. *Invest Ophthalmol Vis Sci, 53*(8), 4787-4796. doi: 10.1167/iovs.12-9951

June, C. H., Blazar, B. R., & Riley, J. L. (2009). Engineering lymphocyte subsets: tools, trials and tribulations. *Nat Rev Immunol, 9*(10), 704-716. doi: 10.1038/nri2635

Kebriaei, P., Huls, H., Jena, B., Munsell, M., Jackson, R., Lee, D. A., . . . Cooper, L. J. (2012). Infusing CD19-directed T cells to augment disease control in patients undergoing

autologous hematopoietic stem-cell transplantation for advanced B-lymphoid malignancies. *Hum Gene Ther, 23*(5), 444-450. doi: 10.1089/hum.2011.167

Keefe, A. C., Lawson, J. A., Flygare, S. D., Fox, Z. D., Colasanto, M. P., Mathew, S. J., . . . Kardon, G. (2015). Muscle stem cells contribute to myofibres in sedentary adult mice. *Nat Commun, 6*, 7087. doi: 10.1038/ncomms8087

Kerr, J. P., Ward, C. W., & Bloch, R. J. (2014). Dysferlin at transverse tubules regulates Ca(2+) homeostasis in skeletal muscle. *Front Physiol, 5*, 89. doi: 10.3389/fphys.2014.00089

Kerr, J. P., Ziman, A. P., Mueller, A. L., Muriel, J. M., Kleinhans-Welte, E., Gumerson, J. D., . . . Bloch, R. J. (2013). Dysferlin stabilizes stress-induced Ca2+ signaling in the transverse tubule membrane. *Proc Natl Acad Sci U S A, 110*(51), 20831-20836. doi: 10.1073/pnas.1307960110

Kesari, A., Fukuda, M., Knoblach, S., Bashir, R., Nader, G. A., Rao, D., . . . Hoffman, E. P. (2008). Dysferlin deficiency shows compensatory induction of Rab27A/Slp2a that may contribute to inflammatory onset. *Am J Pathol, 173*(5), 1476-1487. doi: 10.2353/ajpath.2008.080098

Klinge, L., Harris, J., Sewry, C., Charlton, R., Anderson, L., Laval, S., . . . Bushby, K. (2010). Dysferlin associates with the developing T-tubule system in rodent and human skeletal muscle. *Muscle Nerve, 41*(2), 166-173. doi: 10.1002/mus.21166

Klinge, L., Laval, S., Keers, S., Haldane, F., Straub, V., Barresi, R., & Bushby, K. (2007). From T-tubule to sarcolemma: damage-induced dysferlin translocation in early myogenesis. *FASEB J, 21*(8), 1768-1776. doi: 10.1096/fj.06-7659com

Kong, K. Y., Ren, J., Kraus, M., Finklestein, S. P., & Brown, R. H., Jr. (2004). Human umbilical cord blood cells differentiate into muscle in sjl muscular dystrophy mice. *Stem Cells, 22*(6), 981-993. doi: 10.1634/stemcells.22-6-981

Koo, T., Malerba, A., Athanasopoulos, T., Trollet, C., Boldrin, L., Ferry, A., . . . Dickson, G. (2011). Delivery of AAV2/9-microdystrophin genes incorporating helix 1 of the coiled-coil motif in the C-terminal domain of dystrophin improves muscle pathology and restores the level of alpha1-syntrophin and alpha-dystrobrevin in skeletal muscles of mdx mice. *Hum Gene Ther, 22*(11), 1379-1388. doi: 10.1089/hum.2011.020

Krahn, M., Beroud, C., Labelle, V., Nguyen, K., Bernard, R., Bassez, G., . . . Levy, N. (2009). Analysis of the DYSF mutational spectrum in a large cohort of patients. *Hum Mutat, 30*(2), E345-375. doi: 10.1002/humu.20910

Krahn, M., Wein, N., Bartoli, M., Lostal, W., Courrier, S., Bourg-Alibert, N., . . . Levy, N. (2010). A naturally occurring human minidysferlin protein repairs sarcolemmal lesions in a mouse model of dysferlinopathy. *Sci Transl Med, 2*(50), 50ra69. doi: 10.1126/scitranslmed.3000951

Kren, B. T., Unger, G. M., Sjeklocha, L., Trossen, A. A., Korman, V., Diethelm-Okita, B. M., . . . Steer, C. J. (2009). Nanocapsule-delivered Sleeping Beauty mediates therapeutic Factor VIII expression in liver sinusoidal endothelial cells of hemophilia A mice. *J Clin Invest, 119*(7), 2086-2099. doi: 10.1172/JCI34332

Kuang, S., Kuroda, K., Le Grand, F., & Rudnicki, M. A. (2007). Asymmetric self-renewal and commitment of satellite stem cells in muscle. *Cell, 129*(5), 999-1010. doi: 10.1016/j.cell.2007.03.044

Kutcher, M. E., & Herman, I. M. (2009). The pericyte: cellular regulator of microvascular blood flow. *Microvasc Res, 77*(3), 235-246. doi: 10.1016/j.mvr.2009.01.007

Lander, E. S., Linton, L. M., Birren, B., Nusbaum, C., Zody, M. C., Baldwin, J., . . . International Human Genome Sequencing, Consortium. (2001). Initial sequencing and analysis of the human genome. *Nature, 409*(6822), 860-921. doi: 10.1038/35057062

Latil, M., Rocheteau, P., Chatre, L., Sanulli, S., Memet, S., Ricchetti, M., . . . Chretien, F. (2012). Skeletal muscle stem cells adopt a dormant cell state post mortem and retain regenerative capacity. *Nat Commun, 3*, 903. doi: 10.1038/ncomms1890

Lek, A., Evesson, F. J., Lemckert, F. A., Redpath, G. M., Lueders, A. K., Turnbull, L., . . . Cooper, S. T. (2013). Calpains, cleaved mini-dysferlinC72, and L-type channels underpin calcium-dependent muscle membrane repair. *J Neurosci, 33*(12), 5085-5094. doi: 10.1523/JNEUROSCI.3560-12.2013

Lek, A., Evesson, F. J., Sutton, R. B., North, K. N., & Cooper, S. T. (2012). Ferlins: regulators of vesicle fusion for auditory neurotransmission, receptor trafficking and membrane repair. *Traffic, 13*(2), 185-194. doi: 10.1111/j.1600-0854.2011.01267.x

Lepper, C., Partridge, T. A., & Fan, C. M. (2011). An absolute requirement for Pax7-positive satellite cells in acute injury-induced skeletal muscle regeneration. *Development, 138*(17), 3639-3646. doi: 10.1242/dev.067595

Leriche-Guerin, K., Anderson, L. V., Wrogemann, K., Roy, B., Goulet, M., & Tremblay, J. P. (2002). Dysferlin expression after normal myoblast transplantation in SCID and in SJL mice. *Neuromuscul Disord, 12*(2), 167-173.

Li, X., Eastman, E. M., Schwartz, R. J., & Draghia-Akli, R. (1999). Synthetic muscle promoters: activities exceeding naturally occurring regulatory sequences. *Nat Biotechnol, 17*(3), 241-245. doi: 10.1038/6981

Li, X., Ewis, H., Hice, R. H., Malani, N., Parker, N., Zhou, L., . . . Craig, N. L. (2013). A resurrected mammalian hAT transposable element and a closely related insect element are highly active in human cell culture. *Proc Natl Acad Sci U S A, 110*(6), E478-487. doi: 10.1073/pnas.1121543109

Liu, J., Aoki, M., Illa, I., Wu, C., Fardeau, M., Angelini, C., . . . Brown, R. H., Jr. (1998). Dysferlin, a novel skeletal muscle gene, is mutated in Miyoshi myopathy and limb girdle muscular dystrophy. *Nat Genet, 20*(1), 31-36. doi: 10.1038/1682

Liu, L., Mah, C., & Fletcher, B. S. (2006). Sustained FVIII expression and phenotypic correction of hemophilia A in neonatal mice using an endothelial-targeted sleeping beauty transposon. *Mol Ther, 13*(5), 1006-1015. doi: 10.1016/j.ymthe.2005.11.021

Lostal, W., Bartoli, M., Bourg, N., Roudaut, C., Bentaib, A., Miyake, K., . . . Richard, I. (2010). Efficient recovery of dysferlin deficiency by dual adeno-associated vector-mediated gene transfer. *Hum Mol Genet, 19*(10), 1897-1907. doi: 10.1093/hmg/ddq065

Lostal, W., Bartoli, M., Roudaut, C., Bourg, N., Krahn, M., Pryadkina, M., . . . Richard, I. (2012). Lack of correlation between outcomes of membrane repair assay and correction of dystrophic changes in experimental therapeutic strategy in dysferlinopathy. *PLoS One, 7*(5), e38036. doi: 10.1371/journal.pone.0038036

Luo, W. Y., Shih, Y. S., Hung, C. L., Lo, K. W., Chiang, C. S., Lo, W. H., . . . Hu, Y. C. (2012). Development of the hybrid Sleeping Beauty: baculovirus vector for sustained gene expression and cancer therapy. *Gene Ther, 19*(8), 844-851. doi: 10.1038/gt.2011.129

Marg, A., Escobar, H., Gloy, S., Kufeld, M., Zacher, J., Spuler, A., . . . Spuler, S. (2014). Human satellite cells have regenerative capacity and are genetically manipulable. *J Clin Invest, 124*(10), 4257-4265. doi: 10.1172/JCI63992

Marg, A., Schoewel, V., Timmel, T., Schulze, A., Shah, C., Daumke, O., & Spuler, S. (2012). Sarcolemmal repair is a slow process and includes EHD2. *Traffic, 13*(9), 1286-1294. doi: 10.1111/j.1600-0854.2012.01386.x

Marty, N. J., Holman, C. L., Abdullah, N., & Johnson, C. P. (2013). The C2 domains of otoferlin, dysferlin, and myoferlin alter the packing of lipid bilayers. *Biochemistry, 52*(33), 5585-5592. doi: 10.1021/bi400432f

Mates, L., Chuah, M. K., Belay, E., Jerchow, B., Manoj, N., Acosta-Sanchez, A., . . . Izsvak, Z. (2009). Molecular evolution of a novel hyperactive Sleeping Beauty transposase enables robust stable gene transfer in vertebrates. *Nat Genet, 41*(6), 753-761. doi: 10.1038/ng.343

Matsuda, C., Aoki, M., Hayashi, Y. K., Ho, M. F., Arahata, K., & Brown, R. H., Jr. (1999). Dysferlin is a surface membrane-associated protein that is absent in Miyoshi myopathy. *Neurology, 53*(5), 1119-1122.

Matsuda, C., Hayashi, Y. K., Ogawa, M., Aoki, M., Murayama, K., Nishino, I., . . . Brown, R. H., Jr. (2001). The sarcolemmal proteins dysferlin and caveolin-3 interact in skeletal muscle. *Hum Mol Genet, 10*(17), 1761-1766.

Matsuda, C., Miyake, K., Kameyama, K., Keduka, E., Takeshima, H., Imamura, T., . . . Hayashi, Y. (2012). The C2A domain in dysferlin is important for association with MG53 (TRIM72). *PLoS Curr, 4*, e5035add5038caff5034. doi: 10.1371/5035add8caff4

Mauro, A. (1961). Satellite cell of skeletal muscle fibers. *J Biophys Biochem Cytol, 9*, 493-495.

McDade, J. R., Archambeau, A., & Michele, D. E. (2014). Rapid actin-cytoskeleton-dependent recruitment of plasma membrane-derived dysferlin at wounds is critical for muscle membrane repair. *FASEB J, 28*(8), 3660-3670. doi: 10.1096/fj.14-250191

McDade, J. R., & Michele, D. E. (2014). Membrane damage-induced vesicle-vesicle fusion of dysferlin-containing vesicles in muscle cells requires microtubules and kinesin. *Hum Mol Genet, 23*(7), 1677-1686. doi: 10.1093/hmg/ddt557

McLoon, L. K., & Wirtschafter, J. (2003). Activated satellite cells in extraocular muscles of normal adult monkeys and humans. *Invest Ophthalmol Vis Sci, 44*(5), 1927-1932.

Mendell, J. R., Campbell, K., Rodino-Klapac, L., Sahenk, Z., Shilling, C., Lewis, S., . . . Walker, C. M. (2010). Dystrophin immunity in Duchenne's muscular dystrophy. *N Engl J Med, 363*(15), 1429-1437. doi: 10.1056/NEJMoa1000228

Meng, J., Adkin, C. F., Xu, S. W., Muntoni, F., & Morgan, J. E. (2011). Contribution of human muscle-derived cells to skeletal muscle regeneration in dystrophic host mice. *PLoS One, 6*(3), e17454. doi: 10.1371/journal.pone.0017454

Meng, J., Bencze, M., Asfahani, R., Muntoni, F., & Morgan, J. E. (2015). The effect of the muscle environment on the regenerative capacity of human skeletal muscle stem cells. *Skelet Muscle, 5*, 11. doi: 10.1186/s13395-015-0036-8

Meng, J., Chun, S., Asfahani, R., Lochmuller, H., Muntoni, F., & Morgan, J. (2014). Human skeletal muscle-derived CD133(+) cells form functional satellite cells after intramuscular transplantation in immunodeficient host mice. *Mol Ther, 22*(5), 1008-1017. doi: 10.1038/mt.2014.26

Meregalli, M., Navarro, C., Sitzia, C., Farini, A., Montani, E., Wein, N., . . . Torrente, Y. (2013). Full-length dysferlin expression driven by engineered human dystrophic blood derived CD133+ stem cells. *FEBS J, 280*(23), 6045-6060. doi: 10.1111/febs.12523

Minasi, M. G., Riminucci, M., De Angelis, L., Borello, U., Berarducci, B., Innocenzi, A., . . . Cossu, G. (2002). The meso-angioblast: a multipotent, self-renewing cell that originates from the dorsal aorta and differentiates into most mesodermal tissues. *Development, 129*(11), 2773-2783.

Mingozzi, F., & High, K. A. (2011). Therapeutic in vivo gene transfer for genetic disease using AAV: progress and challenges. *Nat Rev Genet, 12*(5), 341-355. doi: 10.1038/nrg2988

Miskey, C., Izsvak, Z., Plasterk, R. H., & Ivics, Z. (2003). The Frog Prince: a reconstructed transposon from Rana pipiens with high transpositional activity in vertebrate cells. *Nucleic Acids Res, 31*(23), 6873-6881.

Mitchell, K. J., Pannerec, A., Cadot, B., Parlakian, A., Besson, V., Gomes, E. R., . . . Sassoon, D. A. (2010). Identification and characterization of a non-satellite cell muscle resident progenitor during postnatal development. *Nat Cell Biol, 12*(3), 257-266. doi: 10.1038/ncb2025

Miyoshi, K., Kawai, H., Iwasa, M., Kusaka, K., & Nishino, H. (1986). Autosomal recessive distal muscular dystrophy as a new type of progressive muscular dystrophy. Seventeen cases in eight families including an autopsied case. *Brain, 109 (Pt 1)*, 31-54.

Moldt, B., Miskey, C., Staunstrup, N. H., Gogol-Doring, A., Bak, R. O., Sharma, N., . . . Mikkelsen, J. G. (2011). Comparative genomic integration profiling of Sleeping Beauty transposons mobilized with high efficacy from integrase-defective lentiviral vectors in primary human cells. *Mol Ther, 19*(8), 1499-1510. doi: 10.1038/mt.2011.47

Montarras, D., Morgan, J., Collins, C., Relaix, F., Zaffran, S., Cumano, A., . . . Buckingham, M. (2005). Direct isolation of satellite cells for skeletal muscle regeneration. *Science, 309*(5743), 2064-2067. doi: 10.1126/science.1114758

Montini, E., Held, P. K., Noll, M., Morcinek, N., Al-Dhalimy, M., Finegold, M., . . . Grompe, M. (2002). In vivo correction of murine tyrosinemia type I by DNA-mediated transposition. *Mol Ther, 6*(6), 759-769.

Morgan, J. E., Beauchamp, J. R., Pagel, C. N., Peckham, M., Ataliotis, P., Jat, P. S., . . . Partridge, T. A. (1994). Myogenic cell lines derived from transgenic mice carrying a thermolabile T antigen: a model system for the derivation of tissue-specific and mutation-specific cell lines. *Dev Biol, 162*(2), 486-498. doi: 10.1006/dbio.1994.1103

Morgan, J. E., Gross, J. G., Pagel, C. N., Beauchamp, J. R., Fassati, A., Thrasher, A. J., . . . Partridge, T. A. (2002). Myogenic cell proliferation and generation of a reversible tumorigenic phenotype are triggered by preirradiation of the recipient site. *J Cell Biol, 157*(4), 693-702. doi: 10.1083/jcb.200108047

Morgan, J. E., Hoffman, E. P., & Partridge, T. A. (1990). Normal myogenic cells from newborn mice restore normal histology to degenerating muscles of the mdx mouse. *J Cell Biol, 111*(6 Pt 1), 2437-2449.

Morgan, J. E., Pagel, C. N., Sherratt, T., & Partridge, T. A. (1993). Long-term persistence and migration of myogenic cells injected into pre-irradiated muscles of mdx mice. *J Neurol Sci, 115*(2), 191-200.

Morgan, J. E., & Zammit, P. S. (2010). Direct effects of the pathogenic mutation on satellite cell function in muscular dystrophy. *Exp Cell Res, 316*(18), 3100-3108. doi: 10.1016/j.yexcr.2010.05.014

Muses, S., Morgan, J. E., & Wells, D. J. (2011a). A new extensively characterised conditionally immortal muscle cell-line for investigating therapeutic strategies in muscular dystrophies. *PLoS One, 6*(9), e24826. doi: 10.1371/journal.pone.0024826

Muses, S., Morgan, J. E., & Wells, D. J. (2011b). Restoration of dystrophin expression using the Sleeping Beauty transposon. *PLoS Curr, 3*, RRN1296. doi: 10.1371/currents.RRN1296

Nagaraju, K., Rawat, R., Veszelovszky, E., Thapliyal, R., Kesari, A., Sparks, S., . . . Hoffman, E. P. (2008). Dysferlin deficiency enhances monocyte phagocytosis: a model for the inflammatory onset of limb-girdle muscular dystrophy 2B. *Am J Pathol, 172*(3), 774-785. doi: 10.2353/ajpath.2008.070327

Negroni, E., Riederer, I., Chaouch, S., Belicchi, M., Razini, P., Di Santo, J., . . . Mouly, V. (2009). In vivo myogenic potential of human CD133+ muscle-derived stem cells: a quantitative study. *Mol Ther, 17*(10), 1771-1778. doi: 10.1038/mt.2009.167

Newrzela, S., Cornils, K., Li, Z., Baum, C., Brugman, M. H., Hartmann, M., . . . von Laer, D. (2008). Resistance of mature T cells to oncogene transformation. *Blood, 112*(6), 2278-2286. doi: 10.1182/blood-2007-12-128751

Nicholson, L. V. (1993). The "rescue" of dystrophin synthesis in boys with Duchenne muscular dystrophy. *Neuromuscul Disord, 3*(5-6), 525-531.

Nigro, V., & Savarese, M. (2014). Genetic basis of limb-girdle muscular dystrophies: the 2014 update. *Acta Myol, 33*(1), 1-12.

Ohlfest, J. R., Frandsen, J. L., Fritz, S., Lobitz, P. D., Perkinson, S. G., Clark, K. J., . . . Largaespada, D. A. (2005). Phenotypic correction and long-term expression of factor VIII in hemophilic mice by immunotolerization and nonviral gene transfer using the Sleeping Beauty transposon system. *Blood, 105*(7), 2691-2698. doi: 10.1182/blood-2004-09-3496

Pan, X. J., Ma, Z. Z., Zhang, Q. J., Fan, L., & Li, Q. H. (2012). Sleeping Beauty transposon system is a reliable gene delivery tool for hereditary tyrosinaemia type 1 disease gene therapy: size of the foreign gene decides the timing of stable integration into the host chromosomes. *J Int Med Res, 40*(5), 1850-1859.

Pannerec, A., Formicola, L., Besson, V., Marazzi, G., & Sassoon, D. A. (2013). Defining skeletal muscle resident progenitors and their cell fate potentials. *Development, 140*(14), 2879-2891. doi: 10.1242/dev.089326

Papadakis, E. D., Nicklin, S. A., Baker, A. H., & White, S. J. (2004). Promoters and control elements: designing expression cassettes for gene therapy. *Curr Gene Ther, 4*(1), 89-113.

Paradas, C., Gonzalez-Quereda, L., De Luna, N., Gallardo, E., Garcia-Consuegra, I., Gomez, H., . . . Gallano, P. (2009). A new phenotype of dysferlinopathy with congenital onset. *Neuromuscul Disord, 19*(1), 21-25. doi: 10.1016/j.nmd.2008.09.015

Partridge, T. A., & Morgan, J. E. (2014). Multiple insights from myogenic cell transplants. *Hum Gene Ther, 25*(5), 404-405. doi: 10.1089/hum.2014.035

Perie, S., Trollet, C., Mouly, V., Vanneaux, V., Mamchaoui, K., Bouazza, B., . . . St Guily, J. L. (2014). Autologous myoblast transplantation for oculopharyngeal muscular dystrophy: a phase I/IIa clinical study. *Mol Ther, 22*(1), 219-225. doi: 10.1038/mt.2013.155

Philippi, S., Lorain, S., Beley, C., Peccate, C., Precigout, G., Spuler, S., & Garcia, L. (2015). Dysferlin rescue by spliceosome-mediated pre-mRNA trans-splicing targeting introns harbouring weakly defined 3' splice sites. *Hum Mol Genet*. doi: 10.1093/hmg/ddv141

Piccolo, F., Moore, S. A., Ford, G. C., & Campbell, K. P. (2000). Intracellular accumulation and reduced sarcolemmal expression of dysferlin in limb--girdle muscular dystrophies. *Ann Neurol, 48*(6), 902-912.

Ponting, C. P., Mott, R., Bork, P., & Copley, R. R. (2001). Novel protein domains and repeats in Drosophila melanogaster: insights into structure, function, and evolution. *Genome Res, 11*(12), 1996-2008. doi: 10.1101/gr.198701

Pramono, Z. A., Lai, P. S., Tan, C. L., Takeda, S., & Yee, W. C. (2006). Identification and characterization of a novel human dysferlin transcript: dysferlin_v1. *Hum Genet, 120*(3), 410-419. doi: 10.1007/s00439-006-0230-1

Pramono, Z. A., Tan, C. L., Seah, I. A., See, J. S., Kam, S. Y., Lai, P. S., & Yee, W. C. (2009). Identification and characterisation of human dysferlin transcript variants: implications for dysferlin mutational screening and isoforms. *Hum Genet, 125*(4), 413-420. doi: 10.1007/s00439-009-0632-y

Puttaraju, M., Jamison, S. F., Mansfield, S. G., Garcia-Blanco, M. A., & Mitchell, L. G. (1999). Spliceosome-mediated RNA trans-splicing as a tool for gene therapy. *Nat Biotechnol, 17*(3), 246-252. doi: 10.1038/6986

Rawat, R., Cohen, T. V., Ampong, B., Francia, D., Henriques-Pons, A., Hoffman, E. P., & Nagaraju, K. (2010). Inflammasome up-regulation and activation in dysferlin-deficient skeletal muscle. *Am J Pathol, 176*(6), 2891-2900. doi: 10.2353/ajpath.2010.090058

Recchia, A., Bonini, C., Magnani, Z., Urbinati, F., Sartori, D., Muraro, S., . . . Mavilio, F. (2006). Retroviral vector integration deregulates gene expression but has no consequence on the biology and function of transplanted T cells. *Proc Natl Acad Sci U S A, 103*(5), 1457-1462. doi: 10.1073/pnas.0507496103

Redpath, G. M., Woolger, N., Piper, A. K., Lemckert, F. A., Lek, A., Greer, P. A., . . . Cooper, S. T. (2014). Calpain cleavage within dysferlin exon 40a releases a synaptotagmin-like module for membrane repair. *Mol Biol Cell, 25*(19), 3037-3048. doi: 10.1091/mbc.E14-04-0947

Relaix, F., Montarras, D., Zaffran, S., Gayraud-Morel, B., Rocancourt, D., Tajbakhsh, S., . . . Buckingham, M. (2006). Pax3 and Pax7 have distinct and overlapping functions in adult muscle progenitor cells. *J Cell Biol, 172*(1), 91-102. doi: 10.1083/jcb.200508044

Richardson, S. R., Morell, S., & Faulkner, G. J. (2014). L1 retrotransposons and somatic mosaicism in the brain. *Annu Rev Genet, 48*, 1-27. doi: 10.1146/annurev-genet-120213-092412

Roche, J. A., Ru, L. W., O'Neill, A. M., Resneck, W. G., Lovering, R. M., & Bloch, R. J. (2011). Unmasking potential intracellular roles for dysferlin through improved immunolabeling methods. *J Histochem Cytochem, 59*(11), 964-975. doi: 10.1369/0022155411423274

Rocheteau, P., Gayraud-Morel, B., Siegl-Cachedenier, I., Blasco, M. A., & Tajbakhsh, S. (2012). A subpopulation of adult skeletal muscle stem cells retains all template DNA strands after cell division. *Cell, 148*(1-2), 112-125. doi: 10.1016/j.cell.2011.11.049

Roostalu, U., & Strahle, U. (2012). In vivo imaging of molecular interactions at damaged sarcolemma. *Dev Cell, 22*(3), 515-529. doi: 10.1016/j.devcel.2011.12.008

Rosenblatt, J. D., Lunt, A. I., Parry, D. J., & Partridge, T. A. (1995). Culturing satellite cells from living single muscle fiber explants. *In Vitro Cell Dev Biol Anim, 31*(10), 773-779. doi: 10.1007/BF02634119

Ross, J., Benn, A., Jonuschies, J., Boldrin, L., Muntoni, F., Hewitt, J. E., . . . Morgan, J. E. (2012). Defects in glycosylation impair satellite stem cell function and niche composition in the muscles of the dystrophic Large(myd) mouse. *Stem Cells, 30*(10), 2330-2341. doi: 10.1002/stem.1197

Rostovskaya, M., Fu, J., Obst, M., Baer, I., Weidlich, S., Wang, H., . . . Stewart, A. F. (2012). Transposon-mediated BAC transgenesis in human ES cells. *Nucleic Acids Res, 40*(19), e150. doi: 10.1093/nar/gks643

Rozkalne, A., Adkin, C., Meng, J., Lapan, A., Morgan, J. E., & Gussoni, E. (2014). Mouse regenerating myofibers detected as false-positive donor myofibers with anti-human spectrin. *Hum Gene Ther, 25*(1), 73-81. doi: 10.1089/hum.2013.126

Sacco, A., Doyonnas, R., Kraft, P., Vitorovic, S., & Blau, H. M. (2008). Self-renewal and expansion of single transplanted muscle stem cells. *Nature, 456*(7221), 502-506. doi: 10.1038/nature07384

Saclier, M., Cuvellier, S., Magnan, M., Mounier, R., & Chazaud, B. (2013). Monocyte/macrophage interactions with myogenic precursor cells during skeletal muscle regeneration. *FEBS J, 280*(17), 4118-4130. doi: 10.1111/febs.12166

Salani, S., Lucchiari, S., Fortunato, F., Crimi, M., Corti, S., Locatelli, F., . . . Comi, G. P. (2004). Developmental and tissue-specific regulation of a novel dysferlin isoform. *Muscle Nerve, 30*(3), 366-374. doi: 10.1002/mus.20106

Sambasivan, R., Yao, R., Kissenpfennig, A., Van Wittenberghe, L., Paldi, A., Gayraud-Morel, B., . . . Galy, A. (2011). Pax7-expressing satellite cells are indispensable for adult skeletal muscle regeneration. *Development, 138*(17), 3647-3656. doi: 10.1242/dev.067587

Sampaolesi, M., Blot, S., D'Antona, G., Granger, N., Tonlorenzi, R., Innocenzi, A., . . . Cossu, G. (2006). Mesoangioblast stem cells ameliorate muscle function in dystrophic dogs. *Nature, 444*(7119), 574-579. doi: 10.1038/nature05282

Sampaolesi, M., Blot, S., D'Antona, G., Granger, N., Tonlorenzi, R., Innocenzi, A., . . . Cossu, G. (2013). Corrigendum: Mesoangioblast stem cells ameliorate muscle function in dystrophic dogs. *Nature, 494*(7438), 506. doi: 10.1038/nature11976

Sampaolesi, M., Torrente, Y., Innocenzi, A., Tonlorenzi, R., D'Antona, G., Pellegrino, M. A., . . . Cossu, G. (2003). Cell therapy of alpha-sarcoglycan null dystrophic mice through intra-arterial delivery of mesoangioblasts. *Science, 301*(5632), 487-492. doi: 10.1126/science.1082254

Schoewel, V., Marg, A., Kunz, S., Overkamp, T., Carrazedo, R. S., Zacharias, U., . . . Spuler, S. (2012). Dysferlin-peptides reallocate mutated dysferlin thereby restoring function. *PLoS One, 7*(11), e49603. doi: 10.1371/journal.pone.0049603

Schultz, E., Gibson, M. C., & Champion, T. (1978). Satellite cells are mitotically quiescent in mature mouse muscle: an EM and radioautographic study. *J Exp Zool, 206*(3), 451-456. doi: 10.1002/jez.1402060314

Schwarzwaelder, K., Howe, S. J., Schmidt, M., Brugman, M. H., Deichmann, A., Glimm, H., . . . von Kalle, C. (2007). Gammaretrovirus-mediated correction of SCID-X1 is associated with

skewed vector integration site distribution in vivo. *J Clin Invest, 117*(8), 2241-2249. doi: 10.1172/JCI31661

Seale, P., Sabourin, L. A., Girgis-Gabardo, A., Mansouri, A., Gruss, P., & Rudnicki, M. A. (2000). Pax7 is required for the specification of myogenic satellite cells. *Cell, 102*(6), 777-786.

Sharma, N., Cai, Y., Bak, R. O., Jakobsen, M. R., Schroder, L. D., & Mikkelsen, J. G. (2013). Efficient sleeping beauty DNA transposition from DNA minicircles. *Mol Ther Nucleic Acids, 2*, e74. doi: 10.1038/mtna.2013.1

Shea, K. L., Xiang, W., LaPorta, V. S., Licht, J. D., Keller, C., Basson, M. A., & Brack, A. S. (2010). Sprouty1 regulates reversible quiescence of a self-renewing adult muscle stem cell pool during regeneration. *Cell Stem Cell, 6*(2), 117-129. doi: 10.1016/j.stem.2009.12.015

Shinin, V., Gayraud-Morel, B., Gomes, D., & Tajbakhsh, S. (2006). Asymmetric division and cosegregation of template DNA strands in adult muscle satellite cells. *Nat Cell Biol, 8*(7), 677-687. doi: 10.1038/ncb1425

Sinzelle, L., Kapitonov, V. V., Grzela, D. P., Jursch, T., Jurka, J., Izsvak, Z., & Ivics, Z. (2008). Transposition of a reconstructed Harbinger element in human cells and functional homology with two transposon-derived cellular genes. *Proc Natl Acad Sci U S A, 105*(12), 4715-4720. doi: 10.1073/pnas.0707746105

Sjeklocha, L. M., Wong, P. Y., Belcher, J. D., Vercellotti, G. M., & Steer, C. J. (2013). beta-Globin sleeping beauty transposon reduces red blood cell sickling in a patient-derived CD34(+)-based in vitro model. *PLoS One, 8*(11), e80403. doi: 10.1371/journal.pone.0080403

Sondergaard, P. C., Griffin, D. A., Pozsgai, E. R., Johnson, R. W., Grose, W. E., Heller, K. N., . . . Rodino-Klapac, L. R. (2015). AAV.Dysferlin Overlap Vectors Restore Function in Dysferlinopathy Animal Models. *Ann Clin Transl Neurol, 2*(3), 256-270. doi: 10.1002/acn3.172

Sousa-Victor, P., Gutarra, S., Garcia-Prat, L., Rodriguez-Ubreva, J., Ortet, L., Ruiz-Bonilla, V., . . . Munoz-Canoves, P. (2014). Geriatric muscle stem cells switch reversible quiescence into senescence. *Nature, 506*(7488), 316-321. doi: 10.1038/nature13013

Spuler, S., Carl, M., Zabojszcza, J., Straub, V., Bushby, K., Moore, S. A., . . . Rocken, C. (2008). Dysferlin-deficient muscular dystrophy features amyloidosis. *Ann Neurol, 63*(3), 323-328. doi: 10.1002/ana.21309

Staunstrup, N. H., Moldt, B., Mates, L., Villesen, P., Jakobsen, M., Ivics, Z., . . . Mikkelsen, J. G. (2009). Hybrid lentivirus-transposon vectors with a random integration profile in human cells. *Mol Ther, 17*(7), 1205-1214. doi: 10.1038/mt.2009.10

Stein, S., Ott, M. G., Schultze-Strasser, S., Jauch, A., Burwinkel, B., Kinner, A., . . . Grez, M. (2010). Genomic instability and myelodysplasia with monosomy 7 consequent to EVI1 activation after gene therapy for chronic granulomatous disease. *Nat Med, 16*(2), 198-204. doi: 10.1038/nm.2088

Stringer, J. M., Kainer, R. A., & Tu, A. T. (1971). Ultrastructural studies of myonecrosis induced by cobra venom in mice. *Toxicol Appl Pharmacol, 18*(2), 442-450.

Sula, A., Cole, A. R., Yeats, C., Orengo, C., & Keep, N. H. (2014). Crystal structures of the human Dysferlin inner DysF domain. *BMC Struct Biol, 14*, 3. doi: 10.1186/1472-6807-14-3

Swierczek, M., Izsvak, Z., & Ivics, Z. (2012). The Sleeping Beauty transposon system for clinical applications. *Expert Opin Biol Ther, 12*(2), 139-153. doi: 10.1517/14712598.2012.642358

Szymczak, A. L., Workman, C. J., Wang, Y., Vignali, K. M., Dilioglou, S., Vanin, E. F., & Vignali, D. A. (2004). Correction of multi-gene deficiency in vivo using a single 'self-cleaving' 2A peptide-based retroviral vector. *Nat Biotechnol, 22*(5), 589-594. doi: 10.1038/nbt957

Takahashi, K., Tanabe, K., Ohnuki, M., Narita, M., Ichisaka, T., Tomoda, K., & Yamanaka, S. (2007). Induction of pluripotent stem cells from adult human fibroblasts by defined factors. *Cell, 131*(5), 861-872. doi: 10.1016/j.cell.2007.11.019

Takahashi, K., & Yamanaka, S. (2006). Induction of pluripotent stem cells from mouse embryonic and adult fibroblast cultures by defined factors. *Cell, 126*(4), 663-676. doi: 10.1016/j.cell.2006.07.024

Tanaka, A., Woltjen, K., Miyake, K., Hotta, A., Ikeya, M., Yamamoto, T., . . . Sakurai, H. (2013). Efficient and reproducible myogenic differentiation from human iPS cells: prospects for modeling Miyoshi Myopathy in vitro. *PLoS One, 8*(4), e61540. doi: 10.1371/journal.pone.0061540

Tanaka, K. K., Hall, J. K., Troy, A. A., Cornelison, D. D., Majka, S. M., & Olwin, B. B. (2009). Syndecan-4-expressing muscle progenitor cells in the SP engraft as satellite cells during muscle regeneration. *Cell Stem Cell, 4*(3), 217-225. doi: 10.1016/j.stem.2009.01.016

Tedesco, F. S., Dellavalle, A., Diaz-Manera, J., Messina, G., & Cossu, G. (2010). Repairing skeletal muscle: regenerative potential of skeletal muscle stem cells. *J Clin Invest, 120*(1), 11-19. doi: 10.1172/JCI40373

Tedesco, F. S., Hoshiya, H., D'Antona, G., Gerli, M. F., Messina, G., Antonini, S., . . . Cossu, G. (2011). Stem cell-mediated transfer of a human artificial chromosome ameliorates muscular dystrophy. *Sci Transl Med, 3*(96), 96ra78. doi: 10.1126/scitranslmed.3002342

Therrien, C., Dodig, D., Karpati, G., & Sinnreich, M. (2006). Mutation impact on dysferlin inferred from database analysis and computer-based structural predictions. *J Neurol Sci, 250*(1-2), 71-78. doi: 10.1016/j.jns.2006.07.004

Torrente, Y., Belicchi, M., Marchesi, C., D'Antona, G., Cogiamanian, F., Pisati, F., . . . Bresolin, N. (2007). Autologous transplantation of muscle-derived CD133+ stem cells in Duchenne muscle patients. *Cell Transplant, 16*(6), 563-577.

Torrente, Y., Belicchi, M., Sampaolesi, M., Pisati, F., Meregalli, M., D'Antona, G., . . . Bresolin, N. (2004). Human circulating AC133(+) stem cells restore dystrophin expression and ameliorate function in dystrophic skeletal muscle. *J Clin Invest, 114*(2), 182-195. doi: 10.1172/JCI20325

Turunen, T. A., Laakkonen, J. P., Alasaarela, L., Airenne, K. J., & Yla-Herttuala, S. (2014). Sleeping Beauty-baculovirus hybrid vectors for long-term gene expression in the eye. *J Gene Med, 16*(1-2), 40-53. doi: 10.1002/jgm.2756

Uren, A. G., Mikkers, H., Kool, J., van der Weyden, L., Lund, A. H., Wilson, C. H., . . . Adams, D. J. (2009). A high-throughput splinkerette-PCR method for the isolation and sequencing of retroviral insertion sites. *Nat Protoc, 4*(5), 789-798. doi: 10.1038/nprot.2009.64

Vainzof, M., Anderson, L. V., McNally, E. M., Davis, D. B., Faulkner, G., Valle, G., . . . Zatz, M. (2001). Dysferlin protein analysis in limb-girdle muscular dystrophies. *J Mol Neurosci, 17*(1), 71-80. doi: 10.1385/JMN:17:1:71

van Deutekom, J. C., Janson, A. A., Ginjaar, I. B., Frankhuizen, W. S., Aartsma-Rus, A., Bremmer-Bout, M., . . . van Ommen, G. J. (2007). Local dystrophin restoration with antisense oligonucleotide PRO051. *N Engl J Med, 357*(26), 2677-2686. doi: 10.1056/NEJMoa073108

Venter, J. C., Adams, M. D., Myers, E. W., Li, P. W., Mural, R. J., Sutton, G. G., . . . Zhu, X. (2001). The sequence of the human genome. *Science, 291*(5507), 1304-1351. doi: 10.1126/science.1058040

Vigdal, T. J., Kaufman, C. D., Izsvak, Z., Voytas, D. F., & Ivics, Z. (2002). Common physical properties of DNA affecting target site selection of sleeping beauty and other Tc1/mariner transposable elements. *J Mol Biol, 323*(3), 441-452.

Vink, C. A., Gaspar, H. B., Gabriel, R., Schmidt, M., McIvor, R. S., Thrasher, A. J., & Qasim, W. (2009). Sleeping beauty transposition from nonintegrating lentivirus. *Mol Ther, 17*(7), 1197-1204. doi: 10.1038/mt.2009.94

Walisko, O., Schorn, A., Rolfs, F., Devaraj, A., Miskey, C., Izsvak, Z., & Ivics, Z. (2008). Transcriptional activities of the Sleeping Beauty transposon and shielding its genetic cargo with insulators. *Mol Ther, 16*(2), 359-369. doi: 10.1038/sj.mt.6300366

Walton, J. N., & Nattrass, F. J. (1954). On the classification, natural history and treatment of the myopathies. *Brain, 77*(2), 169-231.

Wang, B., Li, J., Fu, F. H., Chen, C., Zhu, X., Zhou, L., . . . Xiao, X. (2008). Construction and analysis of compact muscle-specific promoters for AAV vectors. *Gene Ther, 15*(22), 1489-1499. doi: 10.1038/gt.2008.104

Wang, D., Zhong, L., Nahid, M. A., & Gao, G. (2014). The potential of adeno-associated viral vectors for gene delivery to muscle tissue. *Expert Opin Drug Deliv, 11*(3), 345-364. doi: 10.1517/17425247.2014.871258

Wang, T. T., Tavera-Mendoza, L. E., Laperriere, D., Libby, E., MacLeod, N. B., Nagai, Y., . . . White, J. H. (2005). Large-scale in silico and microarray-based identification of direct 1,25-dihydroxyvitamin D3 target genes. *Mol Endocrinol, 19*(11), 2685-2695. doi: 10.1210/me.2005-0106

Watt, D. J., Morgan, J. E., Clifford, M. A., & Partridge, T. A. (1987). The movement of muscle precursor cells between adjacent regenerating muscles in the mouse. *Anat Embryol (Berl), 175*(4), 527-536.

Weiler, T., Greenberg, C. R., Nylen, E., Halliday, W., Morgan, K., Eggertson, D., & Wrogemann, K. (1996). Limb-girdle muscular dystrophy and Miyoshi myopathy in an aboriginal Canadian kindred map to LGMD2B and segregate with the same haplotype. *Am J Hum Genet, 59*(4), 872-878.

Wein, N., Avril, A., Bartoli, M., Beley, C., Chaouch, S., Laforet, P., . . . Levy, N. (2010). Efficient bypass of mutations in dysferlin deficient patient cells by antisense-induced exon skipping. *Hum Mutat, 31*(2), 136-142. doi: 10.1002/humu.21160

Weller, B., Karpati, G., Lehnert, S., & Carpenter, S. (1991). Major alteration of the pathological phenotype in gamma irradiated mdx soleus muscles. *J Neuropathol Exp Neurol, 50*(4), 419-431.

Wenzel, K., Carl, M., Perrot, A., Zabojszcza, J., Assadi, M., Ebeling, M., . . . Spuler, S. (2006). Novel sequence variants in dysferlin-deficient muscular dystrophy leading to mRNA decay and possible C2-domain misfolding. *Hum Mutat, 27*(6), 599-600. doi: 10.1002/humu.9424

Wenzel, K., Geier, C., Qadri, F., Hubner, N., Schulz, H., Erdmann, B., . . . Ozcelik, C. (2007). Dysfunction of dysferlin-deficient hearts. *J Mol Med (Berl), 85*(11), 1203-1214. doi: 10.1007/s00109-007-0253-7

Wenzel, K., Zabojszcza, J., Carl, M., Taubert, S., Lass, A., Harris, C. L., . . . Spuler, S. (2005). Increased susceptibility to complement attack due to down-regulation of decay-accelerating factor/CD55 in dysferlin-deficient muscular dystrophy. *J Immunol, 175*(9), 6219-6225.

Wilber, A., Wangensteen, K. J., Chen, Y., Zhuo, L., Frandsen, J. L., Bell, J. B., . . . Wang, X. (2007). Messenger RNA as a source of transposase for sleeping beauty transposon-mediated correction of hereditary tyrosinemia type I. *Mol Ther, 15*(7), 1280-1287. doi: 10.1038/sj.mt.6300160

Williams, D. A. (2008). Sleeping beauty vector system moves toward human trials in the United States. *Mol Ther, 16*(9), 1515-1516. doi: 10.1038/mt.2008.169

Xue, X., Huang, X., Nodland, S. E., Mates, L., Ma, L., Izsvak, Z., . . . Zhou, X. (2009). Stable gene transfer and expression in cord blood-derived CD34+ hematopoietic stem and progenitor cells by a hyperactive Sleeping Beauty transposon system. *Blood, 114*(7), 1319-1330. doi: 10.1182/blood-2009-03-210005

Yant, S. R., Ehrhardt, A., Mikkelsen, J. G., Meuse, L., Pham, T., & Kay, M. A. (2002). Transposition from a gutless adeno-transposon vector stabilizes transgene expression in vivo. *Nat Biotechnol, 20*(10), 999-1005. doi: 10.1038/nbt738

Yant, S. R., Meuse, L., Chiu, W., Ivics, Z., Izsvak, Z., & Kay, M. A. (2000). Somatic integration and long-term transgene expression in normal and haemophilic mice using a DNA transposon system. *Nat Genet, 25*(1), 35-41. doi: 10.1038/75568

Yant, S. R., Wu, X., Huang, Y., Garrison, B., Burgess, S. M., & Kay, M. A. (2005). High-resolution genome-wide mapping of transposon integration in mammals. *Mol Cell Biol, 25*(6), 2085-2094. doi: 10.1128/MCB.25.6.2085-2094.2005

Yin, H., Price, F., & Rudnicki, M. A. (2013). Satellite cells and the muscle stem cell niche. *Physiol Rev, 93*(1), 23-67. doi: 10.1152/physrev.00043.2011

Young, L., Sung, J., Stacey, G., & Masters, J. R. (2010). Detection of Mycoplasma in cell cultures. *Nat Protoc, 5*(5), 929-934. doi: 10.1038/nprot.2010.43

Zayed, H., Izsvak, Z., Walisko, O., & Ivics, Z. (2004). Development of hyperactive sleeping beauty transposon vectors by mutational analysis. *Mol Ther, 9*(2), 292-304. doi: 10.1016/j.ymthe.2003.11.024

Zhang, W., Muck-Hausl, M., Wang, J., Sun, C., Gebbing, M., Miskey, C., . . . Ehrhardt, A. (2013). Integration profile and safety of an adenovirus hybrid-vector utilizing hyperactive sleeping beauty transposase for somatic integration. *PLoS One, 8*(10), e75344. doi: 10.1371/journal.pone.0075344

Zhang, W., Solanki, M., Muther, N., Ebel, M., Wang, J., Sun, C., . . . Ehrhardt, A. (2013). Hybrid adeno-associated viral vectors utilizing transposase-mediated somatic integration for stable transgene expression in human cells. *PLoS One, 8*(10), e76771. doi: 10.1371/journal.pone.0076771